Universität für Bodenkultur Wien
University of Natural Resources
and Applied Life Sciences, Vienna

DISSERTATION

Development of innovative methods in radionuclide metrology for applications in natural resources and life sciences

zur Erlangung des Doktorgrades an der Universität für Bodenkultur Wien

Eingereicht von
Dipl.-Ing. Hannah Wiedner, BSc.
00726598

Betreuer:
HR Univ. Prof. Dipl.-Ing. Dr. Franz Josef Maringer

Beratungsteam:
Univ. Prof. Dipl.-Ing. Dr. Dr. h. c. mult. Martin H. Gerzabek
Ass. Prof. Dipl.-Ing. Dr. techn. Karin Poljanc

Gutachter:
Univ. Prof. Dipl.-Ing. Dr. Dr. h. c. mult. Martin H. Gerzabek
Prof. Dr. Georg Steinhauser

Wien, February 2019

Abstract

The presented work starts with an overview over current state of the art techniques for the evaluation of activity concentration in naturally occurring radioactive materials (NORM). The thesis focuses on the development of innovative methods in radionuclide metrology for applications in natural resources and life science research. For this purpose, an extensive study of particular problems arising in γ-ray spectrometry of NORM samples has been conducted. Common challenges and problematic γ-lines are highlighted, and a best practice recommendation on the evaluation of naturally occurring radionuclides is given. Special attention is given to the evaluation of radon tightness of used sample containers. A simple and sensitive method for the estimation of ^{222}Rn leakage is proposed.

The general demand in industry and science for NORM reference materials for instrument calibration and method verification led to the preparation and characterization of a traceable NORM material and its use in a proficiency test of nine European laboratories concerned with radioactivity measurements and environmental monitoring by γ-ray spectrometry. Both the preparation and characterization process of a new NORM material made of quartz sand with significantly elevated levels of ^{226}Ra obtained from the back flush of a drinking water treatment facility, and the results of the proficiency test are presented in this thesis.

As an alternative to classical γ-ray spectrometry, the application of artificial neural networks (ANNs) has been tested in a feasibility study. ANNs are mathematical software tools that can "learn" by generalizing "knowledge" gained from training datasets and apply it to new problems. An ANN that is able to decide from the raw γ-spectrum, whether the activity concentrations in a sample are above or below the exemption limits was trained.

Furthermore, a comparison of two ionization chamber measurement techniques was conducted using water samples of drinking water quality. It was shown, that the results and uncertainties of an old and inexpensive, self-built ionization chamber are in good agreement with the results of a commercially available AlphaGUARD radon monitor. A fit to compensate for measurements made in non-equilibrium state was applied and the detection limit is estimated.

The results of this work give the scientific basis for practical solutions concerning the implementation of the European Radiation Protection Directive in the field of NORM.

Keywords: radionuclide metrology, gamma-ray spectrometry, NORM, traceably reference material, artificial neural networks, radon in water

Zusammenfassung

Die vorliegende Arbeit gibt zuerst einen Überblick über den aktuellen Stand der Technik in der Radionuklidmetrologie natürlicher Radionuklide und beschreibt übliche Methoden und Probleme bei der Bestimmung der Aktivitätskonzentration in natürlich radioaktiven Stoffen (NORM). Darauf aufbauend wurden in dieser Dissertation neue und innovative Methoden für die Radionuklidmetrologie entwickelt, die insbesondere dazu dienen sollen, den Strahlenschutz betroffener Personen in allen Gebieten der natürlichen Ressoucen und Lebenswissenschaften zu verbessern. Eine zu diesem Zweck durchgeführte, umfangreiche Studie beleuchtet die speziell bei der Gammaspektrometrie von Radionukliden der natürlichen Zerfallsketten auftretende Schwierigkeiten und stellt optimierte Vorgehensweisen zur Bestimmung der Aktivitätskonzentration, sowie eine einfache Methode zur Beurteilung der Radondichtheit von Probenbehältern vor.

Um der hohen Nachfrage nach NORM Referenzmaterialen zur Kalibrierung von Detektorsystemen und Methodenverifikation nachzukommen, wurde im Rahmen dieser Dissertation ein NORM Vergleichsmaterial mit einem hohen ^{226}Ra Gehalt hergestellt und charakterisiert. Dieses wurde zu einem Eignungstest verwendet, an dem neun europäische Gammaspektrometrielaboratorien teilnahmen. Der Herstellungs- und Charakterisierungsprozess, sowie die Ergebnisse des Eignungstests werden beschrieben.
Als Alternative zur klassischen Gammaspektrometrie wurde eine Machbarkeitsstudie zur Verwendung von künstlichen neuronalen Netzen (Artificial Neural Networks, ANNs) durchgeführt. ANNs sind Computertools, die in begrenztem Ausmaß lernfähig sind. Durch die Auswahl geeigneter Trainingsbeispiele kann die Software das „erlernte“ Wissen auf unbekannte Situationen übertragen. Im Rahmen der Studie wurde geprüft, ob ANNs dazu verwendet werden können, aus Gammaspektrometrie-Rohdaten zu entscheiden, ob die Aktivitätskonzentration eines Materials oberhalb oder unterhalb der Freigrenze für NORM liegt.

Weiters wurde ein Vergleich zweier Ionisationskammer-Messmethoden zur Bestimmung der ^{222}Rn-Aktivitätskonzentration in Trinkwasserproben durchgeführt. Messergebnisse und Unsicherheiten einer alten, günstig im Eigenbau hergestellten Ionisationskammer stimmen gut mit den Ergebnissen eines kommerziell verfügbaren Radonmonitors (AlphaGUARD) überein. Ein Fit der Messdaten für Messungen, die außerhalb des Gleichgewichtszustands durchgeführt wurden, und eine Abschätzung der Nachweisgrenze wurden ebenfalls durchgeführt.

Die Ergebnisse der Arbeiten bieten die wissenschaftliche Basis für Fragestellungen bei der Umsetzung der europäischen Strahlenschutzrichtlinie in die Praxis.

Schlagworte: Radionuklidmetrologie, Gammaspektrometrie, NORM, Referenzmaterial, künstliche neuronale Netze, Radon in Wasser

Acknowledgements

I would like to express my gratitude to my supervisor Univ. Prof. Dipl.-Ing. Dr. Franz Josef Maringer for the useful comments, remarks, engagement and open ear through the learning process and writing of this doctoral thesis. Thank you for taking the time and going above and beyond in your supervision of this thesis. I would also like to thank my advisor Ass. Prof. Dipl.-Ing. Dr. techn. Karin Poljanc for her support and helpful suggestions.

Furthermore, I would like to thank Univ. Prof. Dipl.-Ing. Dr. Dr. h. c. mult. Martin H. Gerzabek and Prof. Dr. Georg Steinhauser for taking the time out of their busy schedules to appraise this thesis.

I want to give a big thank you to Virginia and Eduardo and all my colleagues at CIEMAT who have made me feel welcome and at home during my stay abroad. Thank you, Andreas, Michael and Franz, for your scientific insights and discussions, collaboration, and moral support.

This thesis was made possible through the support of Bundesamt für Eich- und Vermessungswesen (BEV), the European Metrology Research Programme, and European Metrology Programme for Innovation and Research, specifically JRP IND57 MetroNORM and 16ENV10 MetroRADON.

Last but not least, I would like to thank my loved ones, who have motivated and supported me throughout the entire process. I will be grateful forever for your love and support.

Contents

List of Figures

List of Tables

List of used abbreviations

ALARA	As Low as Reasonably Achievable
ANN	Artificial Neural Network
BEV	Federal Office of Metrology and Surveying
BIPM	International Bureau for Weights and Measures
CCRI	BIPM Consultative Committee for Ionizing Radiation
CIPM	BIPM International Committee for Weights and Measures
CIPM-MRA	Mutual Recognition Arrangement of the International Committee for Weights and Measures
CMC	Calibration and Measurement Capability
DDEP	Decay Data Evaluation Project
DI	Designated Institute
EURAMET	European Association of National Metrology Institutes
EMPIR	European Metrology Programme for Innovation and Research
EMRP	European Metrology Research Programme
EU-BSS	European Basic Safety Standards, Council Directive 59/2013/Euratom laying down basic safety standards for protection against the dangers arising from exposure to ionising radiation
ICRM	International Committee for Radionuclide Metrology
IRPA	International Radiation Protection Association
ICRP	International Commission on Radiological Protection
NMI	National Metrology Institute
NORM	Naturally Occurring Radioactive Material
PT	Proficiency Test
TCS	True Coincidence Summing
TENORM	Technologically Enhanced Naturally Occurring Radioactive Material

Preface

This thesis is submitted in compliance with the requirements for the degree of Doctorate of Natural Resources and Life Sciences at the University of Natural Resources and Life Sciences, Vienna. The doctoral work has been carried out in the Radioactivity Laboratory of the Federal Office of Metrology and Surveying, Austria.

This thesis is divided into two sections. In the first section an introduction to the field of radionuclide metrology is given. Emphasis is given to highlighting the challenges of this particular field of study and explain the context of the presented work. The second section is comprised of the peer-reviewed international journal papers that are the heart of this thesis. The concepts given in the first section are discussed in more detail in the form of three peer-reviewed first author publications, and one peer reviewed co-author publication, namely:

- Hannah Wiedner, Virginia Peyrés, Teresa Crespo, Marcos Mejuto, Eduardo García-Toraño, Franz Josef Maringer. "Application of an Artificial Neural Network for evaluation of activity concentration exemption limits in NORM industry". *Appl. Radiat. Isot. 126 (2017), 289-292*
- Hannah Wiedner, Jakob Riedl, Franz Josef Maringer, Andreas Baumgartner, Michael Stietka, Franz Kabrt. "Production and characterization of a traceable NORM material and its use in proficiency testing of gamma-ray spectrometry laboratories". *Appl. Radiat. Isot. 134 (2018), 45-50*
- Hannah Wiedner, Konrad Lotter, Patrick Karner, Harry Friedmann, Franz Josef Maringer. "Radon in drinking water: Comparison and evaluation of two ionisation chamber activity measurement methods". *Appl. Radiat. Isot. 134 (2018), 477-481*
- Andreas Baumgartner, Michael Stietka, Franz Kabrt, Hannah Wiedner, Franz Josef Maringer. "Study of particular problems appearing in NORM samples and recommendations for best practice gamma-ray spectrometry". *Appl. Radiat. Isot. 126 (2017), 285-288*

Apart from these publications, the following papers were published in peer-reviewed journals in collaboration with colleagues:

- Faidra Tzika, Mikael Hult, Oleksiy Burda, Dirk Arnold, Goedele Sibbens, Belén Caro Marroyo, Maria Belén Gómez-Mancebo, Virginia Peyrés, Hannah Moser, Laurent Ferreux, Jaroslav Šolc, Pavel Dryák, Aldo Fazio, Aurelian Luca, Branko Vodenik, Mario Reis, Zbigniew Tyminski, Seppo Klemola. "Interlaboratory comparison on ^{137}Cs activity concentration in fume dust. *Radiat Phys Chem 116 (2015), 106-110*
- Faidra Tzika, Oleksiy Burda, Mikael Hult, Dirk Arnold, Belén Caro Marroyo, Pavel Dryák, Aldo Fazio, Laurent Ferreux, Eduardo García-Toraño, Andrej Javornik, Seppo Klemola, Aurelian Luca, Hannah Moser, Marijan Nečemer, Virginia Peyrés, Mario Reis, Lidia Silva, Jaroslav Šolc, Anton Svec, Zbigniew Tyminski, Branko Vodenik, Uwe Wätjen. "^{60}Co in cast steel matrix: A European interlaboratory comparison for the characterisation of new activity standards for calibration of gamma-ray spectrometers in metallurgy". *Appl. Radiat. Isot. (2016), 167-172*
- Jaroslav Šolc, Pavel Dryák, Hannah Moser, Thierry Branger, Eduardo García-Toraño, Virginia Peyrés, Faidra Tzika, Guillaume Lutter, Marco Capogni, Aldo Fazio, Aurelian Luca, Branko Vodenik, Carlos Oliveira, Andre Saraiva, Laszlo Szűcs, Tomasz Dziel, Oleksiy Burda, Dirk Arnold, Jozef Martinkovič, Teemu Siiskonen, Aleksi Mattila. "Characterisation of a radionuclide specific laboratory detector system for the metallurgical industry by Monte Carlo simulations". *Radiat Phys Chem 116 (2015), 189-193*
- Franz Josef Maringer, Andreas Baumgartner, Francesco Cardellini, Philippe Cassette, Teresa Crespo, Julian Dean, Hannah Wiedner, Jiři Hůlka, Mikael Hult, Simon Jerome, Franz Kabrt, Petr Kovář, Cyrus Larijani, Guillaume Lutter, Maria Marouli, Alexander Mauring, Monika Mazánová, Bogusław Michalik, Nathalie Michielsen, Virginia Peyres, Sylvie Pierre, Roy Pöllänen, Stefaan Pommé, Mário Reis, Michael Stietka, László Szűcs, Branko Vodenik. "Advancements in NORM metrology – Results and impact of the European joint research project MetroNORM". *Appl. Radiat. Isot. 126 (2017), 273-278*

Furthermore, the work that was carried out throughout the years has been presented at numerous international and national conferences as talks, posters and proceeding papers:

- Hannah Moser. "Application of Artificial Neural Networks to the analysis of NORM samples", *oral presentation at ANN Seminar, Madrid, Spain, 26 November 2015.*
- H. Moser, V. Peyrés, M. Mejuto, E. García-Toraño. "Application of Artificial Neural Networks to the Analysis of NORM Samples", *CIEMAT technical report in "Informes Técnicos Ciemat 1375", ISSN: 1135-9420, Madrid, Spain, November 2015.*

- Hannah Wiedner, Virginia Peyrés, Teresa Crespo, Marcos Mejuto, Eduardo García-Toraño, Franz Josef Maringer. "Application of an Artificial Neural Network for evaluation of activity concentration exemption limits in NORM industry", *poster at 14th Congress of the International Radiation Protection Association (IRPA14), Cape Town, South Africa, May 9-13, 2016.*

- Hannah Wiedner, Virginia Peyrés, Teresa Crespo, Marcos Mejuto, Eduardo García-Toraño, Franz Josef Maringer. "Application of an Artificial Neural Network for evaluation of activity concentration exemption limits in NORM industry", *paper in the proceedings of the 14th Congress of the International Radiation Protection Association (IRPA14), Cape Town, South Africa, May 9-13, 2016.*

- Hannah Wiedner, Virginia Peyrés, Teresa Crespo, Marcos Mejuto, Eduardo García-Toraño, Franz Josef Maringer. "Application of an Artificial Neural Network for evaluation of activity concentration exemption limits in NORM industry", *poster at International Conference on Radionuclide Metrology and its Applications – Low-Level Radioactivity Measurement Techniques, Seattle, USA, 26-30 September, 2016.*

- Hannah Wiedner, Jakob Riedl, Franz Josef Maringer, Andreas Baumgartner, Michael Stietka, Franz Kabrt. "Production and characterization of a traceable NORM material and its use in proficiency testing of gamma-ray spectrometry laboratories", *oral presentation at 21st International Conference on Radionuclide Metrology and its Applications, Buenos Aires, Argentina, 15-19 May 2017.*

- Hannah Wiedner, Konrad Lotter, Patrick Karner, Harry Friedmann, Franz Josef Maringer. "Radon in drinking water: Comparison and evaluation of two ionisation chamber activity measurement methods", *poster at 21st International Conference on Radionuclide Metrology and its Applications, Buenos Aires, Argentina, 15-19 May 2017.*

- Katharina Newrkla, Hannah Wiedner, Franz Josef Maringer. "A radioecological study of radon and thoron in soil gas and water", *poster at 5th European Congress of the International Radiation Protection Association, The Hague, Netherlands, 4-8 June 2018.*

- Katharina Newrkla, Hannah Wiedner, Franz Josef Maringer. "A radioecological study of radon and thoron in soil gas and water", *paper in the proceedings of the 5th European Congress of the International Radiation Protection Association, The Hague, Netherlands, 4-8 June 2018, in print.*

- Hannah Wiedner,, Virginia Peyrés, Teresa Crespo, Marcos Mejuto, Eduardo García-Toraño, Franz Josef Maringer. "Application of an Artificial Neural Network for evaluation of activity concentration exemption limits in NORM industry" *oral presentation at 5th European Congress of the International Radiation Protection Association, The Hague, Netherlands, 4-8 June 2018.*

1 State-of-the-art in metrology of natural radionuclides

1.1 Natural radioactivity and radiation background

Natural radioactive elements are present in low concentration in earth's crust and are continuously created by interaction of cosmic radiation with earth's atmosphere. Due to their involvement in a whole number of natural processes, radioactive isotopes are – to varying degree – present in all environmental media, even in the human body (UNSCEAR, 2010). For most individuals, exposure to natural background radiation is the largest contribution (world average: 79 %) to the annual effective dose (see Figure 1.1).

Figure 1.1: Distribution of global annual average of effective dose per caput (data according to UNSCEAR (2010)).

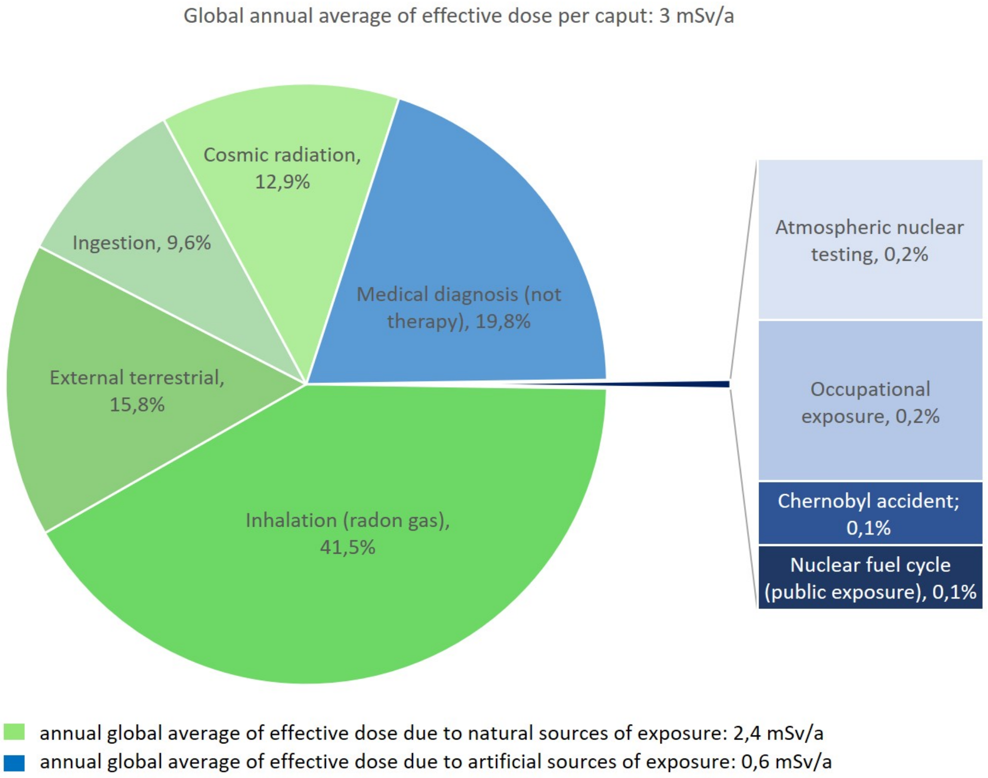

The primordial radionuclides ^{40}K, ^{232}Th, ^{235}U and ^{238}U, as well as their radioactive progeny account for a large portion of human exposure to natural radiation, amounting to an annual global average effective dose from natural background radiation of 2.4 mSv per caput. Of these 2.4 mSv – on global average – 1.6 mSv (52 %) per year can be attributed to the inhalation of radon gas, a radioactive daughter of ^{238}U (see Figure 1.2).

Figure 1.2: Distribution of effective dose due to natural sources of exposure (data according to UNSCEAR (2010)).

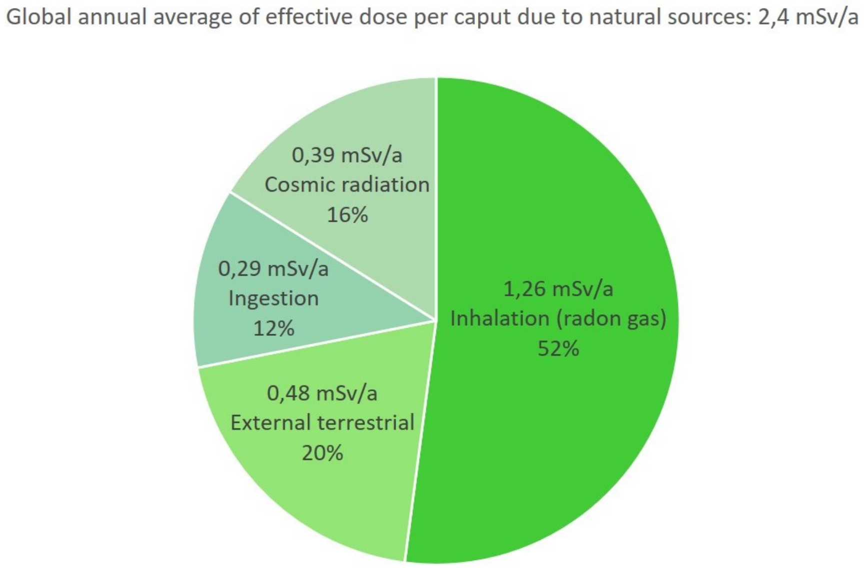

High concentrations of radon gas in dwellings and workplaces with insufficient ventilation pose a health risk to the people occupying those spaces. Exposure rates vary considerably by location, e.g. geological situation and altitude, and building standards and materials influence the concentration of radon gas in dwellings and workplaces. (UNSCEAR, 2010)

1.2 Naturally occurring radioactive materials

Processes involving naturally occurring radioactive materials (NORM) and technologically enhanced naturally occurring radioactive materials (TENORM) can be found in some of the most important industries, such as drinking water production, oil/gas production, coal industry, metallurgy, rare earth industry, phosphate industry, production of TiO_2, etc. and are often used as building materials (e.g. Baumgartner et al., 2017; Anagnostakis et al., 2004; Mantero et al., 2015; IAEA, 2003).

Table 1.1 gives an overview of NORM industries that were deemed significant by the European Union (data from EC, 2003).

Table 1.2 gives an overview of operations in NORM industries that were identified as likely requiring regulatory control on the basis of worker dose (data from IAEA, 2006).

Industrial exploitation of natural resources, such as extraction, processing and purification, can lead to significantly increased activity concentrations (usually in the waste product) that exceed exemption limits as laid down in national legislation and has the potential to harm workers and the public (Maringer, 2016). NORM waste can pose a huge economic and ecological burden if not handled properly (Maringer et al., 2017), and in addition to technical aspects and safety procedures, legislative aspects of the disposal of NORM material and waste have to be considered. Disposal of radioactively contaminated waste is significantly more expensive than regular waste (Maringer, 2016). Accurate assessment of activity concentration of various radionuclides in NORM is paramount for waste disposal, the decision to re-use the material and to ensure radiation protection of workers, the public and the environment as it is used for threat assessment. To accomplish these objectives, traceable, accurate and standardized measurement techniques and instruments are needed, particularly for in-situ applications (Maringer et al., 2017).

Table 1.1: Summary of potentially significant NORM industries in the European Union (data from EC, 2003).

Industry or work activity	**Potentially significant solid residues?**	**Potentially significant liquid discharges?**	**Potentially significant aerial discharges?**	**Is such a facility present in EU member state?**														
				BE	**DK**	**DE**	**EL**	**ES**	**FR**	**IE**	**IT**	**LU**	**NL**	**AT**	**PT**	**FI**	**SE**	**UK**
On-shore oil/gas	yes, sludges, scales	yes, if discharged, but no if injected	no	–	y	y	–	–	y	–	y	n	y	y	–	–	n	y
Off-shore oil/gas	yes, sludges, scales	yes, produced water, scales	no	–	y	y	y	y	n	y	y	n	y	–	n	–	n	y
Phosphoric acid	yes, if phosphogypsum is stockpiled	yes, if phosphogypsum is discharged	no	y	–	–	y	y	y	–	–	–	–	–	–	–	–	–
Phosphate fertilizer[1]	yes/no depending on process	yes/no depending on process	no	y	y	y	y	y	y	–	y	–	y	–	y	y	y	–
Thermal phosphorous	yes, calcine dust and slag	yes, ^{210}Po, ^{210}Pb	yes, ^{210}Po, ^{210}Pb	–	–	–	–	–	–	–	–	–	y	–	–	–	–	–
TiO_2 pigment	yes, solids from liquid waste treatment	yes/no depending on process	no	–	–	y	–	y	y	–	y	–	y	–	–	y	–	y
Steel	yes, blast furnace and sinter dust	yes/no depending on waste water treatment	yes, ^{210}Po, ^{210}Pb	y	y	y	y	y	y	–	y	y	y	y	y	y	y	y
Cement	no	no	yes, ^{210}Po, ^{210}Pb	y	y	y	y	y	y	y	y	y	y	y	y	y	y	y

Continued on next page

---

[1] incl. off-site production of phosphoric acid

Table 1.1: Summary of potentially significant NORM industries in the European Union (data from EC, 2003).

Industry or work activity	**Potentially significant solid residues?**	**Potentially significant liquid discharges?**	**Potentially significant aerial discharges?**	**Is such a facility present in EU member state?**														
				BE	**DK**	**DE**	**EL**	**ES**	**FR**	**IE**	**IT**	**LU**	**NL**	**AT**	**PT**	**FI**	**SE**	**UK**
Coal fuelled power plants	bottom and fly ash	no	no	y	y	y	y	y	y	y	y	y	y	y	y	y	y	y
Bricks and roofing tiles	no	no	yes, ^{210}Po	y	y	y	y	y	y	y	y	y	y	y	y	y	y	y
Tin smelters (closed down)	slag, slag wool, historical	no	yes, ^{210}Po, ^{210}Pb	–	–	–	–	–	–	–	–	–	–	–	–	–	–	–
Metal extraction from tin slag	yes, slag	no	yes, ^{210}Po, ^{210}Pb	–	–	y	–	–	–	–	–	–	–	–	–	–	–	–
Lead/zinc smelter	yes, cobalt-cake	no	yes, ^{210}Po, ^{210}Pb	y	–	y	y	y	y	–	y	–	y	–	y	y	y	y
Copper smelter	not known	no	yes, ^{210}Po, ^{210}Pb	y	–	y	–	y	y	–	–	–	–	–	–	y	y	–

Table 1.2: Types of operations likely to require regulatory control (data from IAEA, 2006).

Type of operation	**Description**	**Radionuclide(s) with highest activity concentration**	**Typical activity concentration (Bq/g)**	**Worker dose (mSv/a)**
Rare earth extraction from monazite	Monazite	^{232}Th series	40 - 600	Average 1-8
	Thorium concentrate	^{232}Th	Up to 800	Could approach or exceed dose limit
	Scale	^{228}Ra	1 000	
	Residue	^{228}Ra	20 - 3 000	

Continued on next page

Table 1.2: Types of operations likely to require regulatory control (data from IAEA, 2006).

Type of operation	**Description**	**Radionuclide(s) with highest activity concentration**	**Typical activity concentration (Bq/g)**	**Worker dose (mSv/a)**
Production of thorium compounds	Thorium concentrates	^{232}Th	Up to 800	Typically 6-15
	Thorium compounds	^{232}Th	Up to 2 000	
Manufacture of thorium containing products	Thorium compounds	^{232}Th	Up to 2 000	$<$ 1 to a significant fraction of dose limit
	Products	^{232}Th	Up to 1 000	
Processing of niobium/tantalum ore	Ore	^{232}Th series	1 - 8	Could reach significant fraction of dose limit
	Pyrochlore concentrate	^{232}Th	80	
	Residue	^{228}Ra	20 - 500	
	Slag	^{232}Th	2 0- 120	
Some underground mines and similar workplaces	Ore	^{226}Ra, ^{228}Ra	Up to 10	$<$ 1 to a significant fraction of dose limit[2]
	Scales from Ra rich water		Up to 200	
Oil and gas production	Scales during removal from pipes/vessels	^{226}Ra	0.1 - 15 000	$<$ 1 to a significant fraction of dose limit
TiO_2 pigment production	Scales during removal from pipes/vessels	^{226}Ra, ^{228}Ra	$<$ 1 - 1 600	$<$ 1 - 6

Continued on next page

---

[2] Effective dose from radon is highly variable and difficult to predict due to its high dependence on ventilation conditions and other factors.

Table 1.2: Types of operations likely to require regulatory control (data from IAEA, 2006).

Type of operation	**Description**	**Radionuclide(s) with highest activity concentration**	**Typical activity concentration (Bq/g)**	**Worker dose (mSv/a)**
Thermal phosphorus production	fume and precipitator dust	^{210}Pb	Up to 1 000[3]	0.2 - 5 (average ca. 1)
Fused zirconia production	fume and precipitator dust	^{210}Pb, ^{210}Po	Up to 600[3]	0.25 - 4.5

---

[3] Values refer to activity concentration of the precipitator dust

1.3 Metrology – The science of measurement

1.3.1 General overview

Metrology is the science of measurement and its application, including all theoretical and practical aspects of measurement, regardless of their uncertainty (JCGM, 2012). It is concerned with the definition and scientific realisation of internationally accepted units of measurement, and the establishment of traceability chains (Howarth and Redgrave, 2008). This means that the measurement result can be related to a reference through a documented unbroken chain of calibrations, that each contribute to the measurement uncertainty (JCGM, 2012). Figure 1.3 shows a visual representation of how traceability chains are established in practice.

Figure 1.3: Measurement traceability pyramid indicating the metrological infrastructure and establishment of the traceability chain.

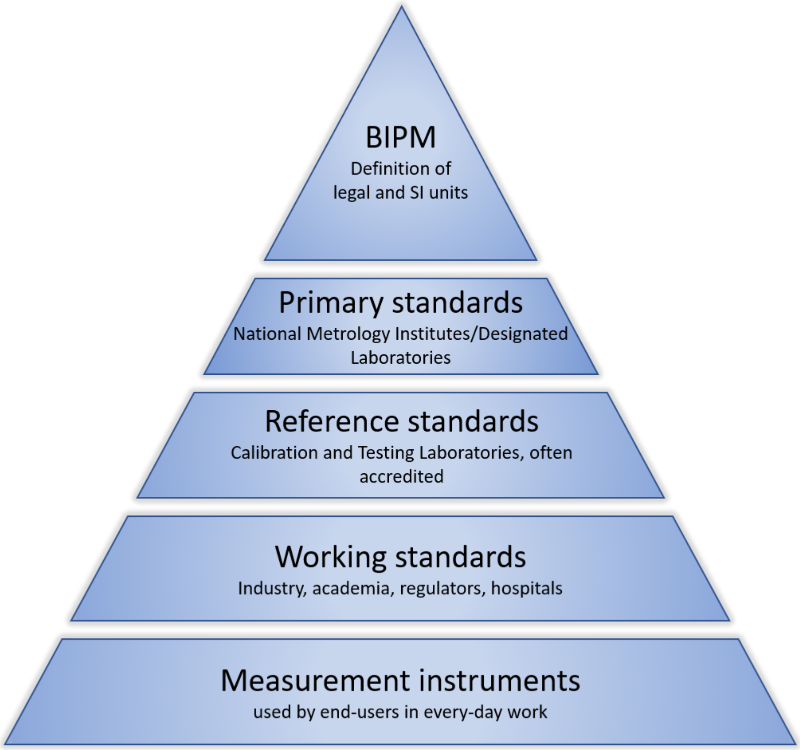

Taking accurate and traceable measurements is not purely the domain of scientists. An innumerable number of measurements is conducted world-wide everyday. A general need for harmonization and international agreement on units and quantities led to the signing of the Metre Convention on 20 May 1875, thus founding the International Bureau for Weights and Measures (BIPM – Bureau International des Poids et Mesures) based in Paris. Through the BIPM "Member States act together on matters related to measurement science and measurement standards", therefore, the BIPM "has the mandate to provide the basis for a single, coherent system of measurements throughout the world, traceable to the International

System of Units (SI)" and to enable and "promote and advance the global comparability of measurements" (BIPM, 2018a).

Under the umbrella of the BIPM, the Mutual Recognition Arrangement of the International Committee for Weights and Measures (CIPM-MRA) ensures mutual recognition of other Member's calibration and measurement capabilities (CMCs). To ensure that quality standards are met, National Metrology Institutes (NMIs) or Designated Laboratories (DIs) – the holders of the national standards – have to prove their competence in international key comparisons. These key comparisons are usually carried out by Regional Metrology Organisations (RMOs) such as EURAMET (European Association of National Metrology Institutes, RMO for Europe). Within the area of ionizing radiation, such key comparisons are conducted by the CIPM Consultative Committee for Ionizing Radiation (CCRI), that is divided into three subsections:

- Section I: x- and gamma rays, charged particles
- Section II: Measurement of radionuclides
- Section III: Neutron measurements

In addition, EURAMET has the objective of coordinating the cooperation of the European NMIs "in fields such as research in metrology, traceability of measurements to the SI units, international recognition of national measurement standards and related Calibration and Measurement Capabilities (CMC)" and to facilitate knowledge transfer and cooperation among EURAMET members, and the development and advancement of national metrology infrastructures (EURAMET, 2018). This includes the coordination and execution of the European Metrology Research Programme (EMRP) and the European Metrology Programme for Innovation and Research (EMPIR) with the aim to encourage collaboration between European National Metrology Institutes (NMIs) and partners from industry or academia (EURAMET, 2018).

1.3.2 Radionuclide metrology

The field of radionuclide metrology in general is concerned with the science behind measuring radioactivity (see CCRI Section II: Measurement of radionuclides). The advancement and development of new, accurate and reliable measurement techniques, traceability of the measured quantities to national and international standards, and a sound understanding and assessment of the associated measurement uncertainties are integral parts of this field. A strong intradisciplinary cooperation and collaboration with all fields of industry and radiation protection is an important prerequisite to enable uptake of developed methods by end-users and benefit everyone, be it by protecting the general public and workers in industries using radioactivity from unnecessary exposure to ionizing radiation or further our understanding of the world.

In the field of radionuclide metrology, the International Committee for Radionuclide Metrology (ICRM) is particularly relevant. It is an association of radionuclide metrology laboratories and scientists engaged in the study and application of radioactivity that serves as an international forum for the dissemination of information on techniques, applications and data in the field of radionuclide metrology. The main focus points are general research, industrial, medical and environmental applications, emergency preparedness, decommissioning of nuclear facilities, public interest related to radioactivity, etc. A number of specialized working groups like Life Sciences, Gamma-ray Spectrometry, Low-Level Measurement Techniques, Nuclear Data, etc. are coordinated to engage the particular needs of each branch. ICRM regularly collaborates with CCRI and hosts the scientific biannual International Conference on Radionuclide Metrology and its Applications as a platform for knowledge transfer under experts and to exchange new findings. (NIST, 2018)

Radionuclides are used in many different industries and applications, for example in material science and testing, life sciences, medicine, nuclear power, modelling and monitoring of environmental processes, dating, environmental fingerprinting, etc. NORM are widely used in the building industry and accumulate as a by-product in many other industries. Depending on the area of application (e.g. medicine, industry, environment, etc.), source materials can vary widely by activity concentration, origin (naturally occurring or artificially manufactured), chemical composition (liquid, solid, gaseous or a mixture thereof), etc. The recycling industry focuses on the detection and evaluation of man-made radionuclides such as ^{60}Co and ^{137}Cs which is rather straight forward and for which many reference materials exist (Maringer et al., 2017; Maringer and Ramer, 1997). The precise determination of activity concentrations in various natural sample material is of high importance and is particularly difficult, even for established laboratories due to the presence of ^{232}Th, ^{235}U, ^{238}U and their progeny (Wiedner et al., 2018b; Shakhashiro et al., 2010; Anagnostakis et al., 2004). These primordial radionuclides decay in a series of up to 14 subsequent α- and β-decays (omitting some stages with very low probability) with half-lives between 14.02 (6) $\cdot$ 10^{10} a (^{232}Th) and 300 (2) $\cdot$ 10^{-9} s (^{212}Po) until a stable lead isotope is formed. Only some of the radionuclides of the natural decay series emit γ-rays and can therefore be evaluated using γ-ray spectrometry. Figure 1.4 shows the uranium series as an example.

Many of the γ-rays are subject to true coincidence summing and a large number of spectral interferences occur between the many nuclides of the natural decay series (Baumgartner et al., 2017). An example of this is the ^{235}U peak at 185.720 (4) keV that is almost at the same energy as the ^{226}Ra peak at 186.211 (13) keV. Resolution of such peaks is usually difficult, if not impossible.

The detector background is often comprised of radionuclides of the natural decay chains surrounding the detector, thus sample activity must be distinguished from the background radiation and noise. Moreover, activity concentration in environmental samples is usually low and often does not significantly exceed the background. This leads to long measurement

Figure 1.4: Uranium decay series.

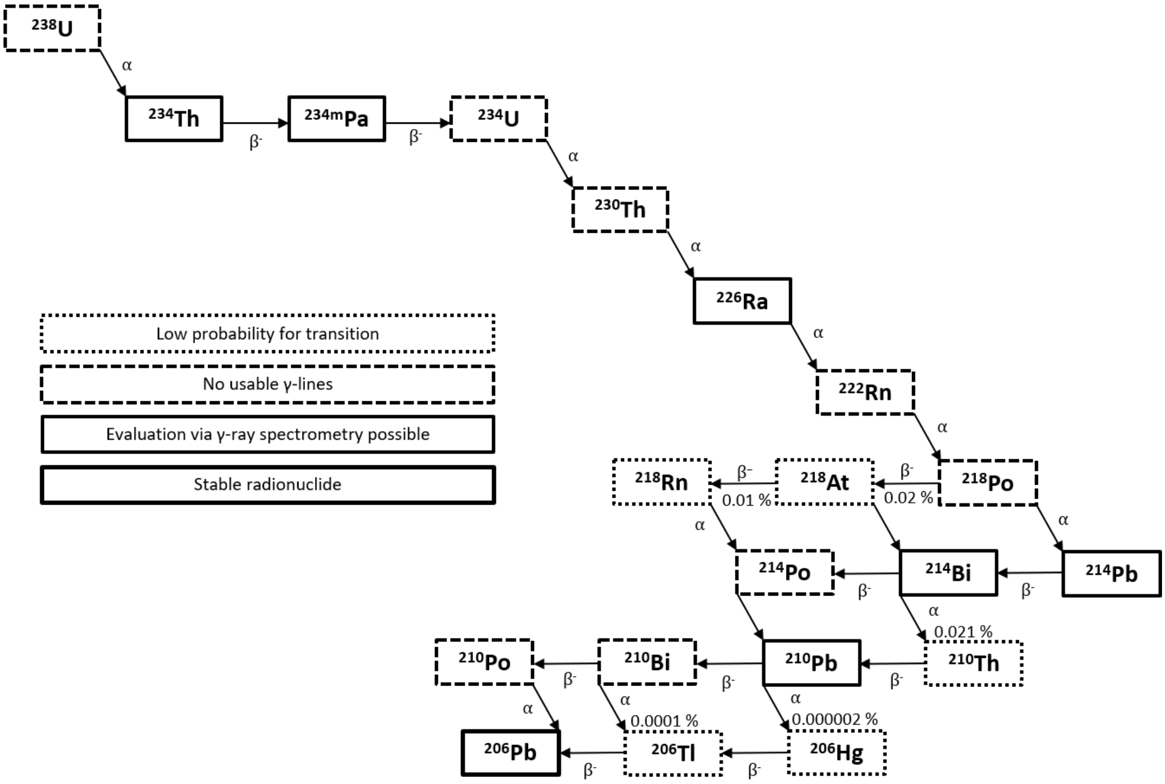

times in order to obtain significant results with sufficiently low uncertainties, especially if it is not possible to use specialized low-level detectors. In order to accurately and traceably quantify activity concentration in NORM samples via γ-ray spectrometry, robust calibration methods using NORM reference materials, and high methodical and metrological standards in the laboratory are necessary (Maringer, 2010).

1.3.3 Scientific contribution of this thesis to radionuclide metrology

This dissertation concentrates on the study and development of new and innovative methods in radionuclide metrology for the application in natural resources and life science research, particularly in the field of natural radioactivity. This involves an in-depth study of methods used to accurately determine activity concentrations in NORM samples, focusing mainly on γ-ray spectrometry and particular problems arising when using this method (Baumgartner et al., 2017). As a result of this study a traceable NORM has been produced, characterized and used in proficiency testing of specialized γ-ray spectrometry laboratories (Wiedner et al., 2018b). Furthermore, a feasibility study to test if artificial neural networks (ANNs) can be used to determine if NORM samples are above or below the exemption limit of 1 Bq/m^3, as laid down in Council Directive 59/2013/Euratom ("European Basic Safety Standards" – EU-BSS, Council of the European Union, 2013) has been conducted (Wiedner et al., 2017) and a comparison of currently used methods for the determination of ^{226}Ra activity concentration in drinking water samples has been undertaken (Wiedner et al., 2018a).

The papers presented in this dissertation are a result of research associated to EMRP and EMPIR projects MetroNORM and MetroRADON, and were presented at ICRM conferences.

1.4 Radiation protection against natural radiation

1.4.1 General radiation protection

Due to the fact that one source of natural radiation comes is soil and radioactive particles are continuously produced in the atmosphere, radiation protection against natural radiation can be difficult in comparison to other sources of exposure. For the other, artificial, sources, like those used in research, industrial or medical applications, radiation protection focusses on three main principles:

- Limiting time(s) of exposure: reduce time spent near the sources, limit number of exposures (e.g. number of radiological exams at the doctor).
- Increasing distance to the source of exposure: radiation dose follows the inverse-square law and is, therefore, significantly reduced with increasing distance to the source.
- Maximizing shielding of sources, or, if not possible, people: e.g. medical x-ray exams where radiation is required on certain body parts and others are shielded with lead gowns.

In addition to this, the so-called ALARA principle of radiation protection is applied: Radiation exposure should always be kept as low as reasonably achievable (ALARA) (NBS, 1954).

In the same vein, the International Committee on Radiological Protection (ICRP) proposes the principle of justification, optimisation and limitation. Every exposure situation must be justified, meaning that every change in radiation exposure should do more good than harm. Is an exposition justified, it has to be optimised so that the number of exposures, people exposed and individual doses are kept as low as reasonably achievable while taking the economic and societal situation into account. Additionally, in all planned exposure situations excluding medical exposures, dose limits as determined by regulatory authorities in agreement with international recommendations, should not be exceeded. (ICRP, 2007)

In many cases the application of these principles is not feasible with natural radiation exposure and it is impossible for the general population to completely avoid natural sources of exposure. Furthermore, sources of natural radiation cannot easily be controlled.

Where high levels of radiation are known to exist, these principles can be applied. It is comparatively easy to replace certain building materials that are known to have high levels or radioactivity with other building materials. At industrial sites it can be feasible to prevent the pile-up of large amounts of NORM waste. As an example the phosphate fertilizer production industry uses separation processes to separate the phosphate from phosphate rock. The remaining rock is then treated as waste but has a much higher activity concentration due to the extraction of the phosphate. Such waste pile-ups should be kept at a minimum and work processes should be designed in a way that workers spend as little time as possible near such areas of concentrated radioactivity.

As was shown in section 1.1, in most areas inhalation of radon gas constitutes the largest part (often more than half) of the radiation dose gained through natural sources of exposure for the general population.

1.4.2 The special role of radon

All of the three natural decay chains include radon isotopes (^{222}Rn, ^{220}Rn, ^{219}Rn and ^{218}Rn). Radon is a radioactive noble gas that is very volatile due to its gaseous nature. This characteristic can make determination of activity concentration in sample material difficult. ^{218}Rn only occurs in trace amounts and can be neglected on the grounds of its short half-life of 162.3 (12) μs. ^{220}Rn and ^{219}Rn have rather short half-lives of 55.8 (3) s and 3.98 (3) s, respectively, and sample equilibrium will be re-established within minutes after sealing the material in a radon-tight container. In case of the the longer lived ^{222}Rn (in the following simply called radon) with a half-life of 3.8232 (8) d, equilibrium is only re-established after about a month. Due to the aforementioned interference of the strongest γ-lines of ^{226}Ra and ^{235}U, and their low emission probabilities, radon daughters are often used to establish ^{235}U activity concentration. When radon gas escapes the measurement container, it affects the determination of activity concentration of the parent. Loss of radon happens if an unsuitable container material or form is chosen, leading to (depending on the used container, sometimes severe) underestimations of the activity concentration which, in turn, can lead to health and financial impacts.

Radiation protection of the population can be assured by modern, regionally appropriate building codes that consider the region's particular radon potential. Remedial action for older buildings, like the installation of ventilation systems that remove accumulated radon gas can be undertaken easily and at relatively low cost. Time limits and monitoring of accumulated effective dose for workers at industrial sites, in water treatment, mines, caves, radon spas, etc. are also options to ensure radiation protection. Radon and its impact on health will be discussed in more detail in chapter 3.

1.4.3 Scientific contribution of this thesis to radiation protection

In the framework of this dissertation a NORM material has been characterized and used in a proficiency test with 9 European laboratories concerned with radioactivity measurements and environmental monitoring by γ-ray spectrometry (Wiedner et al., 2018b). It was shown that even established specialized laboratories have problems with the measurement of ^{226}Ra due to radon loss and values diverged up to 35 % from the reference value. Challenges of γ-ray spectrometry of NORM samples will be discussed in more detail in chapter 2. The study contributes to a better understanding of the interferences of γ-lines and gives recommendation on which lines should be preferred for the evaluation of activity concentration which enables the user to more accurately determine activity concentrations in (environmental) samples. Furthermore, a method to quickly and easily check sample containers for radon leakage and quantify said leakage, is proposed. Additionally, a quick method for evaluating if certain NORMs are above or below the exemption limit laid down by the EU Basic Safety Standards using Artificial Neural Networks is proposed. As soon as the system is set up, no specialized knowledge in γ-ray spectrometry is required by the user.

The inhalation of radon gas poses a health risk. α-particles from radon and its progeny damage the delicate cells of the bronchial epithelium, playing a large role in the development of lung cancer. While the inhalation of radon gas in open air is of no particular consequence, radon gas can accumulate in unventilated spaces like buildings (e.g. dwellings and workspaces), in mines, and natural formations such as caves. Accurate establishment of radon activity concentrations is of utmost importance for workers and the public, and reliable measurements at low activity concentrations are necessary in order to quantify the risk and propose remedial actions. As a part of this dissertation, an ionisation chamber measurement method for radon activity concentration in drinking water was set up and verified against Austria's national standard.

1.5 Decay data

All decay data used in this thesis are the values recommended by the Decay Data Evaluation Project (DDEP). The DDEP is an international collaboration formed in 1995 and includes members of dedicated research facilities, National Metrology Institutes (NMIs) and Designated Institutes (DIs) such as BNM-CEA/LNHB (France), PTB (Germany), INEEL (USA), KRI (Russia), LBNL (USA), NPL (United Kingdom), CIEMAT (Spain), CNDC (China), NIM (China), NIST (USA) and IFIN-HH (Romania) who evaluate nuclear and atomic data, such as half-life, decay mode and branchings, radiation energies and emission probabilities with the objective of providing carefully produced recommended data for research and detector calibrations (Nucleide, 2018). The recommended values are also published as *Monographie BIPM-5 – Table of radionuclides* by the International Bureau for Weights and Measures (Bureau International des Poids et Mesures – BIPM), see BIPM (2018b) for details.

2 Novel metrological methods for the measurement of naturally occurring radioactive materials

2.1 Evaluation of activity concentration and study of particular problems occurring in γ-ray spectrometry of NORM samples

Knowledge about activity or activity concentration in a natural material significantly influence decisions about waste disposal, re-usage of material, safety installations, exposure time of workers, transport procedures, etc. It is, therefore, of utmost importance to carefully and accurately establish activity concentrations.

The detection and evaluation of artificial (man-made) radionuclides such as ^{60}Co and ^{137}Cs is an essential part of the recycling industry. Naturally occurring radionuclides are often only included as part of the background (Maringer, 2016). While the detection and assessment of activity concentrations of these artificial radionuclides is relatively straight forward and usually not problematic (Brettner-Messler et al., 2007), this is much more complicated for the naturally occurring radionuclides.

Activity concentrations of NORM samples are usually evaluated using low-level γ-ray spectrometry as it is a versatile and non-destructive method with which several radionuclides can be evaluated at the same time (Mantero et al., 2015). However, there are a few problems that arise when using γ-ray spectrometry which necessitate that spectral deconvolution requires expert knowledge.

Firstly, not all photons will deposit their whole energy in the active detector volume. Secondly, detector resolution is finite and photons with energies close together can be summarized in the same energy window, leading to them being indistinguishable in the spectrum. To alleviate this issue, high purity germanium semiconductor detectors with relatively high energy resolutions are commonly used. Finally, independent photons that interact with the detector medium in a time shorter than the detector's resolving time are counted as a single photon with the combined energy of both photons (summing). While the count-rate dependent random summing is usually witnessed quite seldom in the analysis of environmental samples due to the commonly very low count rates, true coincidence summing (TCS), which is the summing of γ-rays that are emitted nearly simultaneously from a nucleus, is quite common in environmental samples (Živanović et al., 2012; Gilmore, 2008). Examples for radionuclides that show TCS are ^{234}Th, ^{234m}Pa, ^{214}Pb, ^{214}Bi ^{235}U, ^{231}Pa, ^{228}Ac, ^{212}Bi, ^{208}Tl and ^{40}K. The last two phenomena were studied by Baumgartner et al., 2017 which was conducted within the MetroNORM project and is a part of this dissertation. Table 2.1 gives an overview of the evaluated radionuclides.

In addition to the difficulties related to detector resolution and resolving time there are a few other problems that arise specifically when dealing with NORM samples.
As mentioned before, there are many different γ-lines present in NORM spectra due to the presence of ^{232}Th, ^{235}U, ^{238}U and their progeny. Many of the γ-lines have very low emission probabilities, are subject to true coincidence summing and a large number of spectral interferences occur between the many nuclides of the natural decay series (Baumgartner et al., 2017). Resolution of such peaks is usually difficult, if not impossible. Activity concentration in environmental samples is usually low and often does not significantly exceed the background. This leads to long measurement times in order to obtain significant results with sufficiently low uncertainties, especially if it is not possible to use specialized low-level detectors. In addition to that the detector background is often comprised of radionuclides of the natural decay chains that surround the detector and can emanate from building materials. Since sample activity in NORM samples is usually quite low, it must be distinguished from this background. This necessitates the use of special shielding methods that can range from simple lead shields, to low-level lead shields made from low activity lead, to special low-level laboratories with climate control and air filters (Aiginger et al., 1986).
Moreover, radioactive equilibrium may also be disturbed due to natural events or processing of the material (Anagnostakis et al., 2004; Živanović et al., 2012), making it impossible to use the activity concentration of the daughter nuclides to establish activity concentration for parents that have no or unsuitable γ-lines.

2.2 Detector calibration

NORM samples have a wide variety of composition, density and physical form, and are often quite heterogeneous. Therefore, a robust efficiency calibration is necessary in order to correctly quantify the activity concentration in the sample (Wiedner et al., 2018b). This calibration accounts for the mainly energy- and density-dependent self-absorption of the sample, as well as the absorption in the sample container. It also takes geometric effects such as sample geometry and height, and sample-detector configuration into consideration. Efficiency calibration can be achieved using physical standards or mathematical models (Monte Carlo simulation).

Table 2.1: Evaluation of particular γ-ray spectrometry problems on the basis of selected NORM samples including the calculation of interference contributions, a comparison of BIPM (Nucleide, 2016) and IAEA (IAEA, 2016) γ-emission intensities for selected natural radionuclides as well as radon leakage effects.

Nuclide	Gamma line keV	Spectral interferences and radon leakage	Gamma emission intensities (BIPM) %	Gamma emission intensities (IAEA) %	Deviation due to choice of gamma intensities %	Deviation due to spectral interferences and radon leakage (except true coincidence summing) %			
						Tuff	TiO_2	Ion exchange resin	Filter residue
^{234}Th	63.3	TCS; interference with the 62.9 keV / 0.0164 (28) % γ-line of ^{234}Th and with the 63.8 keV / 0.259 (15) % γ-line of ^{232}Th	3.75 (8)	3.7 (4)	1.4	7.7	–	0.4	–
$^{234\,m}$Pa	1001.0	TCS	0.847 (8)	0.842 (8)	0.6	0.0	–	0.0	–
^{230}Th	67.7	–	no data available	0.38 (3)		0.0	–	–	0.0
^{226}Ra	186.2	Interference with the 185.7 keV / 57.0 (3) % γ-line of ^{235}U and with the with the 186.1 keV / 0.0088 (7) % γ-line of ^{230}Th	3.555 (19)	3.64 (4)	−2.3	104.3	0.0	107 kBq/kg[b]	1 Bq/kg[b]
^{214}Pb	295.2	TCS, insignificant interference with the 296 keV / 79 (10) % γ-line of ^{210}Tl	18.414 (36)	18.42 (4)	0.0	−0.6	−0,6	–	−0.6
^{214}Bi[a]	609.3	TCS	45.49 (19)	45.49 (16)	0.0	−0.6	−0.6	–	−0.6
^{214}Bi[a]	1120.3	TCS	14.91 (3)	14.92 (3)	−0.1	−0.6	−0.6	–	−0.6
^{210}Pb	46.5	Interference with the 46,4 keV / 0.19 (1) % γ-line of ^{231}Pa	4.252 (40)	4.25 (4)	0.0	0.0	0.0	–	40.7
^{235}U	163.4	TCS; interference with the 163.1 keV / 0.156 (5) % γ-line of ^{231}Th	5.08 (3)	5.08 (6)	0.0	3.1	–	3.1	–
^{235}U	205.3	TCS; interference with the 204.0 keV / 0.114 (8) % γ-line of ^{228}Ac	5.02 (3)	5.02 (6)	0.0	41.7	377 Bq/kg[b]	0.0	–
^{231}Pa	283.7	TCS	1.72 (3)	1.70 (10)	1.2	–	–	–	0.0
^{227}Th	256.2	–	6.8 (4)	7.0 (6)	−2.9	–	0.0	–	0.0
^{223}Ra	323.9	–	4.06 (8)	3.99 (9)	1.8	–	0.0	–	0.0
^{228}Ac	911.2	TCS	26.2 (8)	25.8 (4)	1.6	0.0	0.0	–	–
^{212}Pb	238.6	–	43.6 (5)	43.6 (5)	0.0	0.0	0.0	–	–
^{212}Bi	727.3	TCS; interference with 726,9 keV / 0.68 (8) % γ-line of ^{228}Ac	6.65 (4)	6.67 (9)	−0.3	8.4	9.9	–	–
^{208}Tl	583.2	TCS; interference with the 583.4 keV / 0.120 (11) % γ-line of ^{228}Ac	85.0 (3)	85.0 (3)	0.0	0.3	0.3	–	–
^{40}K	1460.8	Interference with 1459.1 keV / 0.87 (5) % γ-line of ^{228}Ac	10.55 (11)	10.66 (13)	−1.0	1.1	1405 Bq/kg[b]	–	–

[a] Corrected for the radon leakage regarding the calculation of the ^{226}Ra activity concentration.

[b] The activity concentration of the target nuclide is lower than the MDA. Therefore, the contribution of the interfering nuclide can cause a false positive detection. The reported activity concentration values represent such false positive values of the target nuclides. These values were calculated for the applied detector system with use of the intensities of the target nuclides.

2.2.1 Mathematical efficiency calibration

When performing efficiency calibrations on a detector using Monte Carlo codes, mathematical models are used to calculate detection efficiencies. To achieve a reliable result, exact knowledge of the used detector system, sample composition and geometry, and measurement set-up are necessary. Manufacturer information is often not sufficiently reliable or cannot be translated appropriately to the simulation model (Moser and Maringer, 2015; Maleka and Maučec, 2005; Peyres and García-Toraño, 2007; Hurtado et al., 2004; Padilla Cabal et al., 2010; J. C. Hardy and V. E. Iacob and M. Sanchez-Vega and R. T. Effinger and P. Lipnik and V. E. Mayes and D. K. Willis and R. G. Helmer, 2002) and chemical analysis of the sample is often not feasible or possible.

The main advantage of using mathematical models is their versatility. Once the detector model is validated, efficiencies for all materials, geometries and photon-energies can be calculated with very good agreement to experimental values (Moser and Maringer, 2015, Peyres and García-Toraño, 2007 and Šolc et al., 2015). An alternative to using mathematical models is to calibrate the detector system with traceable certified reference materials. After calibration, the activity of an unknown source can be determined through comparison with the reference material of known activity concentration. This comparison is only valid, if the unknown sample and the calibration material and geometry, and measurement geometry of both sources are (ideally exactly) the same or sufficiently similar (Gilmore, 2008).
Mathematical efficiency calibration is of special interest for laboratories that deal with many different sample materials and measurement geometries, since certified reference materials can be very expensive and stability of the material is usually only certified for a certain time frame. In addition to that, reference materials containing radionuclides with short half-lives decay too much or structurally disintegrate until they are no longer usable.

2.2.2 Reference materials

For laboratories that routinely analyse the same material in a standard geometry, the use of certified reference materials can be easier to use and cheaper in the long term. Since there are many different requirements to be met for each application and laboratory, there is a general need for certified NORM reference materials in science and industry with sufficiently low uncertainties to achieve traceability, validate methods and calibrate instruments (Maringer, 2016; Maringer et al., 2017; Harms and Gilligan, 2010).
Reference materials can basically be divided into two groups: reference materials that have a simple matrix, such as water, and are artificially spiked with a known activity, and reference materials consisting of complex matrices. Depending on application and origin these more complex reference materials can be made from material that is naturally rich in radioactivity (NORM, Wiedner et al., 2018b; Merešová et al., 2012; Shakhashiro et al., 2011), technologically enhanced (TENORM, e.g. through concentration of radionuclides due to processing

of material or activation in a nuclear reactor (Harms and Gilligan, 2010)) or by artificial spiking of a material (Tzika et al., 2016). Since it is possible to produce spiked reference material in a controlled laboratory environment, traceability is usually easily ensured for the spiked materials. The downside is that the matrix of the material is often quite different from the analysed material in terms of composition and density (Larijani et al., 2017). Simple transfer of efficiency calibrations conducted with reference material can, depending on the composition and density of the unknown sample, lead to wrong results due to neglect of factors like self-absorption.

In the past, the Austrian Federal Office of Metrology and Surveying (BEV) has organised and evaluated a number of comparison exercises with ^{57}Co, ^{60}Co and ^{137}Cs in water and spiked natural matrices like diaphanous earth and quartz (Brettner-Messler et al., 2007; Maringer and Ramer, 1997). Laboratory proficiency in general was high for these “standard radionuclides” and deviations from the reference value were generally below 10 %. The evaluation of activity concentrations for samples with densities $\neq 1$ and radionuclides of the natural decay chain is much more complex.

2.3 Production and characterization of a traceable NORM material and its use in proficiency testing of gamma-ray spectrometry laboratories

Part of the presented work is the production and characterization of a NORM material traceable to the national standard for activity of the Austrian Federal Office of Metrology and Surveying (BEV), Austria’s national metrology institute. The aim was to produce a realistic reference material that is close to the samples usually evaluated by laboratories concerned with environmental monitoring in terms of physical properties and activity concentration. The material was manufactured and characterized, then used in a proficiency test exercise of 9 European laboratories. ISO 17025 standard requires laboratories to use reference materials to ensure traceability to national or international standards and for calibration purposes. Furthermore, laboratories operating under the requirements of ISO 17025 have to demonstrate and monitor the quality of their results by regularly participating in proficiency tests or intercomparison exercises (ISO/IEC 17025:2017, 2017).

A natural, non-spiked NORM made of quartz sand with elevated levels of radioactivity due to its usage in the treatment of drinking water was chosen. Sand is commonly found and used as a building material in many parts of the world (Anagnostakis et al., 2004). In this case, the sand was taken from the back flush of a drinking water treatment facility in Lower Austria, a region where the water contains significantly elevated levels of ^{226}Ra due to the predominant occurrence of magmatite, granite and clastic sediments such as clays, gravel, and sand. At the treatment facility, drinking water is oxygenated and passed through a bed of quartz sand. The quartz sand acts as a filter in which hydroxides of iron, manganese and radium precipitate. The result of this process is a quartz sand rich in ^{226}Ra. The material was homogenized, characterized, and used in a proficiency test of 9 European laboratories concerned with the measurement of radioactivity (Wiedner et al., 2018b).

Preliminary γ-spectrometric results at the homogenization stage showed that the samples were quite heterogeneous. Upon investigation it was concluded that the very fine grain size fraction ($<$ 0.56 mm) is the cause of the inhomogeneity. Measurements showed that the activity concentration in this fraction of the sample material is higher by a factor of up to 9 when compared to the activity concentration in the 0.8 mm – 2 mm grain size fraction (see Table 2.2).

Table 2.2: Comparison of activity concentration of two grain size fractions of one test sample.

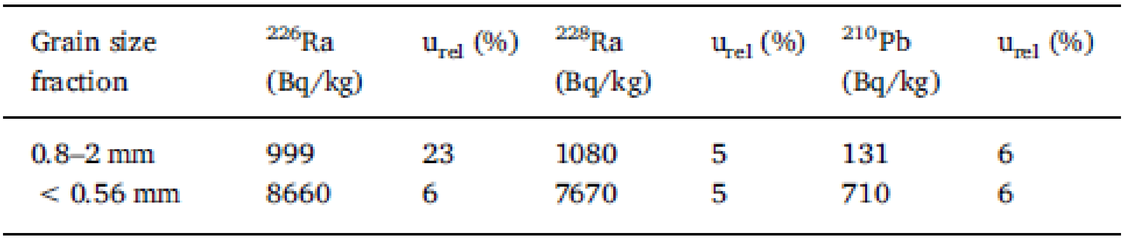

Grain size fraction	^{226}Ra (Bq/kg)	u_{rel} (%)	^{228}Ra (Bq/kg)	u_{rel} (%)	^{210}Pb (Bq/kg)	u_{rel} (%)
0.8–2 mm	999	23	1080	5	131	6
< 0.56 mm	8660	6	7670	5	710	6

Since the dust-like grain size fraction $<$ 0.56 mm is also the most volatile fraction and prone to moving around in the sample container, causing instability of the material, it was decided to sift the material again and only use the grain size fraction of 0.8 mm – 2 mm in the final material. Additionally, removing the fraction with high activity concentration has the positive side effect that the material can easily be shipped via courier without any radiation protection concerns. It was decided against finely grinding the material in order to increase sample homogeneity and keep the material's matrix as realistic as possible for use in smaller laboratories that do not have the resources (time and equipment) for complex sample preparation.

Sample homogeneity was assessed by comparing the count rates of strong emission lines like the 46.5 keV line of ^{210}Pb, 1460.8 keV line of ^{40}K, 186.2 keV line of ^{226}Ra as well as the 583.4 keV and 911.2 keV lines of ^{228}Ac for different grain size fractions.

Five samples were excluded from the exercise as they were deviating too much from the mean, but most samples were deemed sufficiently homogeneous (Figure 2.1). Better homogeneity could be ensured by finely grinding the quartz sand but would also result in a less "realistic" reference material since grinding would destroy the material's natural matrix.

The reference values of the NORM radionuclides were then established traceable to the national standards of Austria and Germany as 0.605 ± 0.024 Bq/g ^{40}K, 1.003 ± 0.015 Bq/g ^{226}Ra, and 0.806 ± 0.013 Bq/g ^{228}Ra (105 °C dry weight basis) via γ-ray spectrometry. Laboratories participating in the proficiency test were tasked to analyse the material using γ-ray

Figure 2.1: Results of the homogeneity testing for the quartz sand samples (grain size fraction (0.8 mm – 2 mm) for ^{40}K, ^{226}Ra and ^{228}Ra combined, measured directly and via its progeny. The image shows the weighted mean of the relative deviations of all considered energy lines of the respective radionuclide for each sample. The final uncertainties of the respective sums of relative deviations were calculated using Gaussian propagation of uncertainties.

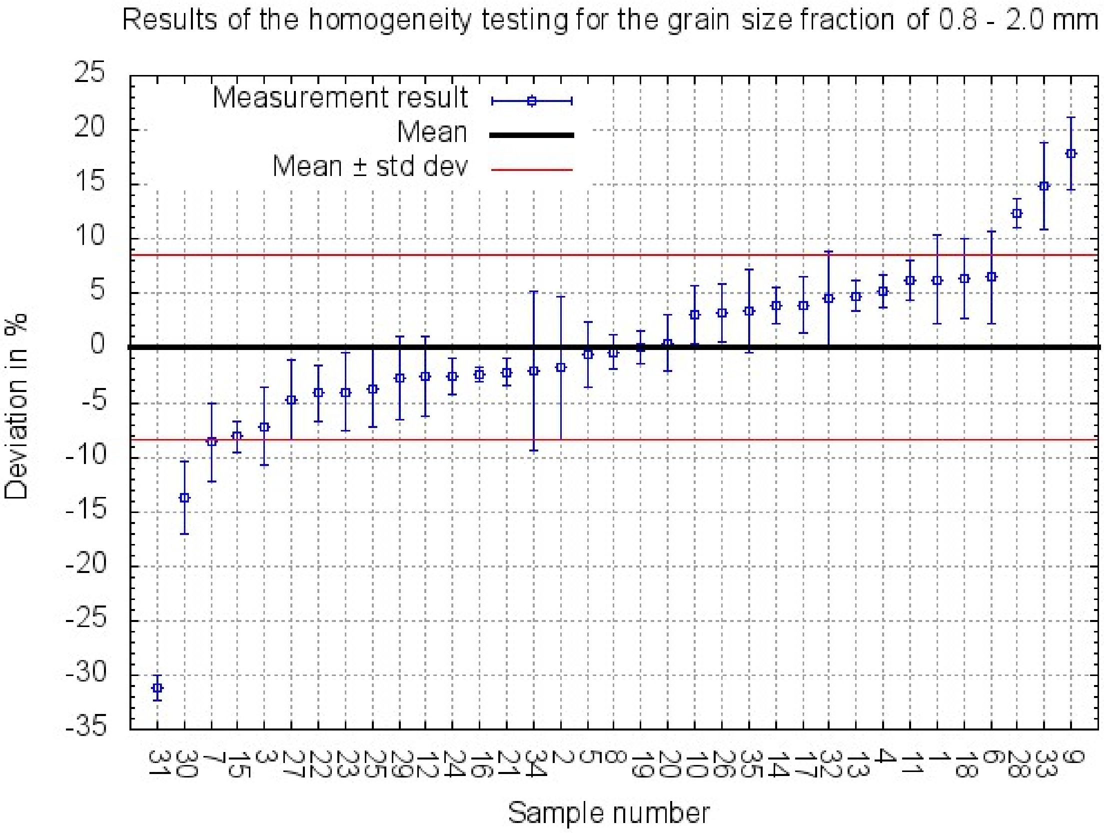

spectrometry and to report their results for these three radionuclides.

Proficiency of the participating laboratories in the evaluation of naturally occurring radionuclides is generally acceptable but leaves room for improvement. One reason for that may be that approximately half the participating laboratories had only little experience in analysing naturally occurring radionuclides. The results of the NORM proficiency test showed the expected behaviour of larger deviations from the mean and reference value, and a larger spreading of results compared to proficiency tests using simple matrices and anthropogenic radionuclides like ^{57}Co, ^{60}Co and ^{137}Cs. Internal comparison exercises conducted in the framework of the MetroNORM project between established laboratories showed the same behaviour, and it is even evident in CCRI(II)[1] supplementary comparisons (Shakhashiro et al., 2010). Nonetheless, in case of ^{40}K and ^{228}Ra the mean values of the participant's results show sufficient agreement with the reference value. In case of ^{226}Ra the participant's

---

[1] Bureau International des Poids et Mesures (BIPM, International Bureau of Weights and Measures) Consultative Committee for Ionizing Radiation – Section II: Measurement of Radionuclides

mean value is lower than the reference value by approximately 11 %. This can be attributed to the aforementioned difficulties with the evaluation of the strongest γ-line of ^{226}Ra and will be discussed in more detail in the next section.

Figures 2.2 to 2.4 show the detailed results. A Grubbs outlier test (Grubbs and Beck, 1972) was performed on the results. Laboratory 3's results for ^{40}K and ^{228}Ra were classified as outliers and, therefore, eliminated from the evaluation.

Figure 2.2: Outlier-corrected results of the proficiency test for ^{40}K.

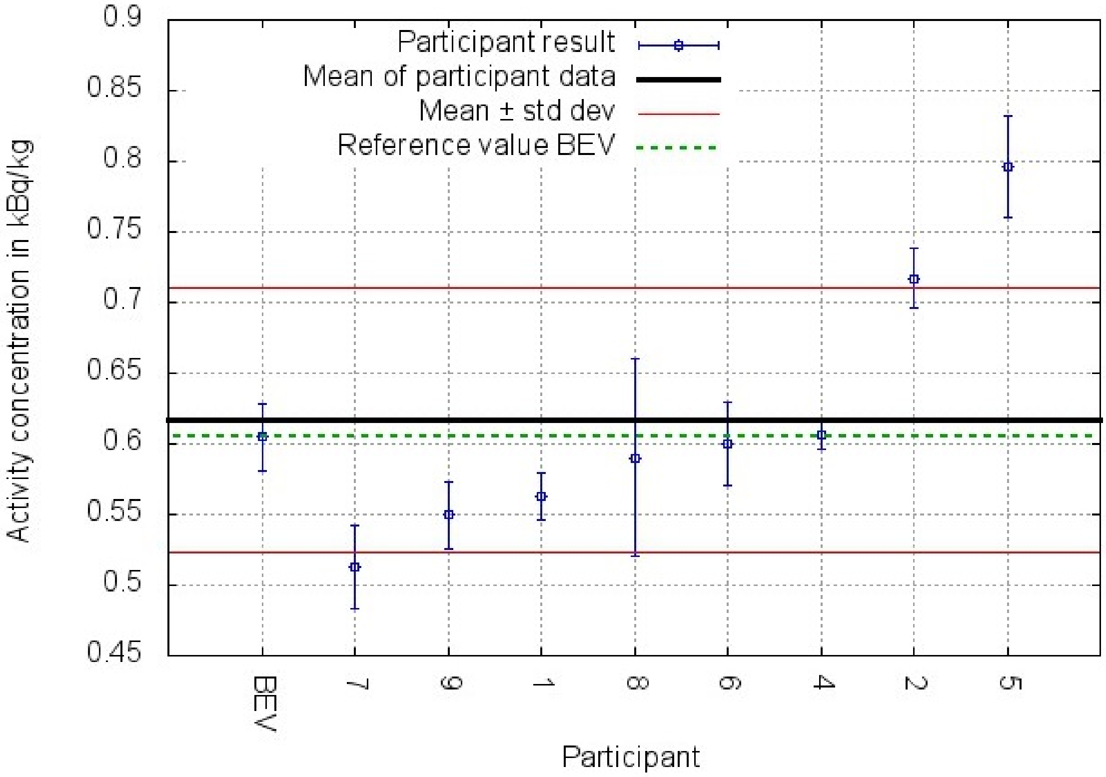

Figure 2.3: Outlier-corrected results of the proficiency test for ^{226}Ra.

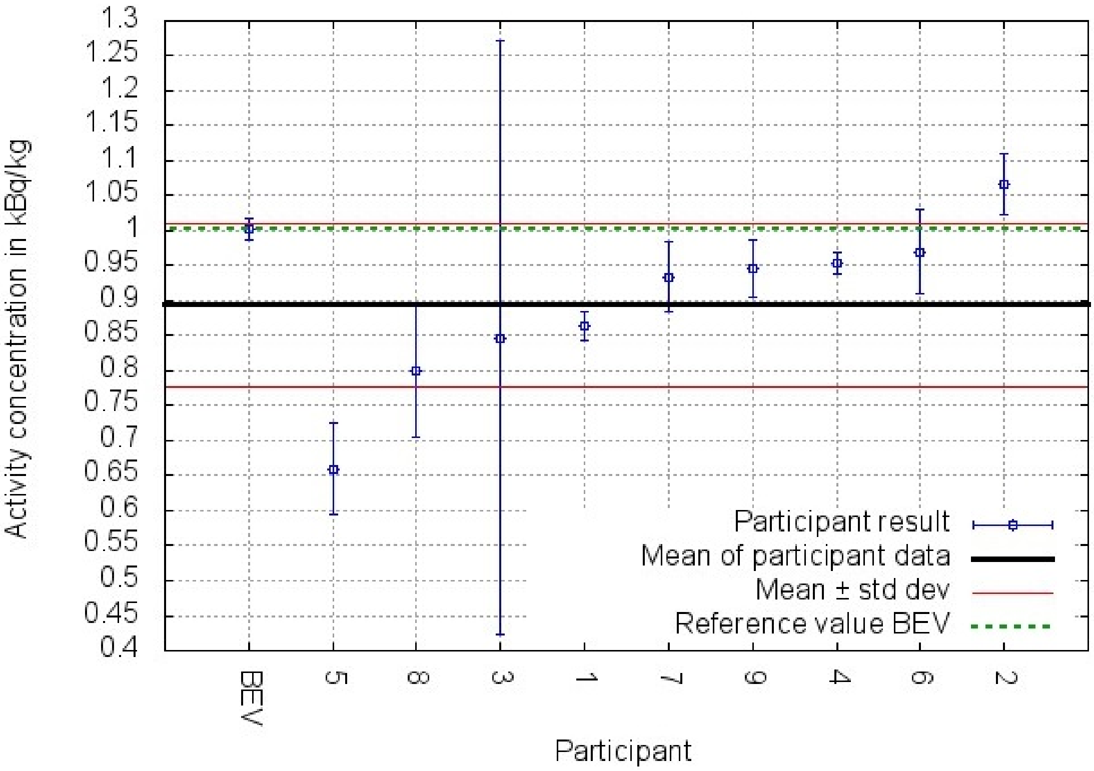

Figure 2.4: Outlier-corrected results of the proficiency test for ^{228}Ra.

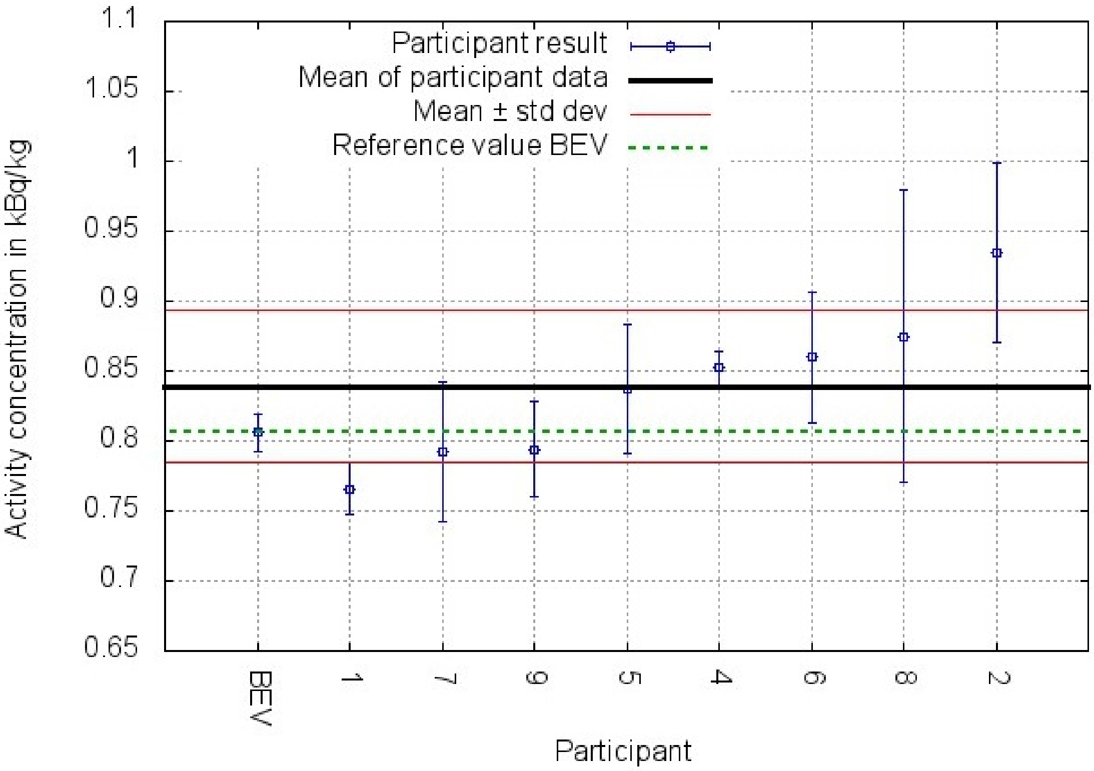

2.4 γ-ray spectrometry of ^{226}Ra

^{226}Ra is a radioactive daughter of ^{238}U. The radionuclide decays via α-dacay into ^{222}Rn and returns to ground state via emission of five γ-rays with quite low emission probabilities. The strongest γ-line can be found at 186.211 (13) keV with an emission probability of only 3.555 (19) % (Nucleide, 2018). Most of the time radionuclides from all three natural decay chains are present in samples of natural origin. ^{235}U has its strongest γ-line at 185.720 (4) keV with an emission probability of 57.0 (3) %. Since both peaks are very close together, it is very difficult to separate them. In theory, it is possible to perform a peak stripping operation and use the other ^{235}U peaks to estimate the contribution to the common peak but high uncertainties must be applied since emission probabilities are quite low and the other lines themselves may be subject to interference or TCS, rendering most ^{226}Ra results unsatisfactory. If one is sure that the natural isotope ratio and radioactive equilibrium between ^{226}Ra and its mother ^{238}U is undisturbed, the contribution to the peak can be calculated mathematically using the half-lives and emission probabilities. (Gilmore, 2008)

In an undisturbed sample ^{226}Ra is in secular equilibrium with its daughters ^{214}Bi and ^{214}Pb due to its comparatively long half-live ($t_{1/2}$ (^{226}Ra) = 1600 (7) a, $t_{1/2}$ (^{214}Bi) = 19.8 (1) min, $t_{1/2}$ (^{214}Pb) = 26.916 (44) min). Once it has been established that the sample is in equilibrium, interference-free (or corrected) γ-lines of the daughter nuclides can be used to establish ^{226}Ra activity concentrations. Due to the fact that ^{226}Ra will transition to gaseous ^{222}Rn before ^{214}Bi or ^{214}Pb is formed, it is necessary to ensure that the sample container is radon tight. Depending on the used sample container and its radon tightness, non-negligible amounts of radon gas can leave the measurement container leading to (sometimes severe) underestimations of ^{226}Ra activity concentration. Depending on sample composition and geometry, filling height of the sample container, container material and container lid, errors of 15-20 % are common (Mauring and Gäfvert, 2013).

From the results of the proficiency test it is apparent that many of the participating laboratories had problems with the correct determination of the activity concentration of ^{226}Ra. Figure 2.5 shows the relative deviations of the participant's results. It can be seen that the mean value of the participants lies approximately 11 % below the reference value. This is due to the fact that in many cases ^{226}Ra activity concentration was deduced using post-radon radionuclides while using non-radon-tight sample containers and/or not waiting sufficiently long for equilibrium to establish.

Figure 2.5: Outlier-corrected results of the proficiency test for ^{226}Ra giving the deviation from the reference value in %.

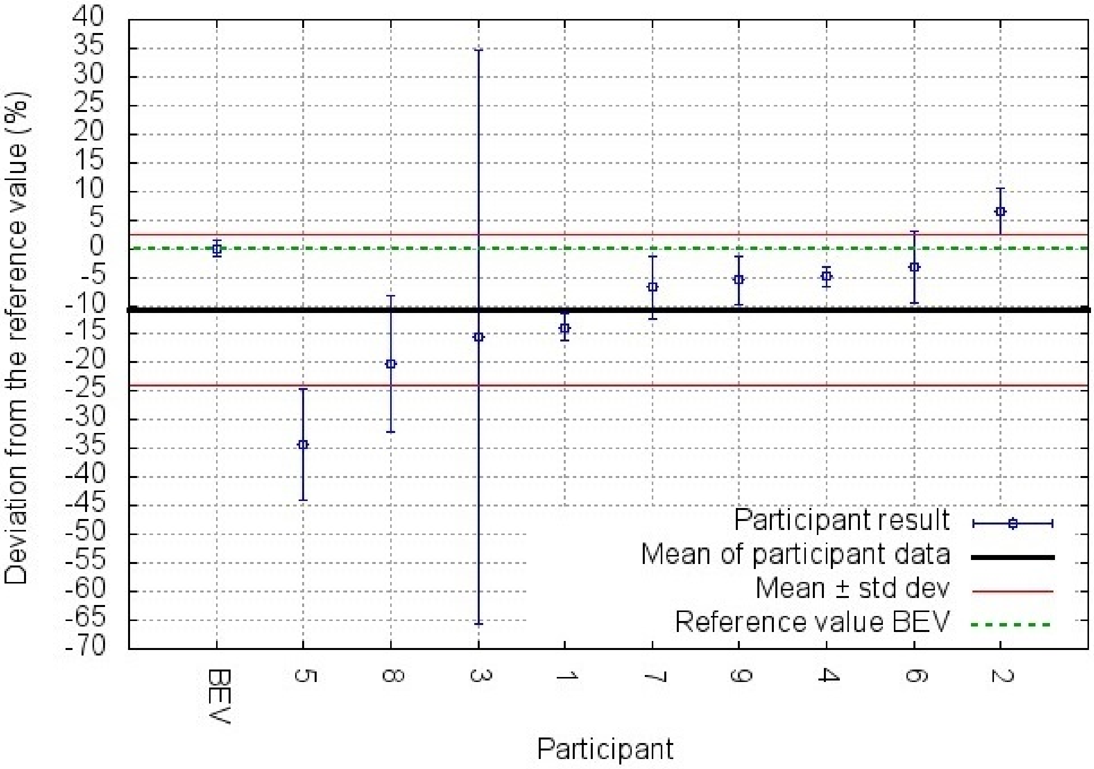

Figure 2.6: Results of the proficiency test for ^{226}Ra giving the deviation from the reference value in % for the more experienced laboratories.

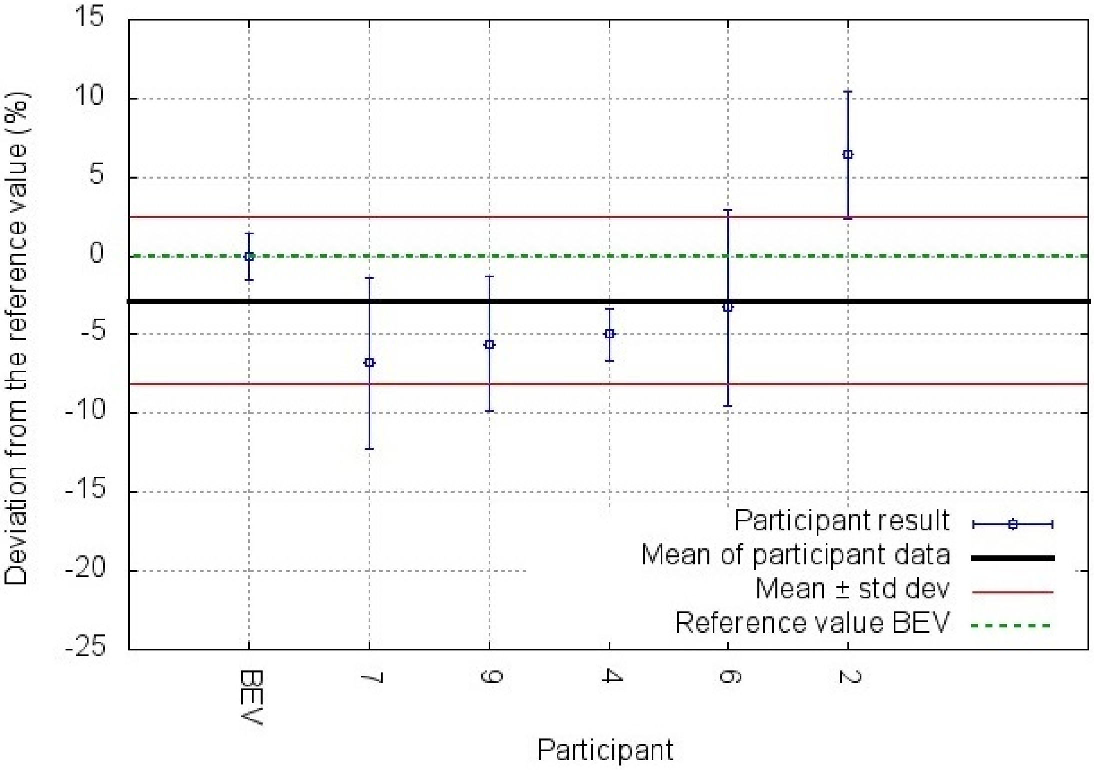

An easy solution to this problem is to use radon tight sample containers or enclose standard sample containers in radon tight material. One commonly used method is to vacuum-seal standard measurement containers in thin aluminium lined bags. This technique yields solid results and is time and cost efficient. Completely filling the sample container is also important to reduce radon exhalation. (Mauring and Gäfvert, 2013).

Figure 2.6 shows the relative deviations using only results of laboratories more experienced with the evaluation of naturally occurring radionuclides. It can be seen that the deviation of the average activity concentration from the reference value is reduced to approx. 3 %.

2.5 A simple and sensitive method to assess ^{222}Rn leakage from sample containers

As a part of this thesis, a simple and sensitive method to assess ^{222}Rn leakage of sample containers was proposed (Baumgartner et al., 2017). A sample container and a ^{222}Rn in air measuring device are placed inside a desiccator to measure the ^{222}Rn build-up curve. For this study a Canary Pro measuring device, a small hand-held passive diffusion chamber used to monitor the leaked radon, was placed in a desiccator together with two samples. Canary Pro uses silicon photo-diodes to both count and measure the energy of alpha particles resulting from the decay of radon gas (Gammadata Instrument AB, 2018). The equilibrium activity concentration in the desiccator is a measure for the radon tightness of the sample. Radon tightness of the desiccator was verified through measurements inside a radon calibration barrel of Genitron Ltd. One of the samples was a polystyrene container completely filled with certified soil (C_{max}=220 kBq/m^3), the other half-filled with ^{226}Ra standard solution (C_{max}=1.442 MBq/m^3). C_{max} describes the theoretical maximum activity concentration in the desiccator corresponding to 100 % container leakage. Due to the large void-space in the half-filled sample and the bad radon retention of the liquid, a high radon exhalation rate is expected. Figure 2.7 shows the results fitted with a two parameter exponential function to estimate container leakage. The results show an asymptotic ratio of C/C_{max} of approximately 0.6 % for the soil sample and a ratio of approximately 0.7 % for the half-filled liquid sample. Comparing the results to Mauring and Gäfvert (2013) who report radon leakage of up to 20 % suggests that not only the material of the used sample containers has a large influence on radon leakage but also their closing mechanism. The beakers used in Mauring and Gäfvert (2013) all had screw on lids with relatively coarse threading while the container tops used for this study were smooth and mounted by simply sliding on which provides the sample container with a relatively tight seal. Mauring and Gäfvert (2013)'s results suggested that a large portion of the leakage takes place at the cracks between container and lid which was tightly closed in Baumgartner et al. (2017).

Figure 2.7: Relative ^{222}Rn build-up curves inside a desiccator resulting from leakage of the sample container. The ratio C/C$_{max}$ is given with the combined standard uncertainty ($k = 1$). The left graph shows the sample container filled completely with certified soil. The right shows the sample container half-filled with a certified ^{226}Ra standard solution.

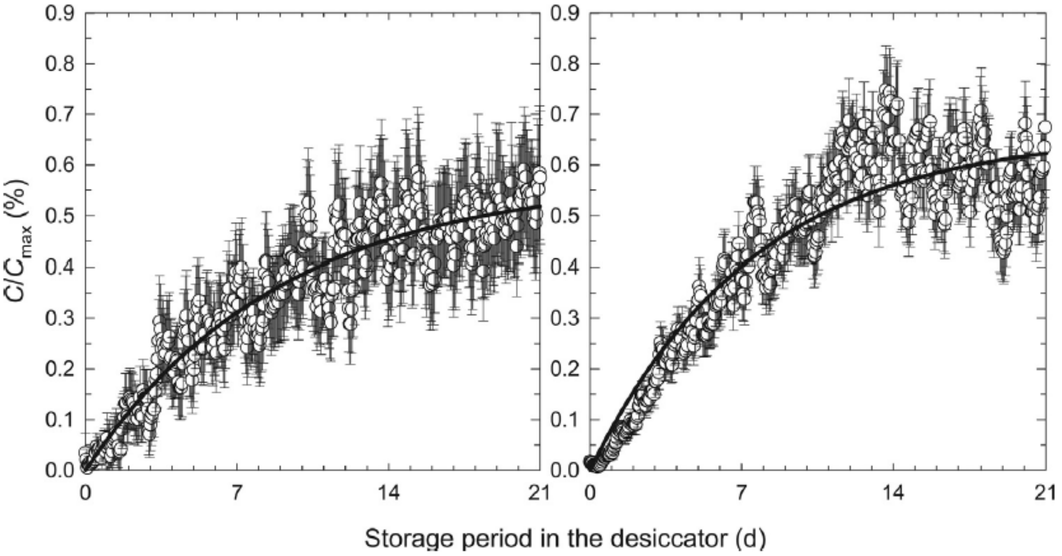

2.6 Innovative Application of Artificial Neural Networks for evaluation of NORM

As can be seen from the above chapters, the evaluation of activity concentration by γ-ray spectrometry is a complicated process that requires expert knowledge. Furthermore, quick and reliable methods are needed to determine activity concentration in raw materials and waste, e.g. at industrial sites (Maringer, 2016). As part of this thesis a feasibility study (Wiedner et al., 2017) was undertaken to test if artificial neural networks (ANNs) can be used to determine if NORM samples are above or below the exemption limit of 1 Bq/m^3 (as laid down in Council Directive 59/2013/Euratom (Council of the European Union, 2013)) from a raw γ-spectrum, thus avoiding the complex analysis associated with spectral deconvolution. ANNs are very versatile and can handle imprecise and noisy information. Once the ANN is set up, no detector calibration or specialized end-user knowledge is required. The final ANN serves as an alternative detector calibration and can function like a black box for the end-user. The following details how an ANN was created that can analyse six different materials and the main challenges that come with training artificial neural networks. The study was undertaken in cooperation with Centro de Investigaciones Energéticas, Medioambientales y Tecnológicas (CIEMAT).

ANNs are mathematical software tools that can learn from training datasets and apply that "knowledge" to unknown problems. In order to do that, ANNs imitate the way the human brain works. The human brain constitutes of a number of biological neurons that each generate a signal of a certain intensity and synaptic feeding strength. These signals are fed into another neuron via dendrites and axons. If the signal strength is below a certain threshold, the neuron does not compute the input. If it is above the threshold, the neuron computes the inputs and generates a signal. That signal can then serve again as an input to other neurons (Basheer and Hajmeer, 2000). With ANNs this mechanism is copied on a computer basis. ANNs consist of a number of computing nodes that represent the neurons and connections between them. Each connection has an assigned connection weight (synapses) and threshold (representing activity in the soma). The ANN's knowledge is stored in the connection weights which have to be determined using representative training data.

ANNs consist of an input and an output layer and can include one or more hidden layers. Each layer contains a number of computing nodes. A transfer function, often a non-linear or sigmoidal function, is applied to the weighted sums of each node and represents the significance of the information input. Figure 2.8 gives a schematic representation of how ANNs work.

Figure 2.8: Left: Schematic representation of how basic processes work in human brains (adapted from Basheer and Hajmeer, 2000). Right: Schematic of ANN layer structure.

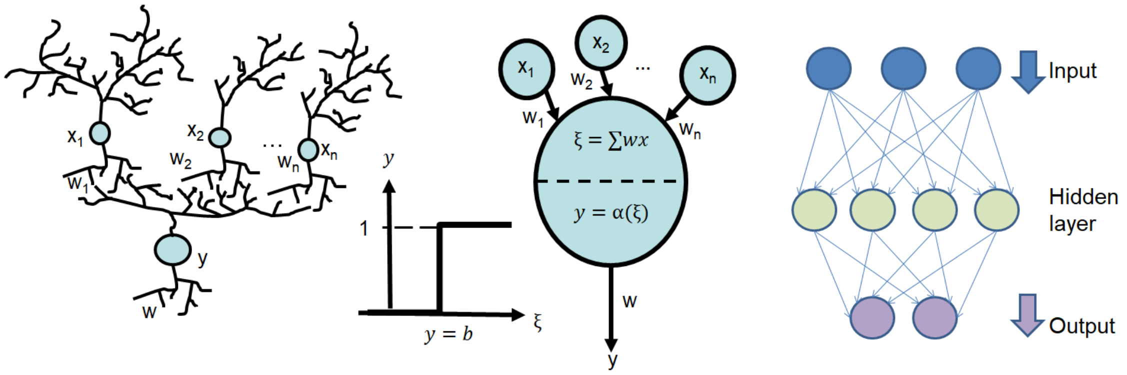

For a functioning ANN, several parameters have to be determined:

- ANN structure
    - Required input information
    - Required output information
    - Number of hidden layers
    - Number of hidden neurons
- Transfer function
- Connection weights

Networks without hidden layer are generally only able to perform linear tasks (Negarestani et al., 2002) while the addition of further hidden layers is only necessary for discontinuous problems (Rafiq et al., 2001). To determine the connection weights, often a backpropagation algorithm is used, in which the ANN is repeatedly presented with a number of training examples. After starting with random weights, the ANN output is compared to the target value and the connection weights are adapted to better fit the target. Then the training material is presented again and the connection weights are adapted once more. This cycle continues until a minimum divergence of the output from the target values is reached. The process of training an ANN can be considered as a robust alternative to a classical calibration method.

In this study, the commonly used backpropagation algorithm (e.g. Dragović et al., 2005) was used to adapt the connection weights by comparing the ANN's output to the target values provided in the training examples. To create a functioning ANN it is paramount to pick representative sample data: The network should be able to predict missing data, but of course it cannot arrive at conclusions for situations where no training material was provided. On the other hand, overtraining is an issue with ANNs. In this case the network loses its ability to generalize its "knowledge", which can be thought of like the difference between understanding something and learning it by heart.

In this study, it was opted to create an ANN with a single hidden layer, even though it may be possible that some non-linear phenomena, such as Compton and back scattering, are better accounted for with more hidden layers. This can be investigated in future work. The optimal input parameters and number of neurons in the hidden layer have to be obtained. This is usually done by employing a trial-and-error method. To keep the mean squared error as low as possible, the number of hidden neurons should be minimized. As a starting point the 2n+1 rule (Azoff in Medhat, 2012), stating that a network with one hidden layer and 2n+1 hidden neurons should be sufficient for n inputs, was employed and later confirmed. Only a limited number of real NORM was available for the project, so it was decided that an ANN will be built and tested for a predefined list of materials and γ-lines. Tables 2.3 and 2.4 show the available materials and analysed lines.

Table 2.3: List of materials and material identifiers used to train the ANN and activity categories assigned to the artificial spectra.

Material	**Material code**
Ilmenita	1
Phosphogypsum Huelva	2
Phosphogypsum MetroNORM	3
Sand	4
TiO_2	5
Tuff 1	6
Tuff 2	7

Table 2.4: List of lines analysed by the ANN.

Radionuclide	**γ-ray energy (keV)**		
^{210}Pb	46.6500		
^{234}Th	63.3100	92.5900*	
^{235}U	143.7700	163.3600	
^{212}Pb	238.6300	300.0900	
^{214}Pb	242.0000	295.2200	351.9300
^{228}Ac	911.2000	968.9600	

*combination of 2 lines that are not well separated: 92.38 keV and 92.80 keV

The materials come from NORM industry and were selected, characterised and used for intercomparison exercises in the MetroNORM project (EMRP JRP IND057) and have each been assigned a material code as an input to the final ANN. The selected γ-lines were chosen because they are relatively strong and interference free, and come from relevant naturally occurring radionuclides, representing the three natural decay chains.

Since only a limited number of real materials was available, and to cover a wider range of experimental conditions and make the ANN applicable to a greater number of situations, only artificial spectra have been used in the training of the ANN. A total of 635 artificial spectra have been created as training input for the ANN, using the Monte Carlo codes PENELOPE v.2014 (Salvat, 2015) and PENNUC (García-Toraño et al., 2017), and a validated model of the used HPGe detector (Peyres and García-Toraño, 2007). To create the training material, a number of $5 \cdot 10^8$ showers have been simulated on CIEMAT's super computer for each radionuclide and density, amounting to a total number of 126 simulations. After separately calculating the efficiency for each radionuclide, material and density from the simulation data, the spectra were convoluted with a Gaussian curve whose width is a function of energy, in order to reproduce the real detector system's response and account for (electronic) noise in a real spectrum. Figure 2.9 illustrates the difference between the data calculated by PENELOPE and the convoluted data.

The final artificial spectra that were used as training input to the ANN were obtained by multiplying the calculated data for each material, density and radionuclide by the target activity and combining them in order to gain one synthetic spectrum including all radionuclides as in the real spectrum. This results in spectra of varying density and activity concentration for each of the materials, containing the counts per second for each energy bin according to the formula

$$A \cdot \epsilon(E) = N \cdot t \tag{2.1}$$

where A is total activity, N is the total number of counts in the peak, ϵ is the detector efficiency and t the measurement time. Correction factors are not used in this equation, since they are already included in the efficiency calculated by PENELOPE and PENNUC. The generation of representative training input requires intensive study of possible material states. A total number of 635 artificial spectra, representing both equilibrium and disequilibrium states with varying distributions of activity concentration, have been calculated according

Figure 2.9: Difference between convoluted and original simulation data.

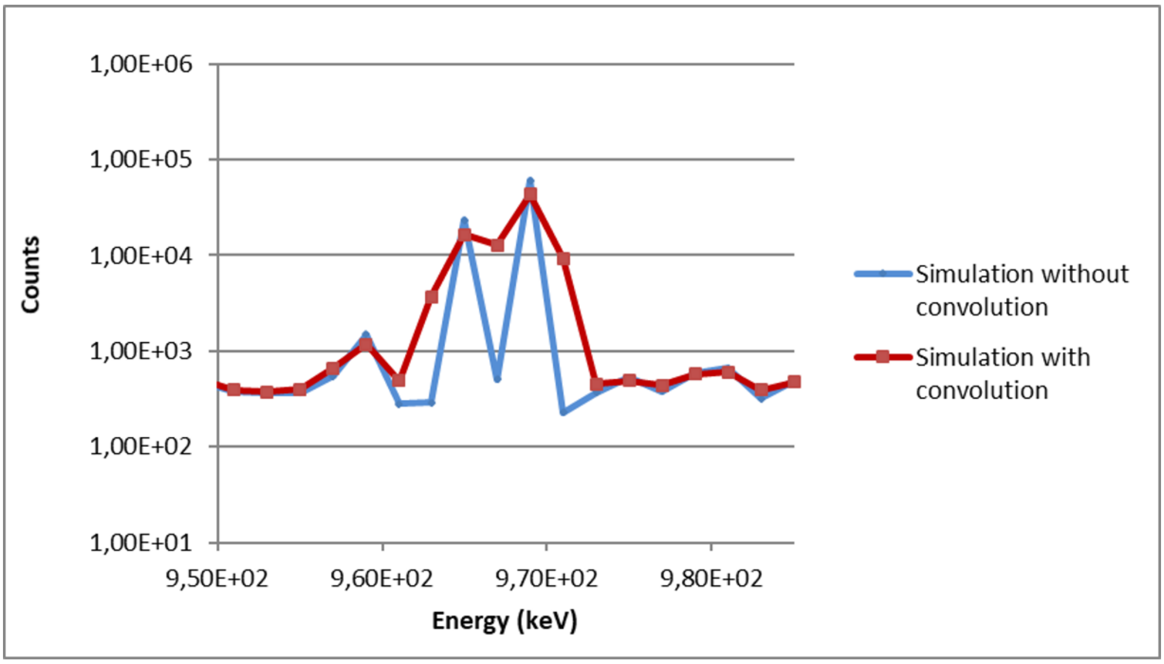

Table 2.5: List of activity categories assigned to the artificial spectra.

Activity concentration	Activity category
0,1 Bq/g	1
0,7 Bq/g	2
1 Bq/g	3
1,2 Bq/g	4
20 Bq/g	5

to five activity categories (see Table 2.5). This minimizes the total number of training samples, relying on the power of the ANN to intrapolate to the missing data, thus avoiding overtraining. The five activity categories represent activity concentrations well below or above the exemption limit, exactly the exemption limit (1 Bq/g) or slightly above or below the exemption limit.

The artificial spectra and their relevant parts that serve as input to the ANN have been calculated and extracted using a Matlab program. Figure 2.10 shows an artificial spectrum for TiO_2. The training input is given by a matrix where each row represents one sample. In each column the counts per second of each individual line to be analysed, followed by density, material identifier and sample mass are given. The ANN's input structure is shown in Figure 2.11. The output is a 1 x 12 matrix giving the activity category for each of the analysed γ-lines. Introducing sample mass as an additional parameter was necessary to ensure good convergence of the data points. Figure 2.12 shows the difference between input including and excluding sample mass in a regression plot.

Figure 2.10: Example of an artificial spectrum of TiO_2 calculated from convoluted simulation data (PENELOPE/PENNUC) using Matlab.

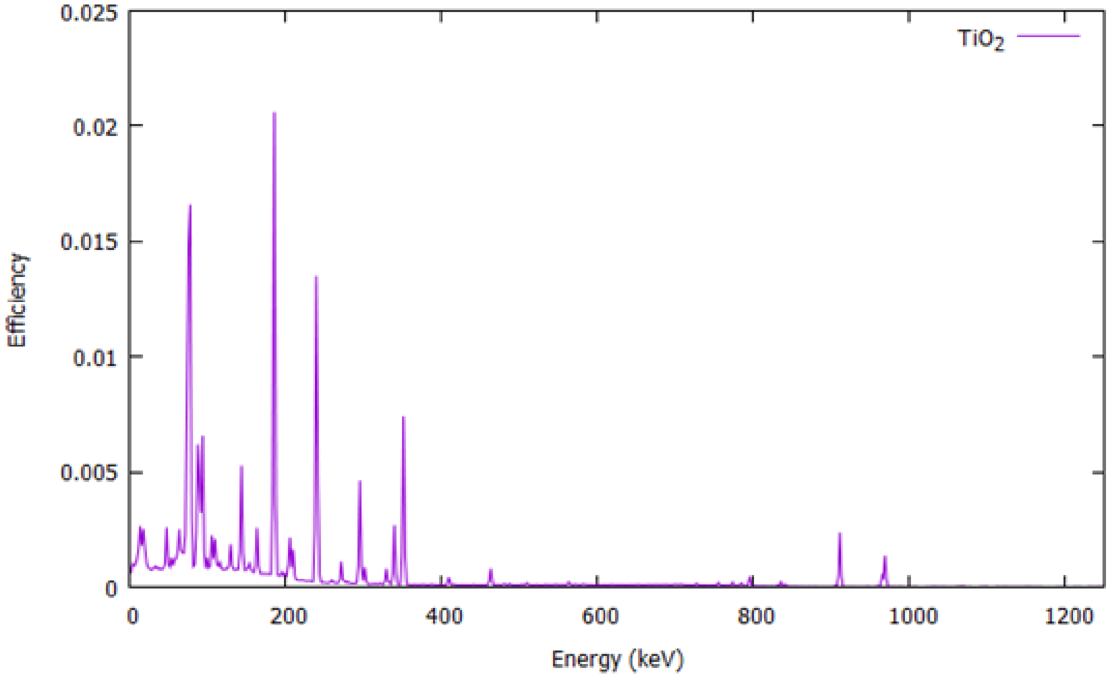

Figure 2.11: Structure of the ANN training input.

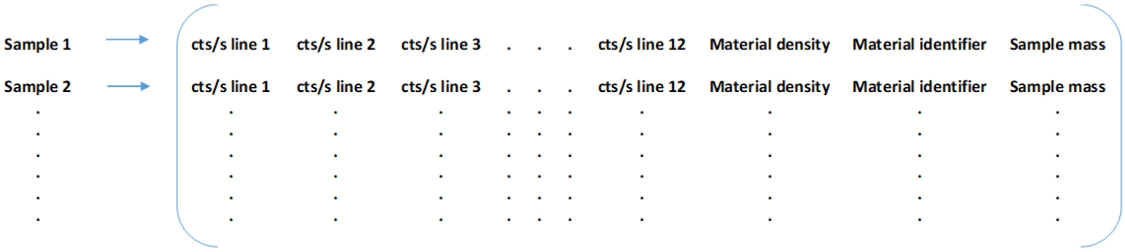

Sample 1	→	cts/s line 1	cts/s line 2	cts/s line 3	. . .	cts/s line 12	Material density	Material identifier	Sample mass
Sample 2	→	cts/s line 1	cts/s line 2	cts/s line 3	. . .	cts/s line 12	Material density	Material identifier	Sample mass
.		.	.	.	. . .	.	.	.	.
.		.	.	.	. . .	.	.	.	.
.		.	.	.	. . .	.	.	.	.
.		.	.	.	. . .	.	.	.	.
.		.	.	.	. . .	.	.	.	.

Figure 2.12: Regression plot with (right) and without (left) sample mass as input parameter.

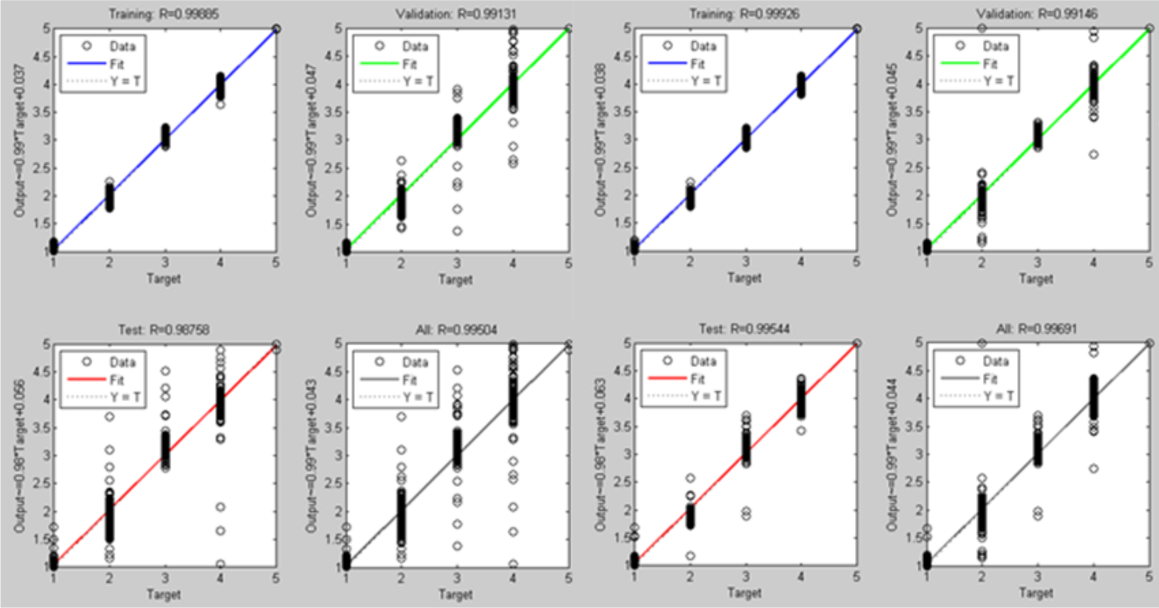

The choice of transfer function depends on the problem to be solved. In case of this study, it was chosen to use a sigmoidal transfer function based on a logarithm (LOGSIG), as it gave the best convergence. Figure 2.13 shows the difference between the transfer function based on a logarithm and on a tangent. The comparatively poor performance of the transfer function based on a tangent and on a purely linear function can be observed in 2.14.

The number of hidden neurons was determined using a trial-and-error approach, keeping in mind the before mentioned 2n+1 rule. A network with 31 hidden neurons provided the best regression and thus confirmed the rule. Figure 2.15 shows the difference of an ANN using 30, 31 and 32 neurons, respectively.

Figure 2.13: Sigmoidal transfer functions LOGSIG (left) and TANSIG (right).

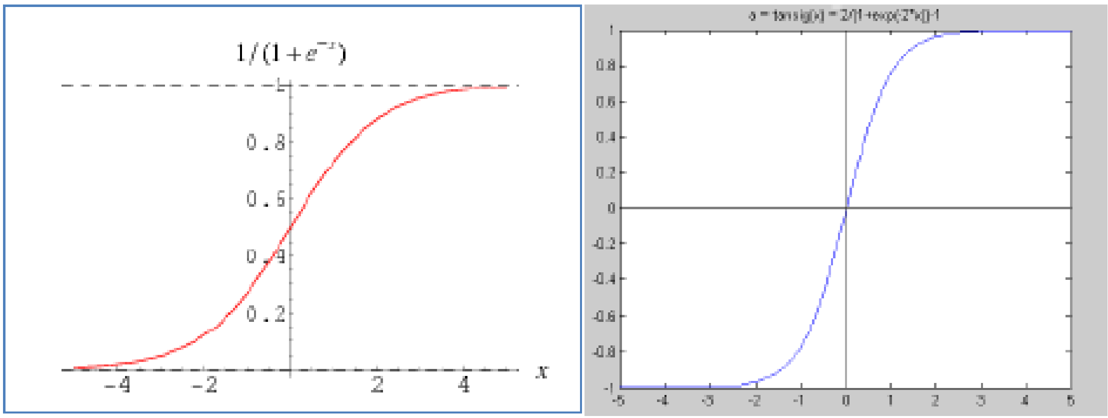

Figure 2.14: ANN using a purely linear transfer function (PURELIN, left) and a transfer function based on a tangent (TANSIG, right). No other parameters were changed from the final ANN that uses a transfer function based on a logarithm (LOGSIG).

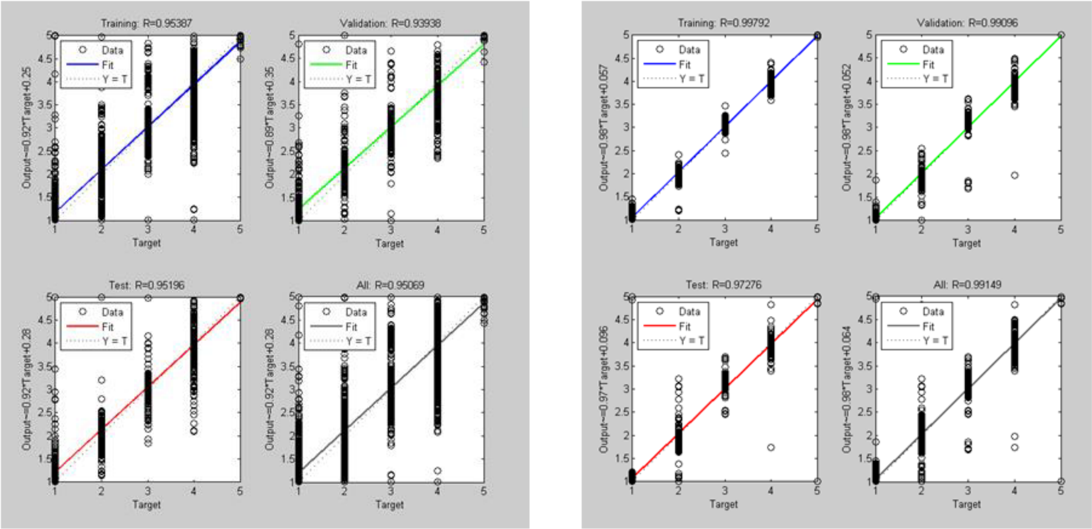

The predictive power of the ANN was verified using data from real γ-spectra of the available NORM. The spectra were obtained by measuring real samples for 200 000 s on an HPGe detector (GX4020) after sample equilibrium was reached. Spectra were obtained using SILENA International SpA EMCA2000 MCA Emulation Software (2000) peak areas were analysed with a non-linear code (GRILS) included in the GANAAS package (IAEA, 1991). Based on the conventional activity evaluation performed with GANAAS, the real sample materials were manually assigned activity categories. The before mentioned Matlab program was used to extract the needed information from the ASCII file of the spectrum and provide an input to the ANN. The ANN's output agrees very well with the manually assigned values. Figure 2.16 shows the results of the verification. Training the ANN in that way resulted in an ANN with an overall regression factor of 0.9975. This shows that ANNs are well suited for the task of deciding if a material is above or below the exemption limit from a raw γ-spectrum. Figure 2.17 gives the performance and regression plots of the final network. The sudden drop in the mean square error of the performance curve can be attributed to the fact that, without reliable a priori information on the connection weights, random weights were used. This causes the ANN to be trapped in a temporary minimum and leaving it requires many cycles of presenting the training dataset to the ANN (Annema, 2012).

Figure 2.15: Comparison of the same ANN using 30 neurons (top left), 31 neurons (bottom) and 32 neurons (top right).

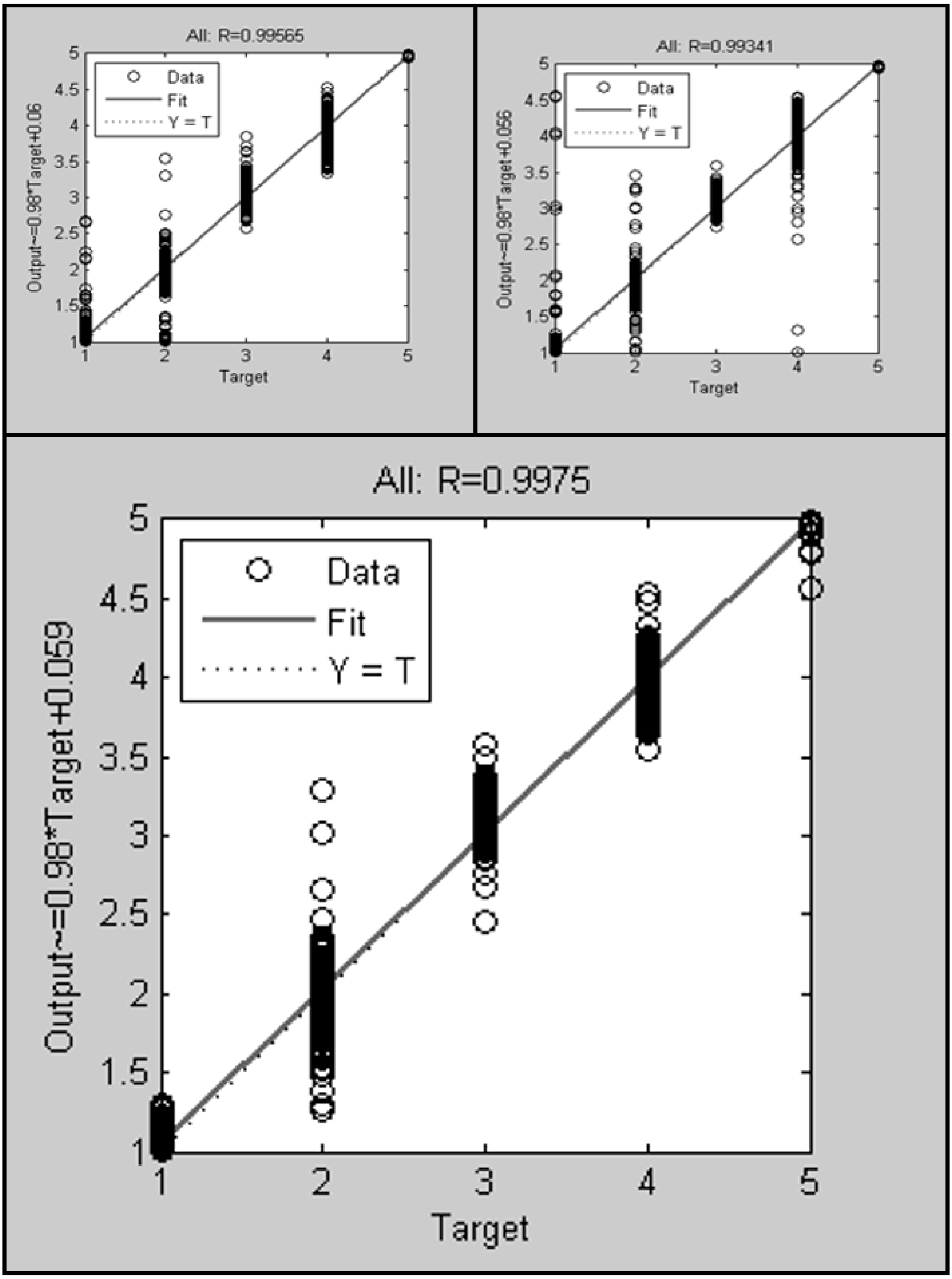

Figure 2.16: ANN output for the six testing materials (activity categories).

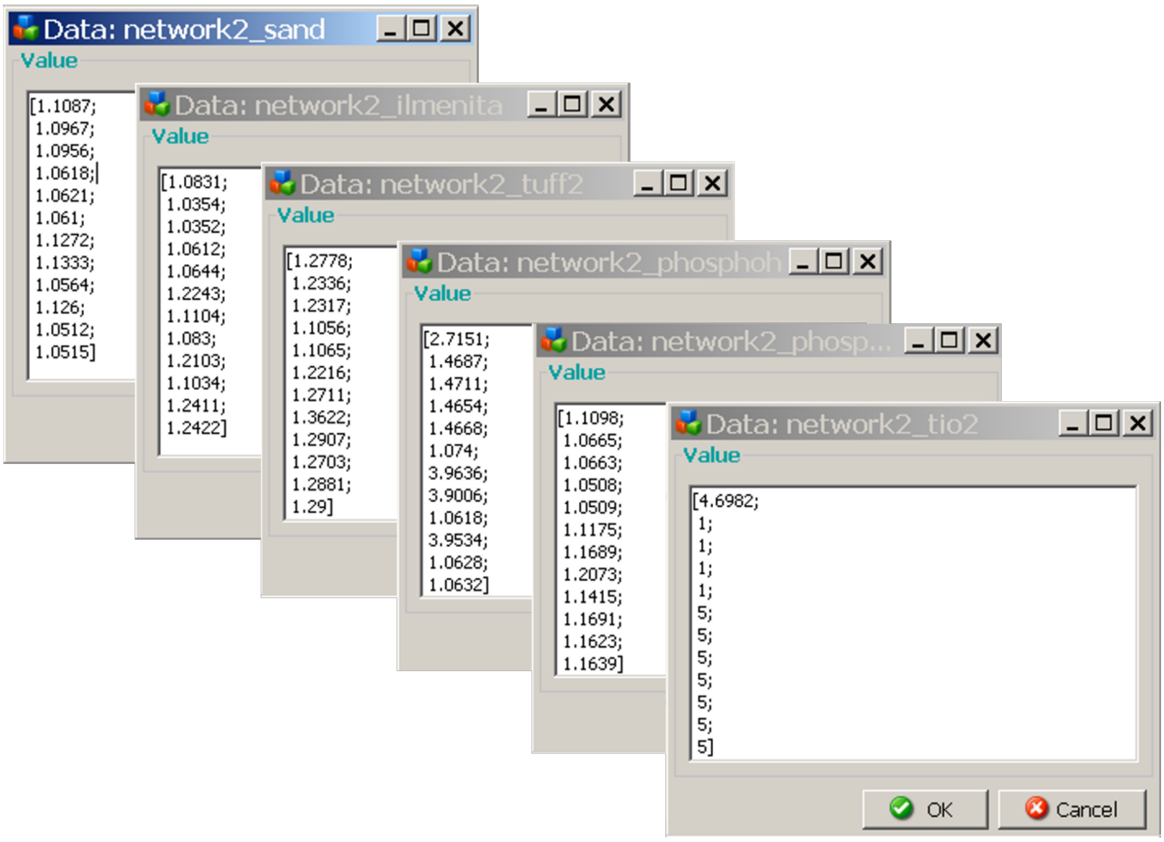

Data: network2_sand

Value

```
[1.1087;
1.0967;
1.0956;
1.0618;
1.0621;
1.061;
1.1272;
1.1333;
1.0564;
1.126;
1.0512;
1.0515]
```

Data: network2_ilmenita

Value

```
[1.0831;
1.0354;
1.0352;
1.0612;
1.0644;
1.2243;
1.1104;
1.083;
1.2103;
1.1034;
1.2411;
1.2422]
```

Data: network2_tuff2

Value

```
[1.2778;
1.2336;
1.2317;
1.1056;
1.1065;
1.2216;
1.2711;
1.3622;
1.2907;
1.2703;
1.2881;
1.29]
```

Data: network2_phosphoh

Value

```
[2.7151;
1.4687;
1.4711;
1.4654;
1.4668;
1.074;
3.9636;
3.9006;
1.0618;
3.9534;
1.0628;
1.0632]
```

Data: network2_phosp...

Value

```
[1.1098;
1.0665;
1.0663;
1.0508;
1.0509;
1.1175;
1.1689;
1.2073;
1.1415;
1.1691;
1.1623;
1.1639]
```

Data: network2_tio2

Value

```
[4.6982;
1;
1;
1;
1;
5;
5;
5;
5;
5;
5;
5]
```

Figure 2.17: Performance and regression plots of the final ANN.

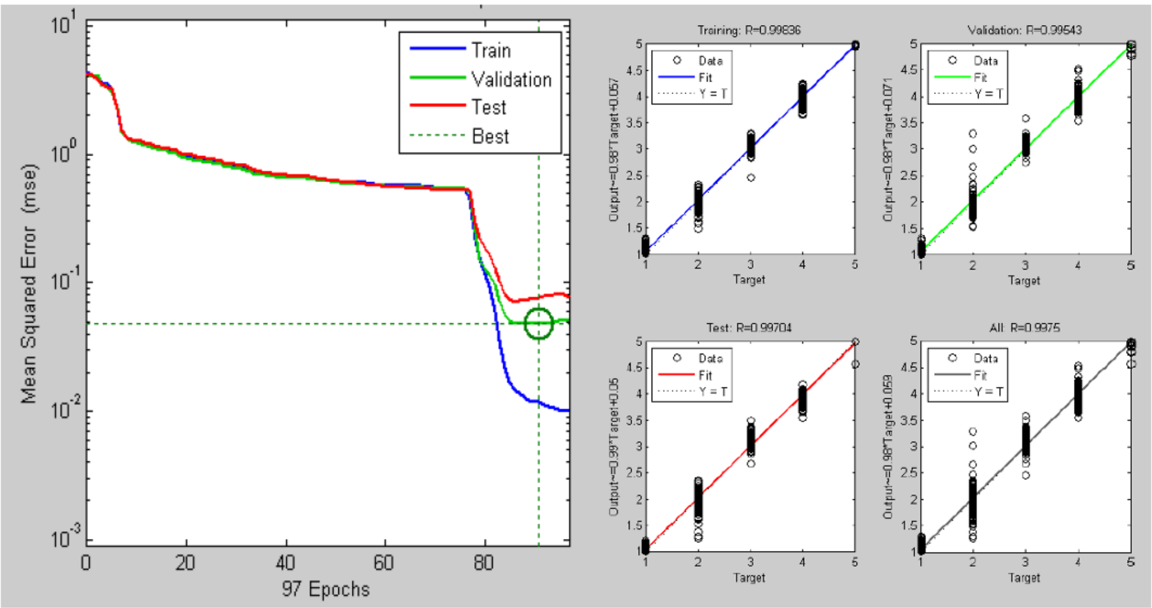

As was shown in the above, ANNs are quite well suited to decide from a raw γ-spectrum if activity concentration in a NORM sample is above or below the exemption limit. In this feasibility study an ANN was created that is able to analyse six different sample materials. In case of specialized industry the number of material can probably be reduced to one or two. The biggest limiting factor for the use of ANNs is the selection of appropriate training material. For specialized industries that already have a large number of γ-ray measurements and knowledge about the material available, the time consuming process of generating artificial spectra can be skipped, speeding up the selection process.

ANNs provide a quick and cost efficient way to manage the large number of routine measurements conducted in NORM industry without specially trained workers. For the end-user only a γ-spectrum in ASCII format as input to the ANN and no knowledge related to spectral deconvolution is required. Reliable assessment of activity concentration helps to protect workers from radiation exposure and reduce costs related to waste management. ANNs can also provide a robust method that can be used outside strict laboratory conditions as the ANN itself serves as the detector calibration.
The work was published as a peer-reviewed paper (Wiedner et al., 2017) that is included in chapter 6, in the IRPA 2016 (Cape Town) Proceedings and also as a CIEMAT Technical Report (Moser et al., 2015) containing more detailed information.

3 Development of innovative methods for radon metrology in life science

3.1 Radon and its impact on health

3.1.1 Radon measurement

Radon is a colourless, odourless and tasteless radioactive noble gas with four naturally occurring isotopes – ^{222}Rn, ^{220}Rn, ^{219}Rn and ^{218}Rn – that are a product from the decay of uranium and thorium. When speaking about radon in the context of radioactivity measurements, it is usually referred to ^{222}Rn, a daughter of ^{238}U and ^{226}Ra, which makes up approx. 90 % of all naturally occurring isotopes. ^{220}Rn, called thoron, accounts for approx. 9 %, while ^{219}Rn, also called actinon, makes up about 1 %. ^{218}Rn only occurs in traces.

All natural radon isotopes decay exclusively via α-decay and only have γ-lines with very low emission probabilities. This makes it impossible to directly analyse the radon concentration with γ-ray spectrometry. Commonly used techniques are ionisation chambers, etched track detectors, scintillation cells, charcoal detectors and electret ionization chambers (Miles, 2004).

3.1.2 Inhalation of radon gas

^{222}Rn has been classified as a Group 1 human carcinogen by the International Agency for Research on Cancer (IACR, 2018). This means that there is "sufficient evidence of carcinogenicity in humans" (IACR, 2006). Since radon is gaseous, it is relatively quickly exhaled. Radon's daughter radionuclides ^{218}Po and ^{214}Po, however, can attach to aerosols that adhere to surrounding surfaces and the walls of the repository tract where sensitive lung tissues, such as the basal cells of the bronchial epithelium, are damaged due to the high linear energy transfer of the alpha particles. Mutations and chromosomic aberrations in the DNA, and a deregulation of the cell cycle can be induced that can ultimately lead to the development of lung cancer (Rodríguez-Martínez et al., 2018). (WHO, 2010)

Inhalation of radon gas is the primary cause of lung cancer for lifelong non-smokers and the second largest cause for lung cancer after smoking. However, there is a large combined risk of smoking and inhalation of radon and most radon-induced lung cancer cases occur among smokers (WHO, 2009; Darby et al., 2005). Radon is estimated to cause between 2 % and

14 % of all lung cancer cases (Darby et al., 2005; WHO, 2009), depending on radon levels and smoking prevalence. In Europe this corresponds to up to 20 000 people per year dying of radon-induced lung cancer (Wiedner, 2018).

3.1.3 Exposure to radon

As shown in section 1.1, most of the exposure due to natural radiation comes from inhalation of radon gas. For most people, the largest portion of this exposure comes from inhalation of radon at home or at the work place (dwellings, underground mines, water works, etc.). Since radon is a daughter of uranium it occurs everywhere where uranium is present. Uranium, radium and radon are soluble in water (WHO, 2011) and, therefore, also present in water that passes through rock-bed. While radon itself is natural, high activity concentrations in indoor air are not and radon can be considered an air pollutant (WHO, 2010). Radon itself is chemically inert and, therefore, very mobile. It can permeate indoors through cracks in the soil and openings in buildings (strip foundations or too thin foundations, holes for pipes, etc.) and accumulate in badly ventilated spaces. The possible degree of indoor radon concentration is of course dependent on the underlying geological conditions (Cosma et al., 2015), but used building materials, building design and ventilation of the space (UNSCEAR, 2010; Park et al., 2018) can lead to very high activity concentrations. Even exposure to low levels of radon over a prolonged time should be avoided as studies have shown an increased excess risk of lung cancer at low radon exposure rates (Kreuzer et al., 2015). A study conducted by Darby et al. (2005) that pooled 13 European case-control studies found that the excess risk of lung cancer is about 16 % per 100 Bq/m^3 throughout a wide range of exposure levels.

3.2 Radiation protection against harmful activity concentrations of radon

Legislation, and development and enforcing of building codes that lay down basic principles of radon protection can help mitigate these factors and reduce exposure for the occupants at moderate to low cost (Darby et al., 2005). As an example, Article 74 of the European basic safety standards lays down that Member States shall establish national reference levels for indoor radon concentrations so that the annual average activity concentration in air is no higher than 300 Bq/m^3 (Council of the European Union, 2013). This necessitates the development of novel reliable SI traceable calibration and measurement methods targeted at low radon activity concentrations to achieve sound measurement results with sufficiently low uncertainties (Wiedner, 2018).

For new buildings, actions to prevent radon from entering inhabited spaces in great quantities can easily be incorporated in the planning phase: Use of at least 10 cm coarse gravel layer underneath a continuous concrete foundation of at least 20 cm, waterproof concrete tanking, plastic sheeting or vapour retarders, and additionally, sealing all openings in the concrete foundation floor and walls, e.g. cracks or holes for water/electrical installation, with polyurethane caulk can prevent radon from entering the building. Vent pipes installed in the gravel layer can remove radon gas before it can enter the building. (Amt der Oö. Landesregierung (2017); US EPA (2017))

Radon mitigation for older buildings is often feasible and of moderate cost – in many cases the installation of soil depressuration or ventilation systems is sufficient (Darby et al., 2005; Cosma et al., 2015; Maringer et al., 2001).

3.3 Soil gas measurements and influence of thoron

3.3.1 Influence of thoron on radon measurements

To reliably measure low activity concentrations of radon gas in air, especially with sufficiently low measurement uncertainties, a significant improvement in the metrological infrastructure in Europe is necessary. New and improved radon calibration procedures at low activity concentrations are a prerequisite to fulfil the requirements of the EU-BSS and currently not available on a large scale. In the future, a large number of traceable and quality assured in-situ and laboratory measurements will have to be conducted in order to ensure that the reference levels laid down in the EU-BSS are met. It is known, that the presence of thoron and its progeny bias radon activity concentration measurements (Beck et al., 2009), however, information on the extent of this effect is currently limited and techniques to reduce or mitigate this influence have to be developed. (Wiedner, 2018)

3.3.2 Radon mapping

In addition to radon reference levels in buildings, Article 103 of the EU-BSS lays down that Member States shall identify areas where the radon concentration in a significant number of buildings is expected to exceed the reference levels and establish a national action plan addressing long-term risks from radon exposures in dwellings, buildings with public access and workplaces. (Wiedner 2018; Council of the European Union 2013)

Radon mapping is an important tool to identify regions that show elevated radon potential (radon priority areas). To create these maps, measurements of radon activity concentrations are taken all over a specific region. Maps can be created from all kinds of measurements, like radionuclide composition of the soil, soil gas or water measurements, but most available maps are created from measurements of indoor air (e.g. JRC, 2018; BMNT, 2018).

Currently many different methodologies for the creation of such maps have been proposed. The MetroRADON consortium is currently working on harmonisation of techniques that will enhance comparability and allow for merging of data sets. (Wiedner, 2018)

3.3.3 Soil gas measurements

To quantify the before mentioned influence of thoron on these measurements, a study of the introduced bias in soil gas measurements was conducted in eight different locations with elevated uranium and thorium occurrence (Newrkla et al., 2018). To extract the soil gas, a hallow steel probe of 1.2 m or 1.6 m length and 12 mm diameter with a separate metal tip was driven into the ground to the desired depth. A thin metal rod was inserted into the probe in order to drive the tip 5 cm further into the ground. This way soil gas can be drawn from the top of the probe, using either a syringe or a pump, and inserted into an AlphaGUARD active radon monitor (model PQ2000 PRO RnTn by Saphymo). For most measurements a volume of 100 mL was extracted, using a syringe. Figure 3.1 shows the set-up.

Figure 3.1: Measurement set-up – Soil gas probe (left) and sampling of soil gas with a syringe(right).

The first sample of soil air is discarded to avoid dilution with air already in the hollow part of the probe. Each sample is measured for at least four 10-minute-cycles, again discarding the first measurement result. This eliminates the effect of thoron on the radon measurement, as it will have decayed almost completely after the first 10 min measurement because of its short half-life.

Activity concentrations of radon and thoron were also measured simultaneously with two radon monitors, one AlphaGUARD in radon/thoron mode and one only measuring radon. Figure 3.2 shows the set-up.

Figure 3.2: Set-up for the evaluation of the influence of thoron on radon activity concentration measurements with two AlphaGUARD radon monitors, measuring the same soil gas sample in a closed circuit.

This confirmed that there is a non-negligible influence on the radon measurement if thoron is present in the sample air (Beck et al., 2009). In addition, the γ dose rate was measured at each measurement location. Values between 81 nSv/h and 225 nSv/h were detected. Figure 3.3 shows the relationship between the radon activity concentration in soil gas and the γ dose rate. Radon progeny in the ground contribute to the dose rate above ground. Since dose rate measurements are faster and easier to carry out than soil gas measurements, such measurements could be used as an alternative way to estimate an area's radon potential.

Figure 3.3: Relationship between ^{222}Rn activity concentration and γ dose rate. ^{222}Rn activity concentrations have been corrected to a depth of 1 m at each measurement location (1-8).

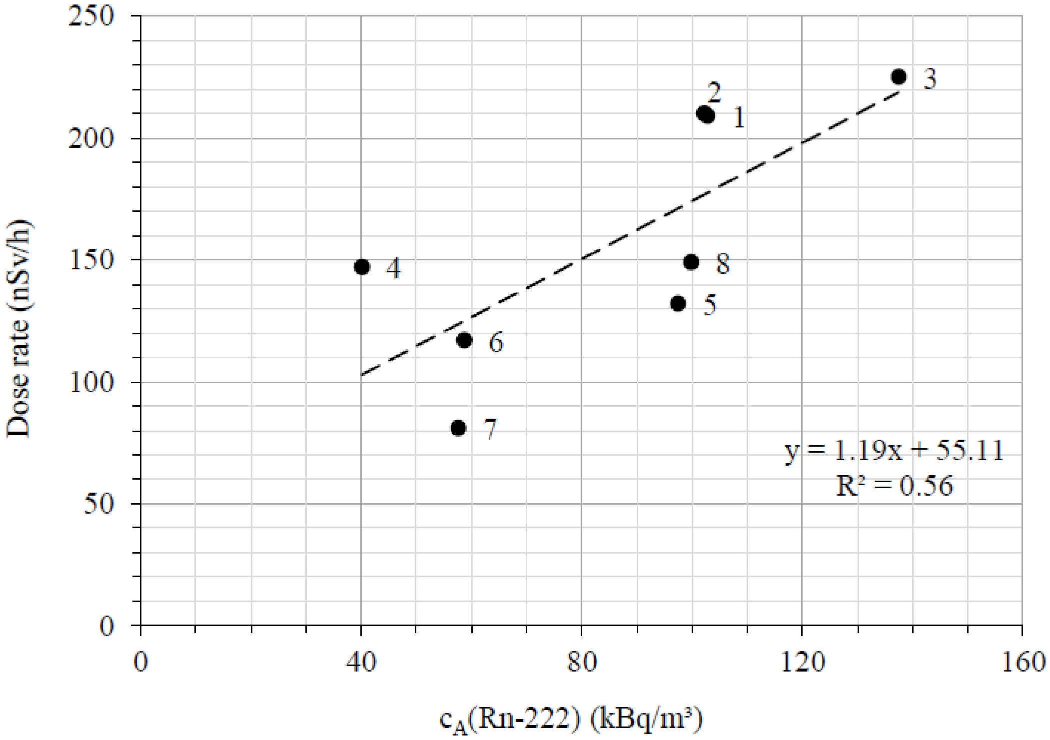

3.4 Radon in drinking water

3.4.1 Risk of cancer due to radon in drinking water

Risk of cancer induced by ingestion of radon is generally considered low (WHO, 2009). Stomach cancer is the most frequently occurring type of cancer to be induced by ingestion of radon. The range of alpha particles emitted by radon and its progeny is too low to reach the especially vulnerable cells in the stomach wall. Therefore, risk of stomach cancer is mainly contingent on diffusion from the ingested substance (generally drinking water) to the stomach wall. Radon can enter the bloodstream through the small intestine or diffusion through the stomach wall and will quickly be expelled through the lungs.

The National Research Council's Committee on Risk Assessment of Exposure to Radon in Drinking Water found that most of the cancer risk associated with radon in drinking water comes from the exhalation of radon gas to the surrounding air from where it can be inhaled (NRC, 1999). The WHO came to the same conclusion, stating that "90 % of the dose attributable to radon in drinking-water comes from inhalation rather than ingestion" (WHO, 2011) and Rühle (1997) calculates an annual dose for an adult of 0.17 mSv due to inhalation and further 0.05 mSv due to ingestion, totalling 0.22 mSv per year for an activity of 100 Bq/L.

Compared to the radiation dose caused by radon in the atmosphere this is ten times lower, but nevertheless underlines the importance of monitoring radon levels in water and the adherence to these limits.

3.4.2 Comparison of two ionization chamber measurement methods for radon in drinking water

Even though ingestion of radon from drinking water does not really pose a health risk under normal circumstances, EU Member states are obligated to continuous monitoring and reporting of levels of environmental radioactivity in air, water and soil by Articles 35 and 36 of the Euratom Treaty (Council of the European Union, 2010). Where water is supplied as part of a commercial or public activity, the European Commission (2001) recommends 100 Bq/L as indication level, below which no remedial action is required. Above 1 000 Bq/L remedial action should be considered for radiation protection purposes.

During the Austrian National Radon Project (Friedmann et al., 2007), new and old measurements of radon concentrations in spring and ground water all over Austria were analysed and merged to create a map of radon in water potential in Austria. Approx. 86 % of the measurements are below 50 Bq/L, but with 3.5 % of measurements above 400 Bq/L, some regions with a high radon potential were identified. Figure 3.4 shows the map created from these measurements, classifying radon potential in Austria into three groups.

The most commonly used detection methods used for this purpose are ionization chambers, liquid scintillation counting, scintillation cells or silicon detectors (Jobbágy et al., 2017). Therefore, a comparison of two ionisation chamber activity measurement techniques has been conducted as part of this thesis (Wiedner et al., 2018a). Water samples in the Austrian Thermenlinie region were analysed with an ionization chamber set-up devised by Prof. Dr. Harry Friedmann (Institute for Isotope Research and Nuclear Physics of the University of Vienna; Friedmann, 1992), and a commercially available and widely used AlphaGUARD (Saphymo) radon monitor. Thermenlinie is the name of a seismic disturbance zone west of Vienna, running from the Northern Limestone Alps to the south of Vienna along the edge of the Vienna Basin. In this region many hot springs, which are often used in spas (Peck and Linsberger, 2007), are located. The Thermenlinie region is mostly part of Class 1, with some municipalities in Class 2 (see Figure 3.4).

The two measurement set-ups that were compared are an AlphaGUARD radon monitor (BEV's national standard for radon activity concentration per volume unit), traceably calibrated at ENEA, and a cylindrical ionization chamber with a volume of 9.3 L. The ionisation chamber is supplied by 260 V and connected to an electrometer. Activity concentration is determined via a charge measurement. This way, electrical current is integrated over a period of time and fluctuations in electrical current have less influence on the result, therefore

Figure 3.4: Class 1: municipalities where all measurement are below 100 Bq/L, with less than 30 % of values above 50 Bq/L, Class 2: municipalities where all measurements are below 300 Bq/L, with less than 30 % of values above 150 Bq/L and not Class 1, Class 3: all other values. Translated from: Friedmann et al. (2007).

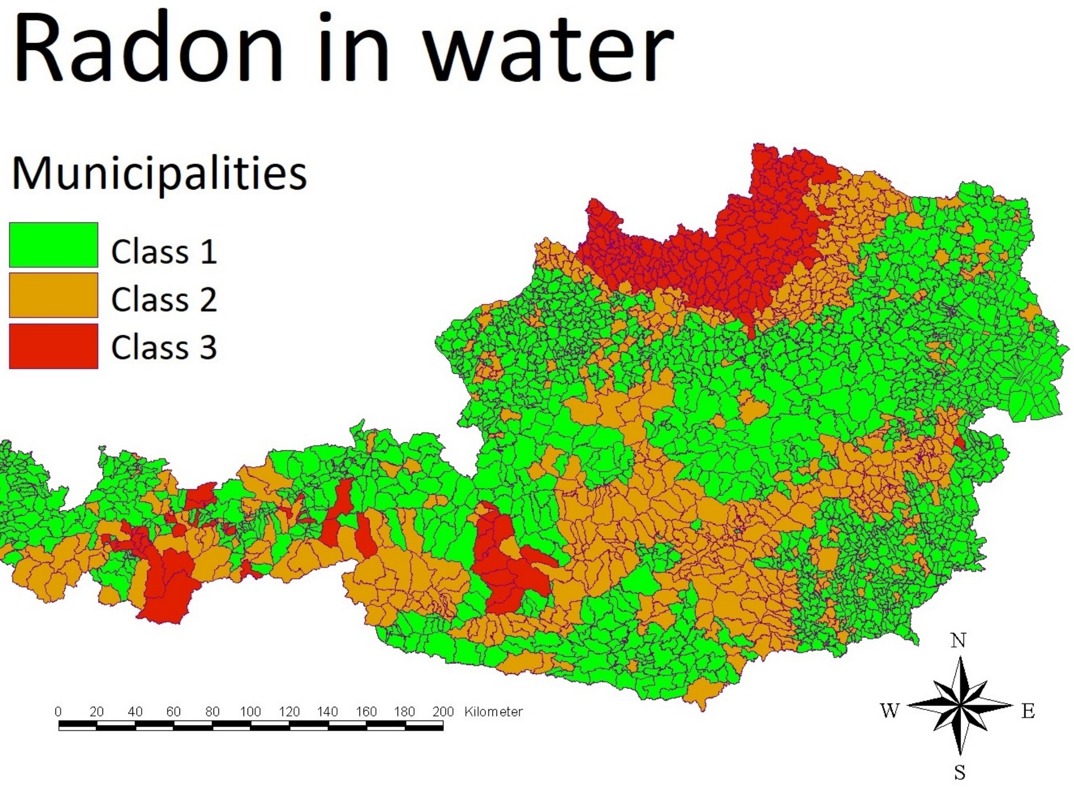

increasing precision. The ionisation chamber's inner pressure was lowered significantly with a water jet pump connected to a tap. The measurement container (a glass water bottle) was attached to the ionisation chamber by using a plug with two hoses. Slightly opening the valve at the chamber results in a flux of ambient air that is slowly sucked through the water and chamber. The flowing air causes the water to bubble and very efficiently emanates radon from the water. A previous study (Friedmann, 1977) showed that three times the volume of the liquid is sufficient to emanate and transfer virtually all the radon from the water into the chamber (chamber volume approx. 9 L vs. approx. 1 L water sample). Once the pressure in the chamber is balanced with the ambient air, equilibrium of radon and its daughters starts to build up. When measurements with the ionization chamber are finished, the outlets of the chamber are fitted with hoses and connected to the AlphaGUARD (see Figure 3.5).

Figure 3.5: Set-up of the measurement system: (a) Ionisation chamber, (b) AlphaGUARD.

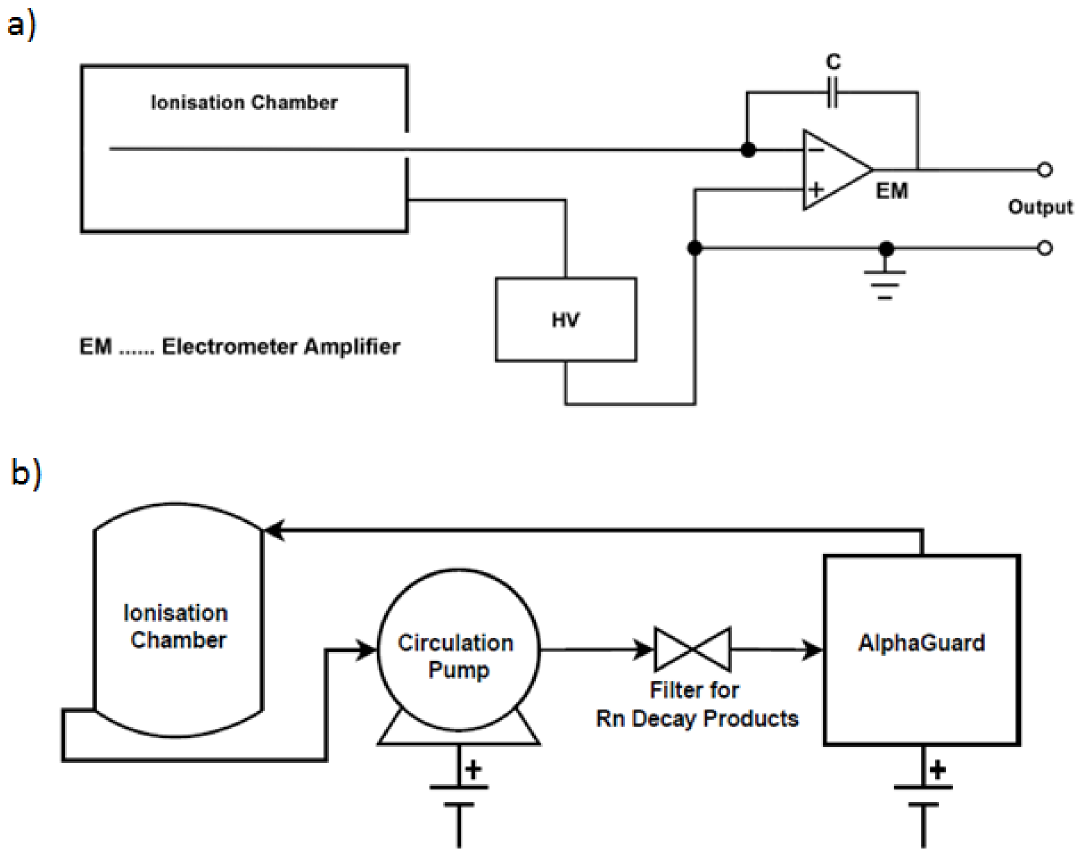

A circulation pump creates a flux of 1 L/min. After ensuring that the air is circulated at least twice through the AlphaGUARD, the pump is shut off and the ionisation chamber disconnected.

Since secular equilibrium is reached after only about ten half-life periods of the longest-lived daughter, ^{222}Rn and its progeny would only be in equilibrium after approx. five hours (ten half-lives (26.8 (9) min) of ^{214}Pb). Due to time constraints, especially when measurements are conducted in the field, it is not always possible to wait for such a long time. Therefore, a fit of the chamber's electrical current was used to correct for the disequilibrium state for measurements performed 20–30 min after insertion of radon gas into the chamber (see Figure 3.6). The results and uncertainties given by both measurement set-ups generally agree (difference factor of 1.00–1.55) with relative uncertainties ranging from 10 % to 35 % ($k = 1$). Figure 3.7 shows the results.

Figure 3.6: Fit of the development of the electrical current (green) for measured values (purple) of a representative sample (approx. 120 Bq/L) using a least squares Marquardt-Levenberg algorithm, where A_0 is considered the only independent variable.

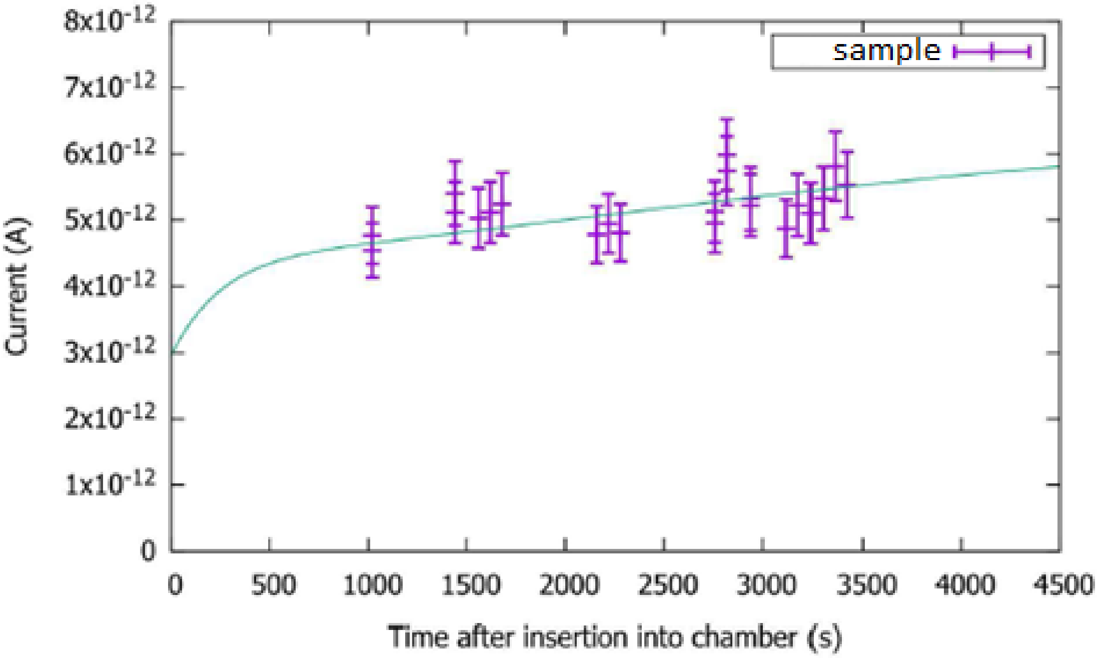

Figure 3.7: Overview of selected samples showing normalised activity and respective measurement technique.

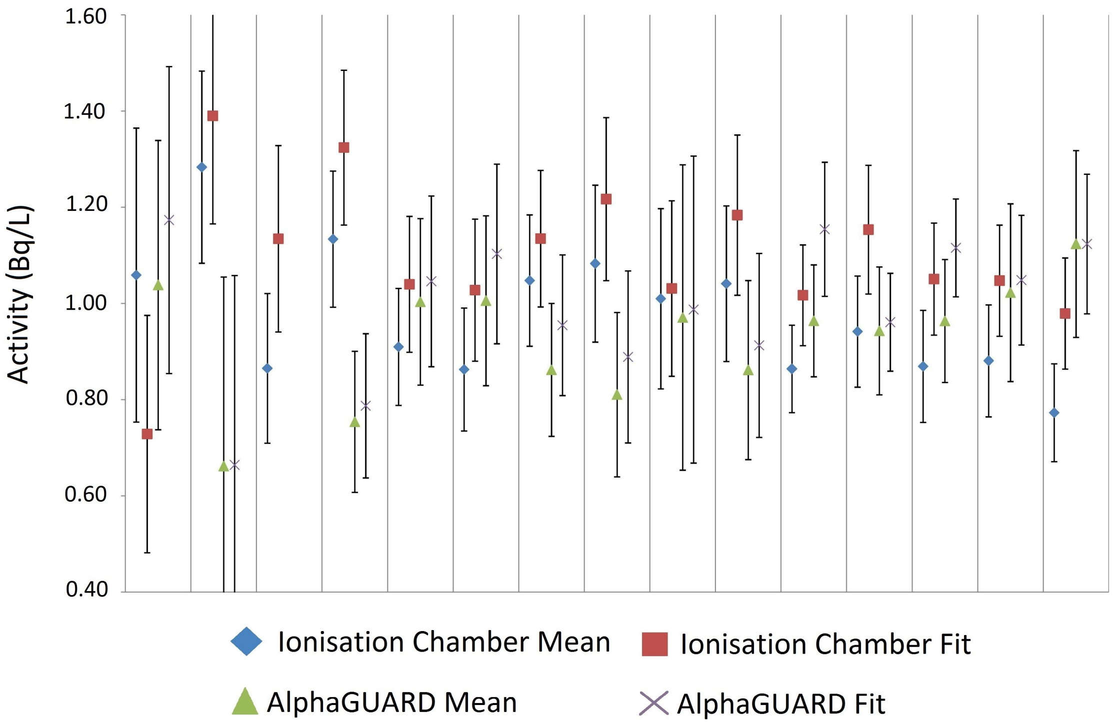

4 Conclusions and outlook

This work describes the current state of the art and challenges related to radionuclide metrology in the field of natural radiation. Emphasis is given to highlight the difficulties connected to γ-ray spectrometry. Another large part of this work is dedicated to radon and its impact on health. Activity concentrations of various radionuclides in water, air and NORM samples are measured and continuously monitored by many institutions to ensure radiation protection of the public, create baselines, study transport processes, dispose of waste, assess contamination, etc. and ensure compliance with the Euratom treaty. This is often done using γ-ray spectrometry, as it is a versatile and non-destructive method with which activity concentrations of many radionuclides can be determined simultaneously.

A study of particular problems appearing in γ-ray spectrometry of NORM samples showed that γ-ray spectrometry of NORM samples is challenging and requires expert knowledge in spectrum deconvolution due to the many different radionuclides of the natural decay chains present within NORM samples. Spectral interferences were studied and a best practice recommendation on suitable γ-lines for the evaluation of activity concentration was published. Furthermore, it was found that the determination of ^{226}Ra based upon ^{214}Bi and ^{214}Pb is strongly dependant on the radon tightness of the sample containers. A simple method to assess leakage of radon gas from the sample containers was proposed.

During the investigation it was found that γ-ray spectrometry of NORM samples heavily relies on the availability of certified reference materials. The use of Monte Carlo codes for simulation of radiation transport can alleviate this problem but exact knowledge of the detector system and measured sample are required. Due to the large number of different NORM, there is a general need for more reference materials in industry and science. Therefore, a natural matrix, non-spiked NORM material made of quartz sand with elevated levels of radioactivity caused by the treatment of drinking water was produced.
Production of reference materials is a complex procedure that requires careful handling and homogeneity testing. To test the proficiency of γ-spectrometry laboratories at the evaluation of NORM samples, the new material was used in a proficiency test exercise with nine European laboratories. The results of the NORM proficiency test showed the expected behaviour: larger deviations from the mean and reference value, and a larger general spreading of results for NORM than for simple matrices and anthropogenic radionuclides like ^{57}Co, ^{60}Co and ^{137}Cs and a general underestimation of the ^{226}Ra activity concentration.

From the results of the proficiency test exercise it became apparent that many laboratories have problems with the determination of the activity concentration of ^{226}Ra, specifically. ^{226}Ra activity concentration was underestimated by up to 35 %. This underestimation is caused by the use of sample containers that are either not sufficiently radon tight or measurement before reaching radioactive equilibrium. It was demonstrated that evaluation of ^{226}Ra is often not correctly performed which underlines the importance of trained γ-ray spectrometry experts.

To alleviate this problem and allow for quick decision making in the field, a feasibility study was undertaken to test if artificial neural networks can be applied to the problem of determining whether the activity concentration in a sample is above or below the exemption limit. An ANN with the ability to analyse a raw γ-spectrum and determine if the activity concentration in 12 γ-lines is above or below the exemption limits laid down in national legislation was created. The ANN was trained using artificially prepared spectra that were calculated using the Monte Carlo codes PENELOPE and PENNUC, and Matlab. The ANN's performance was tested using real γ-spectra. The network was able to correctly classify all of the testing materials. Therefore, ANNs are well suited to carry out this task. For the end-user, only a gamma spectrum in ASCII format and no specialized knowledge in the field of γ-ray spectrometry is required.

The study of measurement techniques to quantify the activity concentration of all radionuclides present in natural samples also showed the difficulties related to accurate measurement of radon. Inhalation of radon gas is the single largest natural factor in the development of lung cancer. Since all naturally occurring radon isotopes are α-emitters, it is impossible to study them by γ-ray spectrometry. Active radon monitors based on an ionization chamber are often used to determine radon concentration in soil gas, water and indoor air. Accurate and robust measurement techniques with sufficiently low uncertainties for radon concentration in air do currently not exist. The 3-year EMPIR joint research project MetroRADON has the objective to develop such methods, study the influence of thoron on radon measurements and harmonize radon mapping methods. In the framework of the project a comparison of two ionization chamber measurement techniques was conducted. It was shown that the results and uncertainties of an old and inexpensive, self-built ionization chamber are in good agreement with the results of a commercially available AlphaGUARD radon monitor. Other meaningful results are expected at the end of the project in 2020.

The results of this thesis will help to improve the efficiency and accuracy of activity concentration measurements in NORM, resulting in a higher level of radiation protection of workers and the public.

5 Bibliography

H. Aiginger, F. Maringer, D. Rank, and E. Unfried. A new laboratory for routine low-level measurements (BVFA Arsenal, Wien). *Nuclear Instruments and Methods in Physics Research Section B: Beam Interactions with Materials and Atoms*, 17(5):435 – 437, 1986.

Amt der Oö. Landesregierung. *Radon Vorsorgemaßnahmen bei Neubauten und Generalsanierungen (Radon prevention for new buildings and major renovations)*, 2017. `https://www.land-oberoesterreich.gv.at/files/publikationen/us_radon_vorsorge.pdf` [Accessed: 2018-10-25].

M. J. Anagnostakis, C. Bolzan, P. D. Felice, A. Fazio, G. Grisanti, S. Risica, T. Turtiainen, and E. van der Graaf. A preliminary intercomparison of gamma-ray spectrometry on building materials. *Applied Radiation and Isotopes*, 61(2):381 – 388, 2004.

A.-J. Annema. *Feed-Forward Neural Networks: Vector Decomposition Analysis, Modelling and Analog Implementation*. Springer US, New York, USA, 2012.

I. Basheer and M. Hajmeer. Artificial neural networks: fundamentals, computing, design, and application. *Journal of Microbiological Methods*, 43(1):3 – 31, 2000.

A. Baumgartner, M. Stietka, F. Kabrt, H. Wiedner, and F. J. Maringer. Study of particular problems appearing in NORM samples and recommendations for best practice gamma-ray spectrometry. *Applied Radiation and Isotopes*, 126:285 – 288, 2017.

T. Beck, H. Buchröder, and V. Schmidt. Performance tests for instruments measuring radon activity concentration. *Applied Radiation and Isotopes*, 67(5):876 – 880, 2009.

R. Brettner-Messler, F. J. Maringer, P. Michai, and M. Kreuziger. Ergebnis der Vergleichsmessung für Gammaspektroskopiesysteme "BEV-Gammaring 2007" (Results of the intercomparison for gamma-ray spectroscopy systems "BEV-Gammaring 2007"). Report, Bundesamt für Eich- und Vermessungswesen, Vienna, Austria, 2007.

Bundesministerium für Nachhaltigkeit und Tourismus (BMNT). *Radonpotentialkarte Österreich (Map of Radon Potential in Austria)*, 2018. `https://www.bmnt.gv.at/umwelt/strahlen-atom/radon/radonpotenzial.html` [Accessed: 2018-09-01].

Bureau International des Poids et Mesures (BIPM). *Bureau International des Poids et Mesures*, 2018a. `https://www.bipm.org/en` [Accessed: 2018-10-25].

Bureau International des Poids et Mesures (BIPM). *Monographie BIPM-5: Table of radionuclides*, 2018b. `https://www.bipm.org/en/publications/scientific-output/monographie-ri-5.html` [Accessed: 2018-08-06].

C. Cosma, B. Papp, A. Cucoş (Dinu), and C. Sainz. Testing radon mitigation techniques in a pilot house from Băiţa-Ştei radon prone area (Romania). *Journal of Environmental Radioactivity*, 140:141 – 147, 2015.

Council of the European Union. *Consolidated Version of the Treaty establishing the European Atomic Energy Community*, 2010. `https://eur-lex.europa.eu/LexUriServ/LexUriServ.do?uri=OJ:C:2010:084:0001:0112:EN:PDF`.

Council of the European Union. *Council Directive 2013/59/EURATOM of 5 December 2013 laying down basic safety standards for protection against the dangers arising from exposure to ionising radiation*, 2013. `https://eur-lex.europa.eu/legal-content/EN/TXT/PDF/?uri=CELEX:32013L0059&from=EN`.

S. Darby, D. Hill, A. Auvinen, J. M. Barros-Dios, H. Baysson, F. Bochicchio, H. Deo, R. Falk, F. Forastiere, M. Hakama, I. Heid, L. Kreienbrock, M. Kreuzer, F. Lagarde, I. Mäkeläinen, C. Muirhead, W. Oberaigner, G. Pershagen, A. Ruano-Ravina, E. Ruosteenoja, A. S. Rosario, M. Tirmarche, L. Tomáscaron;ek, E. Whitley, H.-E. Wichmann, and R. Doll. Radon in homes and risk of lung cancer: collaborative analysis of individual data from 13 European case-control studies. *British Medical Journal*, 330:223–229, 2005.

S. Dragović, A. Onjia, S. Stanković, I. Aničin, and G. Bačić. Artificial neural network modelling of uncertainty in gamma-ray spectrometry. *Nuclear Instruments and Methods in Physics Research Section A: Accelerators, Spectrometers, Detectors and Associated Equipment*, 540(2):455 – 463, 2005.

European Commission. *Commission Recommendation of 20 December 2001 on the protection of the public against exposure to radon in drinking water supplies*, 2001. `https://eur-lex.europa.eu/legal-content/EN/TXT/PDF/?uri=CELEX:32001H0928&from=EN`.

European Association of National Metrology Institutes (EURAMET). *About us*, 2018. `https://www.euramet.org/about-euramet/` [Accessed: 2018-10-29].

European Commission (EC). *Effluent and dose control from European Union NORM industries: Assessment of current situation and proposal for a harmonised community approach. Volume 1: Main Report. Issue No. 135*, 2003. `https://ec.europa.eu/energy/sites/ener/files/documents/135.pdf` [Accessed: 2018-11-03].

H. Friedmann. Modell für die Entemanierung radioaktiver Lösungen. *Anzeiger der mathematisch-naturwissenschaftlichen Klasse der Österreichischen Akademie der Wissenschaften*, 7:120–125, 1977.

H. Friedmann. An inexpensive and highly sensitive method for continuous radon monitoring. *Radon et gaz rares dans les sciences de la terre et de l'environnement*, 32:268–273, 1992.

H. Friedmann, C. Atzmüller, C. Beck1, L. Breitenhuber, P. Brunner, K. Fink, K. Fritsche, D. Gottsbachner, E. Hamernik, W. Hofmann, R. Hover, M. Kafesie1, H. Kaineder, P. Karacson, V. Karg, P. Kindl, M. Kompatscher, C. Kralik, C. Kriha, J. Krischan, S. Lackner, H. Lettner, U. Mack, F. J. Maringer, L. Mossbauer, E. Nadschläger, K. Pock, W. Ringer, C. Schindler1, F. Schönhofer, P. Schönleitner, B. Schramml, T. Singer, S. Sperker, H. Stadtmann, F. Steger, F. Steinhäusler, M. Tschurlovits, I. Weilguni, W. Weiss, R. Weissenbök1, H. Wihlidal, R. Winkler, and P. Zimprich. Das österreichische nationale Radonprojekt – ÖNRAP – Projekt-Endbericht (The Austrian national radon project – final report). Final project report, Bundesministerium für Land- und Forstwirtschaft, Umwelt und Wasserwirtschaft; Bundesministerium für Gesundheit, Familie und Jugend, 2007.

Gammadata Instrument AB. *CANARY pro Data Sheet*, 2018. `http://www.gammadata.se/assets/Uploads/CANARY-pro-DataSheet-V2R1.pdf` [Accessed: 2018-08-17].

E. García-Toraño, V. Peyres, M.-M. Bé, C. Dulieu, M.-C. Lépy, and F. Salvat. Simulation of decay processes and radiation transport times in radioactivity measurements. *Nuclear Instruments and Methods in Physics Research Section B: Beam Interactions with Materials and Atoms*, 396:43 – 49, 2017.

G. Gilmore. *Practical Gamma-ray Spectrometry.* John Wiley & Sons, Ltd., Warrington, United Kingdom, 2008.

F. Grubbs and G. Beck. Extension of sample sizes and percentage points for significance tests of outlying observations. *Technometrics*, 14 (4):847 – 854, 1972.

A. Harms and C. Gilligan. Development of a neutron-activated concrete powder reference material. *Applied Radiation and Isotopes*, 68(7):1471 – 1476, 2010.

P. Howarth and F. Redgrave. Metrology – in short, 3$^{\text{rd}}$ edition). Euramet project 1011, EURAMET, 2008. `https://eur-lex.europa.eu/legal-content/EN/TXT/PDF/?uri=CELEX:32001H0928&from=EN` [Accessed: 2018-09-01].

S. Hurtado, M. García-León, and R. García-Tenorio. GEANT4 code for simulation of a germanium gamma-ray detector and its application to efficiency calibration. *Nuclear Instruments and Methods in Physics Research Section A: Accelerators, Spectrometers, Detectors and Associated Equipment*, 518(3):764 – 774, 2004.

International Agency for Research on Cancer (IACR). *IACR Monographs on the Evaluation of Carcinogenic Risks to Humans – Preamble*, 2006. `https://monographs.iarc.fr/wp-content/uploads/2018/06/CurrentPreamble.pdf` [Accessed:2018-08-29].

International Agency for Research on Cancer (IACR). *IACR Monographs on the Evaluation of Carcinogenic Risks to Humans – List of Classifications*, 2018. `https://monographs.iarc.fr/wp-content/uploads/2018/07/List_of_Classifications.pdf` [Accessed: 2018-08-29].

International Atomic Energy Agency (IAEA). *Nuclear Analysis Software Part 2: Gamma Spectrum Analysis, Activity Calculations and Neutron Activation Analysis (GANAAS).* International Atomic Energy Agency, Vienna, Austria, 1991.

International Atomic Energy Agency (IAEA). Extent of environmental contamination by naturally occurring radioactive material (NORM) and technological options for mitigation. Technical Reports Series No. 419, International Atomic Energy Agency, 2003. `https://www-pub.iaea.org/MTCD/publications/PDF/TRS419_web.pdf` [Accessed: 2018-10-31].

International Atomic Energy Agency (IAEA). Assessing the Need for Radiation Protection Measures in Work Involving Minerals and Raw Materials. Safety Report Series no. 49, International Atomic Energy Agency, 2006. `https://www-pub.iaea.org/MTCD/Publications/PDF/Pub1257_web.pdf` [Accessed: 2018-11-03].

International Atomic Energy Agency (IAEA). *Live Chart of Nuclides*, 2016. `https://www-nds.iaea.org/relnsd/vcharthtml/VChartHTML.html` [Accessed: 2016].

International Commission on Radiological Protection (ICRP). ICRP Publication 103 – The 2007 Recommendations of the International Committee on Radiological Protection. *Annals of the ICRP*, 32:88 ff, 2007.

ISO/IEC 17025:2017. General requirements for the competence of testing and calibration laboratories. Standard, International Organization for Standardization, Geneva, Switzerland, 2017.

J. C. Hardy and V. E. Iacob and M. Sanchez-Vega and R. T. Effinger and P. Lipnik and V. E. Mayes and D. K. Willis and R. G. Helmer. Precise efficiency calibration of an HPGe detector: source measurements and Monte Carlo calculations with sub-percent precision. *Applied Radiation and Isotopes*, 56:65 – 69, 2002.

V. Jobbágy, T. Altzitzoglou, P. Malo, V. Tanner, and M. Hult. A brief overview on radon measurements in drinking water. *Journal of Environmental Radioactivity*, 173:18 – 24, 2017.

Joint Committee for Guides in Metrology (JCGM). *International vocabulary of metrology – Basic and general concepts and associated terms (VIM) – 3rd edition*, 2012. `https://www.bipm.org/utils/common/documents/jcgm/JCGM_200_2012.pdf` [Accessed: 2018-09-01].

Joint Research Centre (JRC). *Atlas of Natural Radiation*, 2018. `https://remon.jrc.ec.europa.eu/About/Atlas-of-Natural-Radiation` [Accessed: 2018-09-01].

M. Kreuzer, N. Fenske, M. Schnelzer, and W. L. Lung cancer risk at low radon exposure rates in German uranium miners. *British Journal of Cancer*, 113(9):1367 – 1369, 2015.

C. Larijani, A. K. Pearce, P. Regan, B. Russell, S. M. Jerome, M. T. Crespo, P. de Felice, G. Lutter, F. Maringer, and M. Mazánová. Reference materials produced for a European metrological research project focussing on measurements of NORM. *Applied Radiation and Isotopes*, 126:279 – 284, 2017.

P. Maleka and M. Maučec. Monte Carlo uncertainty analysis of germanium detector response to γ-rays with energies below 1 MeV. *Nuclear Instruments and Methods in Physics Research Section A: Accelerators, Spectrometers, Detectors and Associated Equipment*, 538(1):631 – 639, 2005.

J. Mantero, M. J. Gázquez, S. Hurtado, J. P. Bolívar, and R. García-Tenorio. Application of gamma-ray spectrometry in a NORM industry for its radiometrical characterization. *Radiation Physics and Chemistry*, 116:78 – 81, 2015.

F. Maringer, M. Akis, H. Kaineder, P. Kindl, C. Kralik, H. Lettner, S. Lueginger, E. Nadschläger, W. Ringer, R. Rolle, F. Schönhofer, S. Sperker, H. Stadtmann, F. Steger, F. Steinhäusler, M. Tschurlovits, and R. Winkler. Results and conclusions of the Austrian radon mitigation project SARAH. *The Science of the Total Environment*, 272:159–167, 2001.

F. J. Maringer. State-of-the-art activity measurement and radionuclide metrology in radiation protection. *Proceedings of the Third European IRPA Congress*, pages 1818 – 1827, 2010.

F. J. Maringer. Final publishable JRP Summary for IND57 MetroNORM – metrology for processing materials with high natural radioactivity. EMRP publishable summary, EURAMET, 2016.

F. J. Maringer and A. Ramer. Mathematisch-statistische Auswertung des Ringvergleichs von Gammaspektrometriemeßplätzen "GAMMARING 97" hinsichtlich der Optimierung der radiometrischen Analytik von Umweltproben in Österreich (Mathematical-statistical evaluation of an intercomparison exercise for gamma-ray spectrometry systems "GAMMARING 97" for optimization of radiometric analysis of environmental samples in Austria). Report, Österreichisches Forschungs- und Prüfzentrum Arsenal, Vienna, Austria, 1997.

F. J. Maringer, A. Baumgartner, F. Cardellini, P. Cassette, T. Crespo, J. Dean, H. Wiedner, J. Hůlka, M. Hult, S. Jerome, F. Kabrt, P. Kovář, C. Larijani, G. Lutter, M. Marouli, A. Mauring, M. Mazánová, B. Michalik, N. Michielsen, V. Peyres, S. Pierre, R. Pöllänen, S. Pommé, M. Reis, M. Stietka, L. Szűcs, and B. Vodenik. Advancements in NORM metrology – Results and impact of the European joint research project MetroNORM. *Applied Radiation and Isotopes*, 126:273 – 278, 2017.

A. Mauring and T. Gäfvert. Radon tightness of different sample sealing methods for gamma spectrometric measurements of ^{226}Ra. *Applied Radiation and Isotopes*, 81:92 – 95, 2013.

M. Medhat. Artificial intelligence methods applied for quantitative analysis of natural radioactive sources. *Annals of Nuclear Energy*, 45:73 – 79, 2012.

J. Merešová, U. Wätjen, and T. Altzitzoglou. Determination of natural and anthropogenic radionuclides in soil – results of an European Union comparison. *Applied Radiation and Isotopes*, 70(9):1836 – 1842, 2012.

J. Miles. Methods of radon measurement and devices. *Proceedings of the 4th European conference on protection against radon at home and at work*, pages 304–312, 2004.

H. Moser and F. J. Maringer. A quick technique to improve the geometry characterisation of aged HPGe detectors for MC code efficiency calculation. *Applied Radiation and Isotopes*, 109:532 – 534, 2015.

H. Moser, V. Peyrés, M. Mejuto, and E. García-Toraño. Application of Artificial Neural Networks to the Analysis of NORM Samples. Informes técnicos CIEMAT - technical report no. 1375, CIEMAT, Madrid, Spain, 2015.

National Bureau of Standards (NBS). Permissible Dose from External Sources of Ionizing Radiation – Recommendation of the National Committee on Radiation Protection. Handbook 59, U.S. Department of Commerce, 1954. `https://inis.iaea.org/collection/NCLCollectionStore/_Public/37/048/37048204.pdf` [Accessed: 2018-11-08].

National Institute of Standards and Technology (NIST). *International Committee for Radionuclide Metrology (ICRM)*, 2018. `https://physics.nist.gov/ICRM/index.html` [Accessed: 2018-10-29].

National Research Council (NRC). *Risk Assessment of Radon in Drinking Water.* National Acedemy Press, Washington, D.C., USA, 1999.

A. Negarestani, S. Setayeshi, M. Ghannadi-Maragheh, and B. Akashe. Layered neural networks based analysis of radon concentration and environmental parameters in earthquake prediction. *Journal of Environmental Radioactivity*, 62(3):225 – 233, 2002.

K. Newrkla, H. Wiedner, and F. J. Maringer. A radioecological study of radon and thoron in soil gas and water. *Proceedings of the Third European IRPA Congress*, 2018.

Nucleide. *Decay Data Evaluation Project*, 2016. `http://www.nucleide.org/DDEP.htm]` [Accessed: 2016].

Nucleide. *Decay Data Evaluation Project*, 2018. `http://www.nucleide.org/DDEP.htm]` [Accessed: 2018-08-06].

F. Padilla Cabal, N. Lopez-Pino, J. L. Bernal-Castillo, Y. Martinez-Palenzuela, J. Aguilar-Mena, K. D'Alessandro, Y. Arbelo, Y. Corrales, and O. Diaz. Monte Carlo based geometrical model for efficiency calculation of an n-type HPGe detector. *Applied Radiation and Isotopes*, 68(12):2403 – 2408, 2010.

J. H. Park, S. Whang, H. Y. Lee, C.-M. Lee, and D. R. Kang. Measurement and modeling of indoor radon concentrations in residential buildings. *Environmental Health and Toxicology*, 33(1), 2018.

D. Peck and A. Linsberger. Baden im Übergang – naturräumliche Analyse (Baden changing – Analysis of natural landscapes). Projekt 2 – Kommunale Entwicklungs- und Flächenwidmungsplanung WS2009/SS2010, Technical University of Vienna, 2007. `https://eur-lex.europa.eu/legal-content/EN/TXT/PDF/?uri=CELEX:32001H0928&from=EN` [Accessed: 2018-09-01].

V. Peyres and E. García-Toraño. Efficiency calibration of an extended-range Ge detector by a detailed Monte Carlo simulation. *Nuclear Instruments and Methods in Physics Research Section A: Accelerators, Spectrometers, Detectors and Associated Equipment*, 580(1):296 – 298, 2007.

M. Rafiq, G. Bugmann, and D. Easterbrook. Neural network design for engineering applications. *Computers & Structures*, 79(17):1541 – 1552, 2001.

Á. Rodríguez-Martínez, M. Torres-Durán, J. M. Barros-Dios, and A. Ruano-Ravina. Residential radon and small cell lung cancer. A systematic review. *Cancer Letters*, 426:57 – 62, 2018.

H. Rühle. *Radon in unserer Umwelt und die damit verbundene Strahlenexposition der Bevölkerung (Radon in our environment and subsequent radiation exposure of the population).* Schriftenreihe des Vereins für Wasser-, Boden- und Lufthygiene, 1997.

F. Salvat. The PENELOPE code system. Specific features and recent improvements. *Annals of Nuclear Energy*, 82:98 – 109, 2015.

A. Shakhashiro, U. Sansone, H. Wershofen, A. Bollhöfer, C. Kim, C. Kim, M. Korun, M. Moune, S. Lee, and S. Tarjan. Technically enhanced naturally occurring radionuclides (TENORM) in phosphogypsum. *Metrologia*, 47 (Tech.Suppl.):201 – 213, 2010.

A. Shakhashiro, U. Sansone, H. Wershofen, A. Bollhöfer, C. Kim, C. Kim, G. Kis-Benedek, M. Korun, M. Moune, S. Lee, S. Tarjan, and M. Al-Masri. The new IAEA reference material: IAEA-434 technologically enhanced naturally occurring radioactive materials (TENORM) in phosphogypsum. *Applied Radiation and Isotopes*, 69(1):231 – 236, 2011.

J. Šolc, P. Dryǎk, H. Moser, T. Branger, E. García-Toraño, V. Peyrés, F. Tzika, G. Lutter, M. Capogni, A. Fazio, A. Luca, B. Vodenik, C. Oliveira, A. Saraiva, L. Szucs, T. Dziel, O. Burda, D. Arnold, J. Martinkovičolc, T. Siiskonen, and A. Mattila. Characterisation of a radionuclide specific laboratory detector system for the metallurgical industry by Monte Carlo simulations. *Radiation Physics and Chemistry*, 116:189 – 193, 2015.

F. Tzika, O. Burda, M. Hult, D. Arnold, B. C. Marroyo, P. Dryák, A. Fazio, L. Ferreux, E. García-Toraño, A. Javornik, S. Klemola, A. Luca, H. Moser, M. Nečemer, V. Peyrés, M. Reis, L. Silva, J. Šolc, A. Svec, Z. Tyminski, B. Vodenik, and U. Wätjen. ^{60}Co in cast steel matrix: A European interlaboratory comparison for the characterisation of new activity standards for calibration of gamma-ray spectrometers in metallurgy. *Applied Radiation and Isotopes*, 114:167 – 172, 2016.

United Nations Scientific Committee on the Effects of Atomic Radiation (UNSCEAR). Sources and effects of ionizing radiation. Volume I: Sources - UNSCEAR 2008 Report to the General Assembly with Scientific Annexes. Technical report, United Nations Publication, 2010.

United States Environmental Protection Agency (US EPA). *Radon-Resistant Construction Basics and Techniques*, 2017. `https://www.epa.gov/radon/radon-resistant-construction-basics-and-techniques` [Accessed: 2018-10-25].

H. Wiedner. Publishable JRP Summary for 16ENV10 MetroRADON – Metrology for radon monitoring. EMPIR publishable summary, EURAMET, 2018.

H. Wiedner, V. Peyrés, T. Crespo, M. Mejuto, and E. G.-T. F. J. Maringer. Application of an artificial neural network for evaluation of activity concentration exemption limits in NORM industry. *Applied Radiation and Isotopes*, 126:289 – 292, 2017.

H. Wiedner, K. Lotter, P. Karner, H. Friedmann, and F. Maringer. Radon in drinking water: Comparison and evaluation of two ionisation chamber activity measurement methods. *Applied Radiation and Isotopes*, 134:477 – 481, 2018a.

H. Wiedner, J. Riedl, F. Maringer, A. Baumgartner, M. Stietka, and F. Kabrt. Production and characterization of a traceable NORM material and its use in proficiency testing of gamma-ray spectrometry laboratories. *Applied Radiation and Isotopes*, 134:45 – 50, 2018b.

World Health Organisation (WHO). *WHO Handbook on Indoor Radon – A Public Health Perspective.* WHO Press, Geneva, Switzerland, 2009.

World Health Organisation (WHO). *WHO Guidelines for Indoor Air Quality – Selected Pollutants.* The Regional Office for Europe of the World Health Organization, Copenhagen, Denmark, 2010.

World Health Organisation (WHO). *WHO Guidelines for Drinking Water Quality – Fourth Edition.* WHO Press, Geneva, Switzerland, 2011.

M. Z. Živanović, J. D. Nikolić, A. I. Apostol, and M. J. Anagnostakis. Analysis of interferences from full energy peaks in gamma-spectrometry of NORM and TENORM samples. *Nuclear Technology & Radiation Protection*, 27:380 – 387, 2012.

6 Peer-reviewed international journal papers

6.1 Paper one

Application of an Artificial Neural Network for evaluation of activity concentration exemption limits in NORM industry

Hannah Wiedner, Virginia Peyrés, Teresa Crespo, Marcos Mejuto, Eduardo García-Toraño, Franz Josef Maringer

Applied Radiation and Isotopes
Volume 126, August 2017, Pages 289-292
http://dx.doi.org/10.1016/j.apradiso.2016.12.044

Application of an Artificial Neural Network for evaluation of activity concentration exemption limits in NORM industry

Hannah Wiedner[1,*], Virginia Peyrés[2], Teresa Crespo[2], Marcos Mejuto[2], Eduardo García-Toraño[2], Franz Josef Maringer[1]

[1] *BEV – Federal Office of Metrology and Surveying, Arltgasse 35, 1160 Wien, Austria*

[2] *CIEMAT – Centro de Investigaciones Energéticas, Medioambientales y Tecnológicas, Avda. Complutense 40, 28040 Madrid, Spain*

[*] *Corresponding author. E-mail address: hannah.wiedner@bev.gv.at (H. Wiedner).*

Abstract

NORM emits many different gamma energies that have to be analysed by an expert. Alternatively, artificial neural networks (ANNs) can be used. These mathematical software tools can generalise “knowledge” gained from training datasets, applying it to new problems. No expert knowledge of gamma-ray spectrometry is needed by the end-user. In this work an ANN was created that is able to decide from the raw gamma-ray spectrum if the activity concentrations in a sample are above or below the exemption limits.

Keywords

Artificial neural network; ANN; Exemption limit; NORM; Monte Carlo; Gamma-spectrometry; PENELOPE; PENNUC

Highlights

- Artificial Neural Networks are well-suited for evaluation of exemption limits
- 635 artificial spectra where produced using Monte Carlo code PENELOPE
- Training different ANNs confirmed the validity of the 2n+1 rule
- Introduction of new parameter (sample mass) leads to better regression

Introduction

Naturally occurring radionuclides like ^{40}K and the decay products of the primordial radionuclides ^{232}Th, ^{235}U and ^{238}U are present in many natural resources. Naturally occurring radioactive materials (NORM) containing these radionuclides are exploited industrially and often exceed the exemption limits of the activity concentration. These industrial activities generate a significant portion of waste, possibly enhancing the potential of exposure of workers and the public. Furthermore, the management and deposition of material above the exemption limit is very costly, making the careful evaluation of activity content one of the crucial challenges when dealing with NORM. The main problem with analysing NORM lies in the variety of compositions and densities of the materials. NORM emits many (interfering) gamma-rays of different energies that have to be analysed by an expert. The evaluation of activity content in a sample also requires the detector to be properly calibrated in terms of energy and efficiency response. The detection efficiency highly depends on source-to-detector and sample geometry, amount and composition of sample material and energy of the gamma-rays to be measured. Self-attenuation of the gamma-rays due to the sample material has to be considered. The individual detection efficiency of each sample has to be determined, either by using standard sources or mathematical models. Within the European Metrology Research Project MetroNORM, that focuses on creating traceable, accurate and standardised measurement methods, reference materials and systems for application in the concerned industries, an artificial neural network (ANN) was created that is able to decide from the data of a raw gamma spectrum if a NORM material is above or below the exemption limit, avoiding the rather complex analysis associated to spectral deconvolution.

Artificial Neural Networks (ANNs)

ANNs imitate the way the human brain works. In the human brain, a number of biological neurons each generate a signal of an intensity x and a synaptic feeding strength w. These signals feed into a neuron with a threshold b using dendrites and axons. If the product of x and w is below the threshold, the neuron does not recognize the input. If the product is above the threshold, the neuron computes the inputs and generates a signal y that can again be an input to another neuron (Basheer and Hajmeer, 2000). An ANN consists of a number of nodes that represent the computing units (or neurons), connections (axons and dendrites) between those nodes, connection weights (synapses) and thresholds (activity in the soma). An ANN contains an input and an output layer and can also include one or more hidden layers. Each layer contains a number of nodes. A non-linear transfer function, often a sigmoidal function, is applied to the weighted sums of each “neuron”, signifying the significance of the information (connection weight). Fig. 1 illustrates the process. Networks with no hidden layer are only able to perform linear tasks (Negarestani et al., 2002) while a second hidden layer is only necessary for discontinuous problems (Rafiq et al., 2001).

Depending on the problem, an even greater number of hidden layers may be necessary. The number of input neurons is defined by the number of input parameters and the number of output neurons reflects the number of output variables. The optimal number of neurons in the hidden layer has to be obtained. In order to keep the mean squared error as low as possible, the number of hidden neurons should be minimized. This is usually done by employing a trial-and-error method. Medhat (Azoff, 1994 in Medhat, 2012) mentions in his work a 2n+1 rule, suggesting that with a number of n input neurons, 2n+1 hidden neurons should be sufficient for any network. The network is trained by providing it with a number of inputs and the corresponding outputs. Unless reliable apriori information is available, the

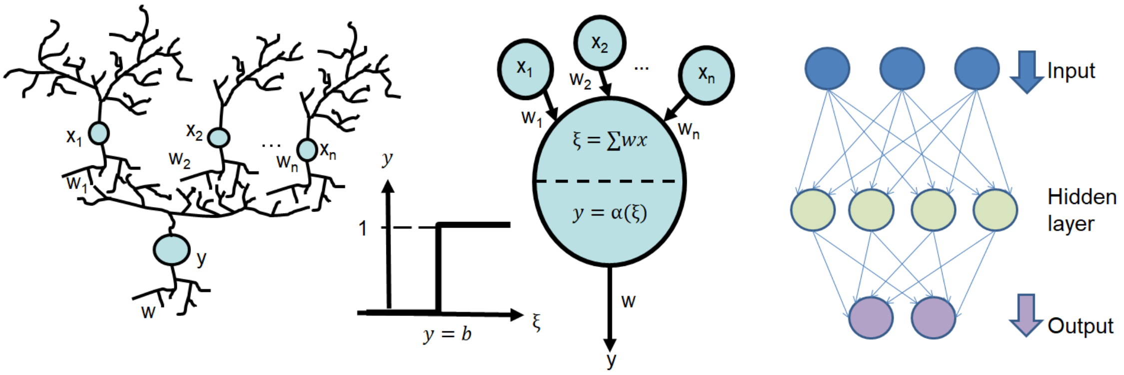

Fig. 1. Left: Basic processes in human brain. Right: ANN schematic.

network algorithm starts out with random connection weights that are changed after each training cycle to reflect the wanted output. Literature research (e.g. Dragović et al., 2005) shows that the most commonly used algorithm to adapt the weights is the backpropagation algorithm that uses the difference between the ANN solution and the actual solution of the training example that is provided for the training process to change the connection weights. ANNs trained in that style are capable of learning and can apply their "knowledge" to unknown situations. The main advantage of such a network is its ability to generalize and handle imprecise and noisy information. This process can be considered as a robust alternative to a classical calibration method. Since only a limited number of samples and materials was available and the aim of this work was to study the feasibility of using ANNs in this context, the ANN was trained for a predefined list of radionuclides and materials relevant to NORM. The spectra are analysed for six radionuclides typically found in NORM materials and representing the three naturally occurring decay chains. Although the nuclides considered for analysis emit several gamma lines, it was decided to analyse only lines free from interferences with other lines.

Measurement Setup

The measurement system used for this project is based on a Canberra Industries GX4020 extended-range coaxial detector with 45.4 % relative efficiency and a carbon-epoxy window. This kind of detectors can extend the usual energy range of Ge detectors down to a few keV. The electronic setup includes a high-voltage power supply from BERTAN, preamplifier, spectroscopy amplifier and pulse generator from CANBERRA and a successive-approximation analog-to-digital converter from SILENA. A prismatic shielding structure of about 80 x 80 x 80 cm surrounds the detector. It is composed by layers of Pb (5 cm), Cd (3 mm) and Cu (1.5 mm) (Peyres and García-Toraño, 2007). The software used for spectrum acquisition is SILENA International SpA EMCA2000 MCA Emulation Software (2000). The peak area was calculated by a non-linear code (GRILS) included in the GANAAS package

(International Atomic Energy Agency, 1991), which is freely distributed by the International Atomic Energy Agency.

Training Samples

To train an ANN that correctly predicts the output, representative samples have to be used as training input. Therefore, artificial spectra of the available materials have been created using the Monte Carlo code PENELOPE v.2014 (Salvat et al., 2001) and CIEMAT's add-on PENNUC (García-Toraño et al., Submitted for publication) in order to cover a wider range of experimental conditions, make up for the limited number of real sample material and provide the network with more training examples. The artificial spectra differ from the original gammaray spectra in density of the sample, radionuclide composition and activity concentration. This requires intensive study of equilibrium and disequilibrium situations and careful sample preparation. With PENNUC the simulation process involves all particles in a cascade, whereas PENELOPE on its own simulates each particle separately. Therefore, coincidence summing and correction factors are not separately calculated, but an integral part of the whole efficiency calculation. The real samples were analysed in CIEMAT's chemical laboratory, carefully weighted and prepared using polypropylene containers. The containers were selected and tested using the radon diffusion coefficient of several materials that were determined using the method described by Jiránek and Hůlka (2000). After equilibrium had been reached (21 days) the samples were measured on CIEMAT's GX4020 detector. To gain significant results, the real materials were measured for 200,000 s on the detector while a number of 5.00E+08 showers have been simulated for each radionuclide and density, amounting to a total number of 126 simulations. After separately calculating the efficiency for each radionuclide, material and density using PENELOPE and PENNUC, the spectra are convoluted with a Gaussian curve whose width is a function of energy in order to reproduce the system's response and include electronic noise. The calculated data of each material and radionuclide was multiplied by the target activity and combined in order to gain one synthetic spectrum per material, density and activity concentration that includes all radionuclides as in a real spectrum. The artificial samples for both equilibrium and disequilibrium states were classified using five nonlinearly spaced categories of activity content, minimizing the total number of samples and relying on the power of the ANN to intrapolate to the missing data. Category 1 corresponds to an activity well below the exemption limit (0.1 Bq), while categories 2 and 3 correspond to an activity a little below (0.7 Bq) or of 1 Bq/g (Council of the European Union, 2013), respectively. Categories 4 and 5 correspond to activities a little above (1.2 Bq) and well above (20 Bq) the exemption limit. That way a total number of 635 artificial spectra with varying distributions of activity concentration have been generated as training input to the ANN. To generate the artificial spectra and train the ANN, the software package Matlab has been used.

Results

The final structure of the input is a matrix (635 x 15) where the rows represent the sample and the columns the individual lines to be analysed, followed by information on density, material and sample mass. The ANN's output layer consists of 12 nodes, each one corresponding to one analysed line. The best results (Table 1) were obtained using an ANN with 15 input nodes, one hidden layer, 31 hidden neurons and 12 output nodes using a backpropagation algorithm and a sigmoidal transfer function based on a logarithm. The ANN was tested using six real gamma-spectra. Introduction of the sample weight as an input parameter caused regression to get significantly better. The output of the ANN agrees very well with the manually assigned activity categories gained through gamma-ray spectrometry. Training the ANN for 91 epochs and then retraining with the same training data resulted in an ANN with an overall regression factor of 0.9975. Good converconvergence of the output can be observed. Fig. 2 shows Matlab's training plot.

Table 1. ANN output (activity category) for each of the six testing materials.

Radionuclide	**γ-ray energy (keV)**	**TiO_2**	**Sand**	**Phosphogypsum Huelva**	**Phosphogypsum MetroNORM**	**Ilmenite**	**Tuff**
^{210}Pb	46.6500	4.1290	1.1106	2.3224	1.1028	1.0873	1.4027
^{234}Th	63.3100	1.0005	1.1162	1.2007	1.0976	1.0721	1.5760
	92.5900*	1.0006	1.1165	1.1992	1.0967	1.0720	1.5747
^{235}U	143.7700	1.0000	1.0843	1.2183	1.0696	1.0565	1.1353
	163.3600	1.0000	1.0841	1.2213	1.0701	1.0562	1.1353
^{212}Pb	238.6300	5.0000	1.0487	1.0569	1.0966	1.2138	1.2004
	300.0900	5.0000	1.1069	4.1687	1.1735	1.0686	1.2905
^{214}Pb	242.0000	5.0000	1.1106	4.1404	1.2009	1.0744	1.3819
	295.2200	5.0000	1.0478	1.0586	1.1147	1.2061	1.2637
	351.9300	5.0000	1.1073	4.1697	1.1724	1.0694	1.2908
^{228}Ac	911.2000	5.0000	1.0458	1.0774	1.1386	1.2256	1.2389
	968.9600	5.0000	1.0459	1.0774	1.1386	1.2243	1.2399

*combination of 2 lines that are not well separated: 92.38 keV and 92.80 keV

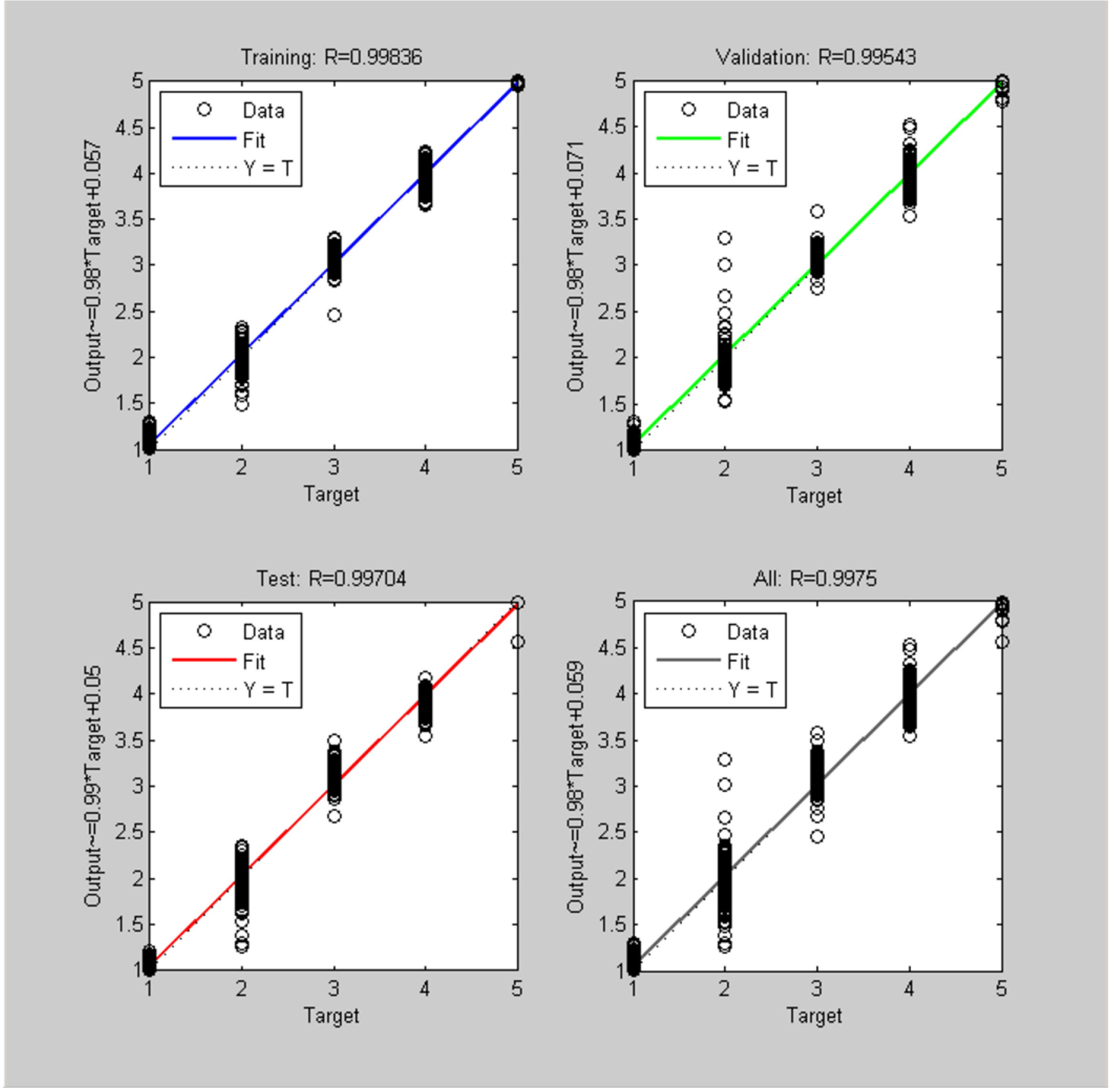

Fig. 2. Performance plot after retraining.

Conclusion

This study was undertaken to find out if ANNs can be applied to the problem of determining if the activity concentration in a sample is above or below the exemption limit. It was shown, that the ANN was able to correctly classify all of the testing materials and ANNs are wellsuited to carry out this task. The lack of real sample material has been sidestepped by calculating artificial spectra using Monte Carlo simulations which necessitates the complicated and time-consuming study of disequilibrium situations. For specialized industries where only one material has to be analysed and a large number of sample spectra are available as training input, the authors propose the use of an ANN specifically trained to only that purpose. For the end-user only a gamma spectrum in ASCII format and no specialized knowledge whatsoever in the field of gamma-ray spectrometry is required.

Acknowledgements

This work has been supported by the European Metrology Research Programme (EMRP), JRP-Contract IND57 MetroNORM (www.emrponline.eu). The EMRP is jointly funded by the EMRP participating countries within EURAMET and the European Union. Hannah Wiedner received an Early Stage Researcher Mobility Grant associated to MetroNORM to complete this work. Thanks are given to the staff of CIEMAT's analysis laboratories characterized the material used in this study.

References

Council of the European Union, 2013. COUNCIL DIRECTIVE 2013/59/Euratom of 5 December 2013 laying down basic safety standards for protection against the dangers arising from exposure to ionising radiation. Annex VII, Table B. Official Journal of the European Union, Brussels.

Basheer, I.A., Hajmeer, M., 2000. Artificial neural networks: fundamentals, computing, design, and application. J. Microbiol. Methods 43, 3–31.

Negarestani, A., et al., 2002. Layered neural networks based analysis of radon concentration and environmental parameters in earthquake prediction. J. Environ. Radioact. 62, 225–233.

Rafiq, M.Y., et al., 2001. Neural network design for engineering applications. Comput. Struct. 79, 1541–1552.

Medhat, M.E., 2012. Artificial intelligence methods applied for quantitative analysis of natural radioactive sources. Ann. Nucl. Energy 45, 73–79.

Dragović, S., et al., 2005. Artificial neural network modelling of uncertainty in gammaray spectrometry. Nucl. Instrum. Methods Phys. Res. A 540, 455–463.

Peyres, V., García-Toraño, E., 2007. Efficiency calibration of an extended-range Ge detector by a detailed Monte Carlo simulation. Nucl. Instrum. Methods Phys. Res. A 580, 296–298.

International Atomic Energy Agency, 1991. Nuclear analysis software, Part 2. Gamma spectrum analysis, activity calculations and neutron activation analysis (GANAAS), Vienna.

Salvat, F.. et al. 2001. PENELOPE. A code system for Monte Carlo Simulation of electron and photon transport. In: Proceedings of a Workshop/Training Course, OECD/NEA 5-7 November 2001 NEA/NSC/DOC(2001)19.

García-Toraño, E., et al. Simulation of decay processes and radiation transport times in radioactivity measurements, to be submitted for publication to Nucl Instr and Meth B.

Jiránek, M., Hůlka, J., 2000. Radon diffusion coefficient in radon-proof membranes – determination and applicability for the design of radon barriers. Int. J. Archit. Sci. 1 (4), 149–155.

6.2 Paper two

Production and characterization of a traceable NORM material and its use in proficiency testing of gamma-ray spectrometry laboratories

H. Wiedner, J. Riedl, F.J. Maringer, A. Baumgartner, M. Stietka, F. Kabrt

Applied Radiation and Isotopes
Volume 134, April 2018, Pages 45-50
http://dx.doi.org/10.1016/j.apradiso.2017.09.025

Production and characterization of a traceable NORM material and its use in proficiency testing of gamma-ray spectrometry laboratories

H. Wiedner[a,b,*], J. Riedl[c], F.J. Maringer[a,b,c], A. Baumgartner[b], M. Stietka[b], F. Kabrt[b]

[a] *BEV – Bundesamt für Eich- und Vermessungswesen, Arltgasse 35, 1160 Wien, Austria*
[b] *BOKU – University for Natural Resources and Life Sciences, Gregor-Mendel-Straße 33, 1180 Wien, Austria*
[c] *TU Wien – Technical University of Vienna, Karlsplatz 13, 1040 Wien, Austria*
[*] *Corresponding author at: BEV – Bundesamt für Eich- und Vermessungswesen, Arltgasse 35, 1160 Wien, Austria. E-mail address: hannah.wiedner@bev.gv.at (H. Wiedner).*

Abstract

This paper outlines the process of characterizing a new NORM material for proficiency testing made of quartz sand with significantly elevated levels of ^{226}Ra obtained from the backflush of a drinking water treatment facility. Samples of the fully characterized NORM material were sent to European laboratories concerned with radioactivity measurements and environmental monitoring by gamma-ray spectrometry for proficiency testing. The paper discusses the results, specific requirements, problems and solutions that were found during the characterization process and the proficiency test.

Keywords

Environmental radioactivity; Gamma-ray spectrometry; NORM; Reference material; Intercomparison; Interlaboratory comparison; Proficiency testing; Quartz sand; Drinking water treatment; Natural radionuclides

Highlights

- A traceably characterized NORM material was produced and studied.
- The NORM material is made of quartz sand from a drinking water production site.
- A proficiency test with the new material was conducted.
- The samples were measured using high-resolution gamma-ray spectrometry.
- The paper outlines common problems with regard to proficiency tests of NORM.

Introduction

Naturally occurring radionuclides, such as ^{40}K and the decay products of the primordial radionuclides ^{232}Th, ^{235}U and ^{238}U are present in many natural resources. Those radionuclides are responsible for the ever present background radiation that results in radiation doses of a few millisieverts per year (UNSCEAR, 2010). (Technologically enhanced) Naturally occurring radioactive materials ((TE)NORM) containing these radionuclides are exploited by industrial endeavours or used as building materials and often exceed the exemption limits of the activity concentration for radionuclides of the U and Th series, depending on mineral composition and geological origin (Maringer et al., 2010). Those industrial and public activities are generating a significant portion of NORM waste and can enhance the potential of radiation exposure of workers and the public, therefore, necessitating a careful determination of activity concentration. Correct quantification of activity concentration and environmental monitoring require high methodical and metrological standards in the respective laboratories (Maringer, 2010). In order to correctly quantify the activity concentration in a sample with unknown activity it is necessary to perform a robust efficiency calibration. This can of course be done mathematically, but exact knowledge of one's measuring system is required as well as the exact sample composition, both of which are often unavailable. Another option is the use of traceable certified reference materials. After the detection system has been calibrated using the reference material, the activity of the unknown sample can be determined through comparison with the reference material. This is only valid, if the sample and the calibration source are similar, or, ideally, of the same composition and geometry (Gilmore, 2008).

There are basically two different kinds of reference materials in existence. Firstly, reference materials that have a simplified matrix, like pure water, and are artificially spiked with a known activity, and secondly, reference materials made from real sample material with a complex matrix depending on the origin of the material that is either naturally rich in radioactive substances or activity concentrations are enhanced by technological endeavours, but can also be spiked. While, on one hand, traceability can usually be ensured easily for the spiked materials, that process can be quite difficult for the naturally occurring materials. On the other hand, reference materials with a simple matrix are often very different from the real samples in terms of composition and density, impeding accurate evaluation of their activity concentration by comparison with the reference materials (Larijani et al., 2017). To simply transfer the efficiency calibration obtained with a simplified matrix can – depending on the composition of the unknown sample – lead to a wrong estimation of activity concentration, due to neglect of factors like the self-absorption of the material. This, in turn, can lead to potentially dangerous situations or entail expensive repercussions because decisions concerning radiation protection, waste disposal, etc. were made based on erroneous measurement results. For the traceable determination of activity concentrations in (TE)NORM, reference materials with a well-established activity concentration as well as a realistic sample matrix are essential.

In Austria and many other countries, accredited laboratories concerned with gamma-ray spectrometric measurements are obligated to participate in intercomparison exercises or proficiency tests in order to prove their competence in the field and prove periodically conformity with the quality and competence requirements of the ISO 17025 standard. In the past, BEV has organised a number of comparison exercises with matrices spiked with ^{57}Co, ^{60}Co and ^{137}Cs and while proficiency in general was high for these "standard radionuclides", the evaluation of activity concentrations for samples with densities $\neq 1$ g/cm^3 and radionuclides of the natural decay chain is much more complex. Many of the radionuclides of the natural decay chains have a number of different emission lines, most with very low emission probabilities, or cannot be directly evaluated using gamma-ray spectrometry. This requires long measurement times and a low background environment, and other factors, like sample equilibrium, have to be considered. Additionally, many of the lines show significant interference with the lines of other nuclides which makes the evaluation of the activity concentration much more complex (Baumgartner et al., 2017) and suitable reference materials are needed.

For this study, a NORM material for proficiency testing was made of quartz sand taken from a drinking water treatment facility in Lower Austria. For the characterization process, methods developed in the European Metrology Joint Research Project EMRP IND57 MetroNORM "Metrology for processing materials with high natural radioactivity" (Maringer et al., 2017) were used. MetroNORM focused on creating traceable, accurate, and standardized measurement methods, reference materials and systems for application in the concerned industries. The NORM material was sent to various laboratories concerned with radioactivity measurements and environmental monitoring, where the activity concentration for ^{40}K, ^{226}Ra and ^{228}Ra was evaluated in the respective laboratory's customary measurement geometry.

Gamma-ray spectrometry detector setup for characterization of the NORM material at BEV

Measurements were conducted with a Canberra Industries HPGe GC3020 p-type standard electrode coaxial germanium detector (crystal diameter: 56 mm, crystal height 54 mm; rel. eff.: 26.8 %, peak to Compton ratio: 58:1; FWHM: 1770 eV at 1332 keV, 834 eV at 122 keV) inside an aluminium end cap and equipped with a lead shielding (100 mm Pb, 1 mm Cd, 1 mm Cu) for verifying homogeneity of the final samples as well as for establishing the reference values. The spectra were analysed with Canberra's Genie2000 software. The detector system is traceably calibrated using standard solutions standardized with the Austrian national standard for activity, an ISOCAL IV ionization chamber traceably calibrated at the National Physical Laboratory (NPL), UK and traceably calibrated reference point sources manufactured by Physikalisch-Technische Bundesanstalt (PTB).

Table 1. Comparison of activity concentration of two grain size fractions of one test sample.

Grain size fraction	^{226}Ra (Bq/kg)	u_{rel} (%)	^{228}Ra (Bq/kg)	u_{rel} (%)	^{210}Pb (Bq/kg)	u_{rel} (%)
0.8–2 mm	999	23	1080	5	131	6
$<$0.56 mm	8660	6	7670	5	710	6

Origin of the material

The material for the proficiency test has been taken from the backflush of a drinking water treatment facility in Lower Austria, in a region where the water contains significantly elevated levels of ^{226}Ra due to the underlying geological conditions. Magmatite, granite and clastic sediments such as clays, gravel, and sand predominate. The water is rich in iron and manganese. At the treatment facility, drinking water is oxygenated, causing iron and manganese (usually in the form of hydrogen carbonates) to oxidize. The water is then passed through a bed of quartz sand acting as a filter where the hydroxides of iron and manganese, as well as of radium, precipitate. A filter holding back the sand closes off the system. Once a month, this filter is cleaned by flushing water in the reverse direction. The result of this water treatment process is a quartz sand rich in ^{226}Ra that has been used as a material in this study.

Sample treatment and homogeneity

The original material taken from the drinking water production plant was roughly homogenized, dried at 105 °C and sifted by passing it over screens of varying size to remove any other material. After drying again for a week at 105 °C, the sand was carefully homogenized using a three-dimensional shaker mixer WAB Turbula T2F.

Preliminary gamma-spectrometric measurements were performed in order to check for homogeneity issues in the quartz sand. This was done by measuring count rates for the 46.5 keV line of ^{210}Pb, 1460.8 keV line of ^{40}K, 186.2 keV line of ^{226}Ra as well as the 583.4 keV and 911.2 keV lines of ^{228}Ac for different grain size fractions. The results showed that the samples were not homogeneous and further homogenisation steps were necessary. Upon further testing it was concluded that the very fine grain size portion ($<$ 0.56 mm) causes problems with homogeneity. Preliminary measurements showed that the activity concentration in the very fine-grained fraction ($<$ 0.56 mm) of the sample material is much higher (see Table 1). Therefore, only material with a grain size between 0.8 mm and 2 mm was used to prepare the samples. 200.00 g ± 1.00 g portions of the grain size fraction of (0.8–2) mm were filled into cylindrical polypropylene sample containers ($r = 3.4$ cm, $h = 7.7$ cm) to produce the samples for the proficiency test.

The homogeneity of the sample collective was studied only between containers, not within containers, by comparison of the count rates of the aforementioned lines. Measurement times for the homogeneity testing varied between 7 h and 12 days, depending on laboratory use. Fig. 1 gives the weighted mean of the relative deviations of all considered energy lines (see above) of the respective radionuclide for each sample.

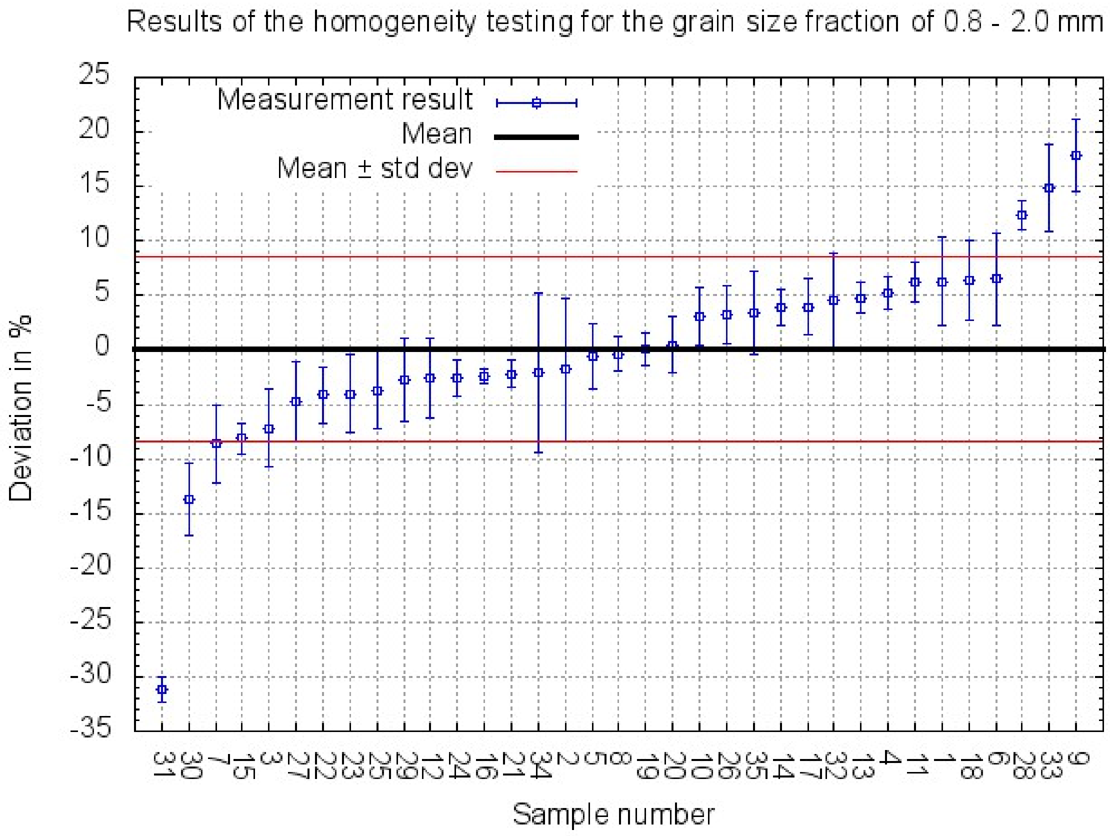

Fig. 1. Results of the homogeneity testing for the quartz sand samples (grain size fraction 0.8–2 mm) for ^{40}K, ^{226}Ra and ^{228}Ra combined, measured directly and via its progeny (see text).

The final uncertainties of the respective sums of relative deviations are calculated using Gaussian propagation of uncertainties.

According to the results of the homogeneity testing of the samples of grain size fraction 0.8–2 mm, the samples 9, 28, 30, 31 and 33 were deviating from the mean at an unacceptable level and eliminated. The eliminated samples show a trend to higher numbers and, therefore, later sample preparation. It is suspected that due to strong manual handling during sample preparation a mechanical disfractioning of the fine-grained, dust-like material from the larger sand particles occurred, causing inhomogeneity in some samples. This specific property of the material was explicitly communicated to the participating laboratories to be taken into account when handling the samples in the laboratories.
Very good homogeneity can only be achieved by finely grinding the material. This was neglected in this study as the aim was to preserve the natural matrix of the material and

create a material as realistic as possible for the use in smaller laboratories that do not have the resources and means (time as well as equipment and money) for complex sample preparation like grinding their samples. Cursory sample stability measurements taken over the course of a few weeks suggested qualitatively that the material is sufficiently stable as PT sample.

Chemical analysis and radionuclide reference values

The chemical analysis of the sample material for correct efficiency calibration (e.g. using Monte Carlo methods, efficiency transfer methods, etc.) was conducted with wavelength dispersive x-ray fluorescence analysis (WDXRF) using a Panalytical Zetium PW 5400 spectrometer. The sample was finely ground using a disc mill with a corundum inlay. Without any further treatment, one part was pressed into a pill with 40 mm diameter and analysed using WDXRF and the software UniQuant. Additionally, the loss on ignition (LOI) at 1 000 °C was evaluated to determine the content of organic matter (carbon, hydrates) in the sample material. The results of the chemical analysis are stated in Table 2. As expected, a high concentration of silicon dioxide from the sand filter matrix was detected. Additionally, aluminium oxide, potassium oxide and iron oxide, as well as manganese oxide are found due to their occurrence in the source water before the water treatment process. The traceable reference values of the NORM radionuclides were established by BEV (the National Metrology Institute of Austria) as (0.605 ± 0.024) Bq/g ^{40}K, (1.003 ± 0.015) Bq/g ^{226}Ra, and (0.806 ± 0.013) Bq/g ^{228}Ra (105 °C dry weight basis).

Discussion of proficiency test

Samples of quartz sand that were deemed homogenous were sent to nine European laboratories concerned with radioactivity measurements and environmental monitoring. The laboratories received one to four samples of 200 g each, depending on their requested amount of material. According to the proficiency test protocol, the sample material was dried at 105 °C at the laboratories and then transferred into the respective laboratory's preferred measurement container where the activity concentration of ^{40}K, ^{226}Ra and ^{228}Ra was determined on HPGe detectors according to the laboratories' quality management procedures. Table 3 gives details of the used detector systems as provided by the respective laboratories. Due to an ambiguous translation in the reporting form some laboratories reported the density of the container material instead of the density of the sample matrix. For future proficiency tests, reporting forms will only be provided in one language (English). This error did not influence the reported results. As can be seen from the table, many laboratories chose not to provide information other than the measurement result or only selectively filled out the reporting form, making it very difficult to establish the source of any discrepancies.

Table 2. Chemical analysis of the sand.

Parameter	**F**	**NaO_2**	**MgO**	**Al_2O_3**	**SiO_2**	**P_2O_5**	**SO_3**	**Cl**	**K_2O**	**CaO**	**TiO_2**	**MnO**	**Fe_2O_3**	**BaO**	**LOI**	**SUM**
Mass content (%)	0.06	0.40	0.08	3.90	89.60	0.03	0.14	$<$0.01	2.70	0.20	0.03	0.14	1.30	0.07	1.20	99.90

Table 3. Information on detector systems as provided by laboratories participating in the proficiency test.

Lab. Code	**Detector system**	**Resolution (FWHM)**	**Sample geometry**	**Measurement geometry**	**Software**	**Measurement time (s)**	**No. of sources**
1	Coaxial and planar HPGe, 51.5/85.50 mm diameter, 30.0/61.5 mm height, window material: Al 0.65/1.1 keV at 122 keV	0.65/1.1 keV at 122 keV 1.8/2 keV at 1 332 keV	Aluminium bottle, 50 mm diameter with 0.5 mm side wall thickness, 1 mm bottom wall thickness, sample height: 165 mm	N/A	Canberra LabSOCS	80 000	2
2	n-type coaxial HPGe, 57.1 mm diameter, 57.2 mm height, window material: Al	0.89 keV at 122 keV 1.42 keV at 661.6 keV 1.95 keV at 1 332 keV	60 mL polyethylene sample container, 73 mm diameter with 2 mm side wall thickness, 2 mm bottom wall thickness, sample height: 14 mm, sample density: ρ=1.5 g/cm^3	Direct contact with detector endcap	ITECH Instruments ORION and Interwinner 7.0	252 000	1
3	N/A	N/A	N/A	N/A	N/A	N/A	N/A
4	Coaxial HPGe, 60.5 mm diameter, 49.0 mm height, window material: N/A	0.875 keV at 122 keV 1.8 keV at 1 330 keV	Marinelli beaker, polypropylene 114 mm diameter with 1.5 mm side wall thickness, 3 mm bottom wall thickness, sample height: 115 mm, sample density: ρ=1.6 g/cm^3	Marinelli beaker	N/A	3 600	1
5	N/A	N/A	N/A	N/A	N/A	N/A	N/A

Continued on next page

Table 3. Continued from previous page

Lab. Code	Detector system	Resolution (FWHM)	Sample geometry	Measurement geometry	Software	Measurement time (s)	No. of sources
6	p-type coaxial HPGe, 82 mm diameter, 30 mm height, window material: carbon epoxy	0.256 keV at 9.5 keV 0.633 keV at 122 keV 1.792 keV at 1 332.5 keV	Cylindrical polystyrene container, 74 mm diameter with 1.9 mm side wall thickness, 1.25 mm bottom wall thickness, sample height: 26 mm, sample density: ρ=1.6 g/cm^3	N/A	N/A	86 400	N/A
7	n-type coaxial HPGe, 81 mm diameter, 31 mm height, window material: Ge (0.0004 mm)	0.7 keV at 122 keV 1.67 keV at 1 332 keV	60 mL polycarbonate sample container, 70 mm diameter with 1 mm side wall thickness, 1 mm bottom wall thickness, sample height: 15.62 mm	N/A	Gespecor	216 000	N/A
8	p-type coaxial HPGe, 66 mm diameter, 63.5 mm height, window material: carbon epoxy	1.0 keV at 122 keV 1.9 keV at 1 330 keV	Cylindrical D15 container, 63.2 mm diameter with 1.3 mm side wall thickness, 1.3 mm bottom wall thickness, sample height: 41 mm	N/A	Canberra LabSOCS	80 000	1
9	p-type coaxial HPGe, 69.6 mm diameter, 41.5 mm height, window material: carbon (0.9 mm)	0.7 keV at 122 keV 1.8 keV at 1 330 keV	250 mL polyethylene container, 96 mm diameter with 1.5 mm side wall thickness, 1.5 mm bottom wall thickness, sample height: 16.9 mm	N/A	Ortec GammaVision 7.02 and LVis, EFFTRAN	N/A	N/A

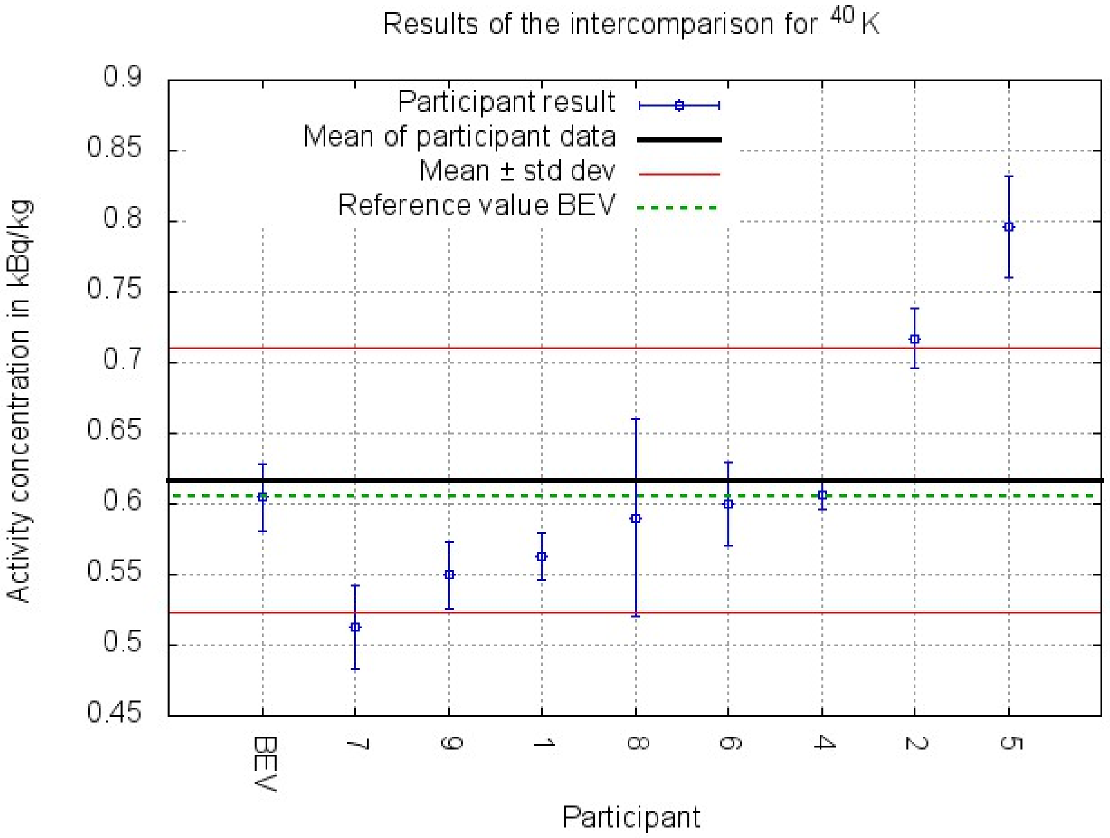

Fig. 2. Outlier-corrected results of the proficiency test for ^{40}K.

On the results of the participating laboratories, a significance test for outlying observations (Grubbs outlier test, Grubbs and Beck, 1972) was performed with a significance threshold of 0.5 % and a rescaled sum of scores. According to this method, laboratory 3's results for ^{40}K and ^{228}Ra had to be excluded. Figs. 2–4 give the outlier-corrected results of the proficiency test in relation to BEV's reference value. The results of the proficiency test of the quartz sand show the expected behaviour: larger deviations from the mean and reference value, and a larger spreading of results in a proficiency test can be expected for NORM than for simple matrices and anthropogenic radionuclides like ^{57}Co, ^{60}Co and ^{137}Cs. This behaviour originates in the complicated evaluation of the activity concentration of the radionuclides of the natural decay chain that is a particular problem arising in NORM sample measurements (Baumgartner et al., 2017). It is also evident in the results of internal comparisons conducted in the framework of the MetroNORM project, and can even be seen in CCRI(II) supplementary comparisons (Shakhashiro et al., 2010).

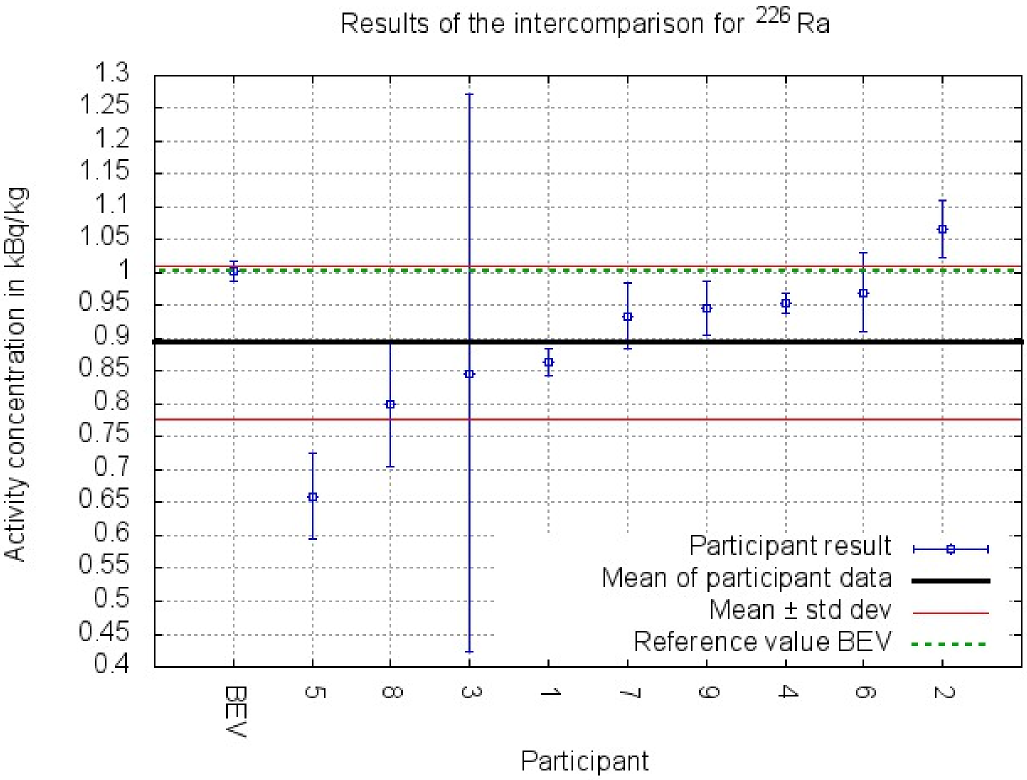

Fig. 3. Outlier-corrected results of the proficiency test for ^{226}Ra.

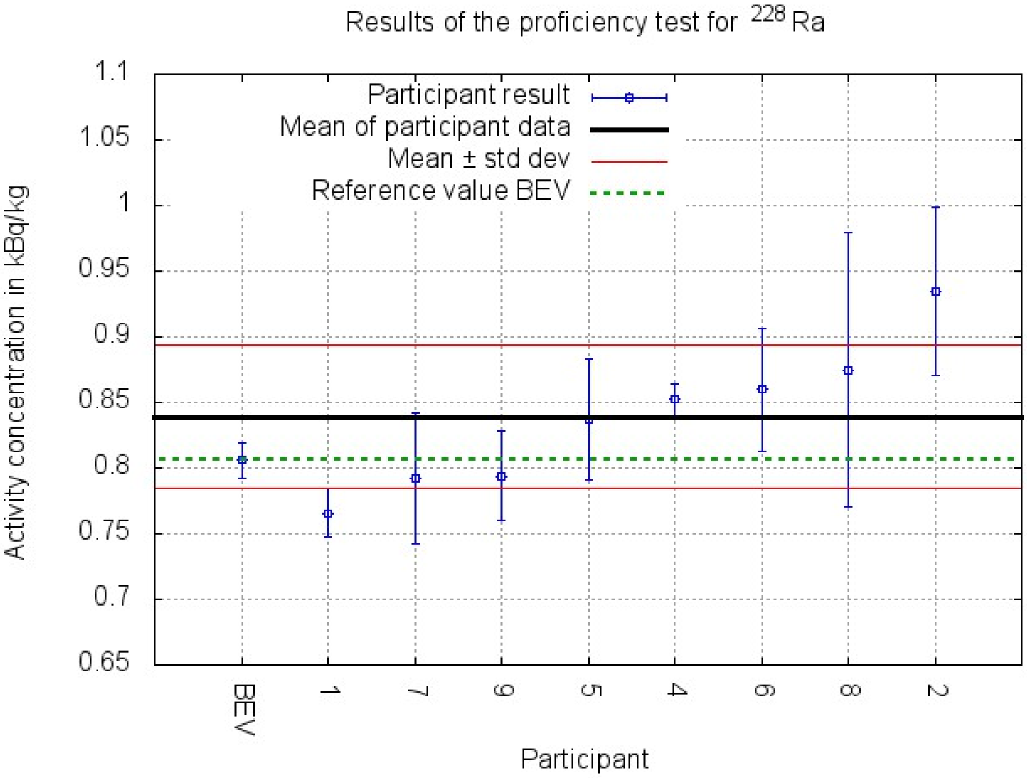

Fig. 4. Outlier-corrected results of the proficiency test for ^{228}Ra.

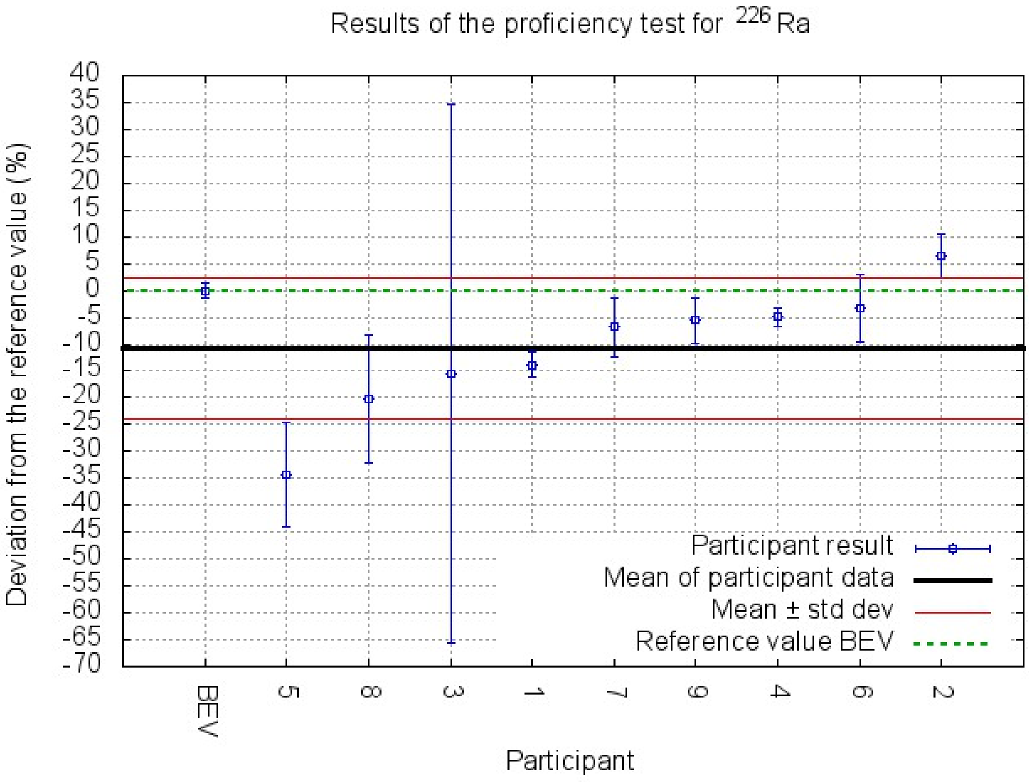

Fig. 5. Outlier-corrected results of the proficiency test for ^{226}Ra showing the deviation from the reference value in %.

With the exception of ^{226}Ra, the reference value and the mean show good agreement despite the large variation of the reported results. In case of ^{226}Ra it is apparent that laboratories 1, 3, 5, and 8 evaluated the activity concentration via ^{222}Rn progeny while using not ^{222}Rn-gastight sample containers and/or not waiting for equilibrium, leading to the severe underestimation of the activity concentration of up to 35 % shown in Fig. 5. Earlier proficiency tests executed by and in cooperation with BEV of ^{57}Co, ^{60}Co and ^{137}Cs in water and natural matrices like diaphanous earth and quartz have shown that deviations of up to 10 % from the reference value can usually be achieved (Brettner-Messler et al., 2007; Maringer and Ramer, 1998). Therefore, the authors propose that with regard to radiation protection the deviations when evaluating the activity concentration of NORM materials should also be minimised to 10 %.

Regarding the reported uncertainties, it can be observed, that many laboratories have problems with the realistic and correct estimation and calculation of uncertainties. Most laboratories only considered uncertainty contributions from counting statistics, while exempting other contributions, whereas other laboratories reported very high uncertainties of up to 50 % ($k = 1$). With current up-to-date equipment, uncertainties of about 4–20 % ($k = 2$) can usually be reached, even for low-level measurements (Maringer, 2010).

Conclusions

The production of NORM materials for intercomparisons and proficiency tests is a complex procedure that requires careful handling. For this study, a natural matrix, non-spiked NORM material made of quartz sand with elevated levels of radioactivity due to the treatment of drinking water was produced and used in a proficiency test exercise with nine European laboratories.

Homogeneity of the samples was assessed by comparing count rates of strong emission lines. Five samples were excluded from the exercise as they were deviating too much from the mean, but most samples were deemed sufficiently homogeneous. Finely grinding the quartz sand would ensure better homogeneity but also result in a less “realistic” reference material since grinding would destroy the material’s natural matrix.

The results of the NORM proficiency test showed the expected behaviour. Proficiency of the participating laboratories is good for some but leaves room for improvement. One reason for this outcome may be that approximately half the participating laboratories had only little experience in analysing NORM radionuclides.

From the results of this proficiency test it is apparent that many laboratories have problems with the determination of the activity concentration of ^{226}Ra, specifically. One reason for the underestimation of the ^{226}Ra activity concentration of up to 35 % is the use of unsealed sample containers or measurement before reaching radioactive equilibrium. During the evaluation of the results it also became evident that many participants had problems with the correct treatment of measurement uncertainties and conversion of quantities, especially when specifying parts and multiples of quantities.

Furthermore, it is obvious that consistent and complete record keeping on sample treatment and activity concentration evaluation is imperative and not typically performed by most laboratories. This necessitates awareness building and training courses for the responsible personnel. One of the lessons learned in this proficiency test is that reporting sheets should be kept as short and simple as possible to ensure that participants will provide complete information and that only one language should be used as translations can produce some ambiguous phrasing. In general, the result of this proficiency test showed the potential for further improvements in correctly analysing the activity concentration of natural radionuclides in NORM, even for expert laboratories.

Acknowledgements

This work is based on the experience and knowledge gained within the Joint Research Project IND57 MetroNORM “Metrology for processing materials with high natural radioactivity” (early impact) in the framework of the European Metrology Research Programme (EMRP)

(Grant Contract no. IND57-REG1). The EMRP is jointly funded by the EMRP participating countries within EURAMET and the European Union. The authors thank the participating laboratories.

References

Baumgartner, A., Stietka, M., Kabrt, F., Wiedner, H., Maringer, F.J., 2017. Study of particular problems appearing in NORM samples and recommendations for best practice gamma-ray spectrometry. Appl. Radiat. Isot. 126, 285–288.

Brettner-Messler, R., Maringer, F.J., Michai, P., Kreuziger, M., 2007. Ergebnis der Vergleichsmessung für Gammaspektroskopiesysteme "BEV-Gammaring 2007" (Results of the intercomparison for gamma-ray spectroscopy systems "BEVGammaring 2007"). Bundesamt für Eich- und Vermessungswesen, Wien.

Gilmore, G., 2008. Practical Gamma-ray Spectrometry, 2nd edition. John Wiley & Sons, Ltd., West Sussex, England, pp. 144.

Grubbs, F., Beck, G., 1972. Extension of sample sizes and percentage points for significance tests of outlying observations. Technometrics 14 (4), 847–854.

Larijani, C., Pearce, A.K., Regan, P.H., Russell, B.C., Jerome, S.M., Crespo, M.T., de Felice, P., Lutter, G., Maringer, F.J., Mazánová, M., 2017. Reference materials produced for a European metrological research project focussing on measurements of NORM. Appl. Radiat. Isot. 126, 279–284.

Maringer, F.J., 2010. State-of-the-art activity measurement and radionuclide metrology in radiation protection (Invited lecture). In: Proceedings of the Third European IRPA Congress, Helsinki.

Maringer, F.J., Ramer, A., 1998. Mathematisch-statistische Auswertung des Ringvergleichs von Gammaspektrometriemeßplätzen "GAMMARING 97" hinsichtlich der Optimierung der radiometrischen Analytik von Umweltproben in Österreich (Mathematical-statistical evaluation of an intercomparison exercise for gamma-ray spectrometry systems "GAMMARING 97 for optimization of radiometric analysis of environmental samples in Austria). Österreichisches Forschungs- und Prüfzentrum Arsenal, Wien.

Maringer, F.J., Baumgartner, A., Seidel, C., 2010. Natural radioactivity of building materials: radiation protection concepts, measurement methods and regulatory implementation. In: Proceedings of the Third European IRPA Congress, Helsinki.

Maringer, F.J., Baumgartner, A., Cardellini, F., Cassette, P., Crespo, T., Dean, J., Wiedner, H., HHůlka, J., Hult, M., Jerome, S., Kabrt, F., Kovář, P., Larijani, C., Lutter, G., Marouli, M., Mauring, A., Mazánová, M., Michalik, B., Michielsen, N., Peyres, V., Pierre, S., Pöllänen, R., Pommé, S., Reis, M., Stietka, M., Szűcso, L., Vodenik, B., 2017. Advancements in NORM metrology – results and impact of the European joint research project MetroNORM. Appl. Radiat. Isot. 126, 273–278.

Shakhashiro, A., Sansone, U., Wershofen, H., Bollhöfer, A., Kim, C.K., Kim, C.K., Korun, M., Moune, M., Lee, S.H., Tarjan, S., 2010. Technically enhanced naturally occurring radionuclides (TENORM) in phosphogypsum. Metrologia 47 (Tech. Suppl.), 06018.

UNSCEAR (United Nations Scientific Committee on the Effects of Atomic Radiation), 2010. Sources and Effects of ionizing radiation, UNSCEAR 2008, Report to the General Assembly with Scientific Annexes Volume I. United Nations, New York.

6.3 Paper three

Radon in drinking water: Comparison and evaluation of two ionisation chamber activity measurement methods

H. Wiedner, K. Lotter, P. Karner, H. Friedmann, F.J. Maringer

Applied Radiation and Isotopes
Volume 134, April 2018, Pages 477-481
http://dx.doi.org/10.1016/j.apradiso.2017.06.031

Radon in drinking water: Comparison and evaluation of two ionisation chamber activity measurement methods

H. Wiedner[a,*], K. Lotter[b], P. Karner[b], H. Friedmann[c], F.J. Maringer[a,b]

[a] *Bundesamt für Eich- und Vermessungswesen, Arltgasse 35, 1160 Wien, Austria*
[b] *Technische Universität Wien – Technical University of Vienna, Karlsplatz 13, 1040 Wien, Austria*
[c] *Universität Wien – University of Vienna, Universitätsring 1, 1010 Wien, Austria*
[*] *Corresponding author. E-mail address: hannah.wiedner@bev.gv.at (H. Wiedner).*

Abstract

In this study the radon activity concentration of water samples from the so called "Thermenlinie" are measured using two different techniques: currents measured with an ionisation chamber setup developed by H. Friedmann are compared with results obtained using a commercially available AlphaGUARD. A fit to compensate for measurements made in non-equilibrium state is applied and the detection limit is estimated.

Highlights

- Comparison and evaluation of radon measurement techniques.
- AlphaGUARD and ionisation chamber measurement generally in good agreement.
- Water samples from spa and drinking water springs were measured.
- Samples taken in “Thermenlinie” region in Austria.

Introdution

As radon is present in many soils, rocks and building materials from where it emanates into the atmosphere it causes by far the largest part of the average annual effective dose to humans due to natural influences (UNSCEAR United Nations Scientific Committee on the Effects of Atomic Radiation, 2010). Accumulation in poorly ventilated buildings or mines can lead to potentially harmful concentrations of activities far exceeding 1000 Bq/m^3. Therefore, radon in air has been investigated in great detail in the last decades.

The emanation of radon from water into air has been identified as a cause of additional radiation dose and measurements are performed to investigate this aspect. The greatest potential danger of radon in water is not the occurrence in drinking water, where concentrations are usually quite low, but the additional amount of radon released to the atmosphere, causing high dose rates, when accumulation happens. A study on 45 water works in Upper Austria showed a yearly dose received by the workers exceeding 6 mSv in three of the investigated sites, two of them even exceeding the limitation for radiation exposed workers of 20 mSv/a (Ditto et al., 2007).

However the exposition of the general public is much lower, as the main part of the radon emanates during water processing. Where water is supplied as part of a commercial or public activity, such as drinking water through a waterwork, the European Commission (2001) recommends 100 Bq/L as indication level, below which no remedial action is required while for higher values, measurements should be conducted as necessary. Above 1 000 Bq/L remedial action is required for radiation protection. For an activity of 100 Bq/L Rühle (1997) calculates an annual dose for an adult of 0.17 mSv due to inhalation and further 0.05 mSv due to ingestion, totalling 0.22 mSv per year. Compared to the radiation dose caused by radon in the atmosphere this is ten times lower, but nevertheless underlines the importance of monitoring the radon levels in water and the adherence to the set limits.

Over the course of the Austrian National Radon Project (Friedmann et al., 2007) measurements where undertaken all over Austria, old measurements of radon concentrations in spring and ground water were analysed and new measurements were conducted to test their credibility. The data shows approx. 86 % of the measurements below a level of 50 Bq/L, but also indicates the high radon potential in some regions with 3.5 % of measurements above 400 Bq/L. The data was divided into three classes to create the map of Radon in Water Potential in Austria depicted in Fig. 1 (Friedmann et al., 2007).

The samples used in this study were mainly taken from locations along the so called "Thermenlinie", a seismic disturbance zone west of Vienna running from the Northern Limestone Alps to the south of Vienna along the edge of the Vienna Basin. Along this line many hot springs are located, which are often used in spas (Peck and Linsberger, 2010). This region is mostly part of Class 1, with some municipalities in Class 2, so radon values are not expected to be as high as in other parts of Austria, like Waldviertel and Mühlviertel in the north, where the uranium content of granite soils leads to some of the highest values in Austria. Although it was decided to take the samples along the "Thermenlinie" the results for the measured springs are not the focus of this study. The main aim is to compare different measurement techniques for radon in water and evaluate the advantages and disadvantages of these methods. Therefore, no strict selection of the measured springs was made, but the samples were taken where access was possible. Between 12 December 2016 and 14 December 2016, 12 springs were sampled by filling two 1 L commercially available glass bottles from each spring (A and B samples).

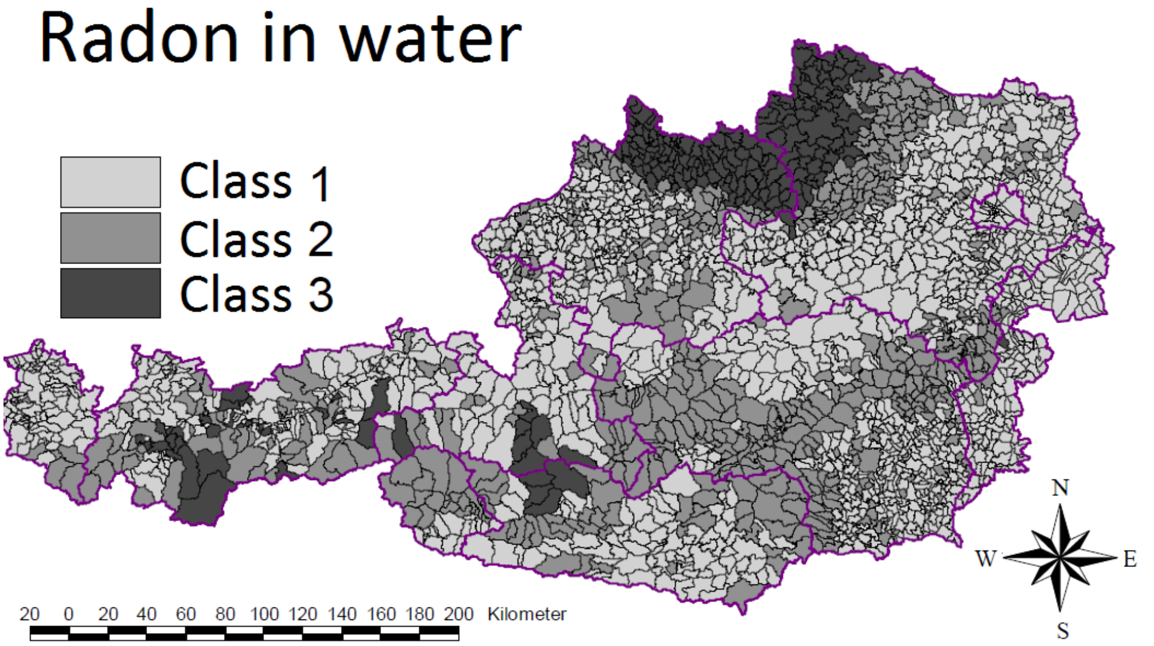

Fig. 1. Class 1: municipalities where all measurement are below 100 Bq/L, with less than 30 % of values above 50 Bq/L, class 2: municipalities where all measurements are below 300 Bq/L, with less than 30 % of values above 150 Bq/L and not class 1, class 3: all other values. Translated from: (Friedmann et al., 2007).

Methods

The springs where the water samples were taken are thermal springs in spas and publicly accessible wells, supplying cold water of drinking water quality. The bottles are cheap, easily available and sufficiently gas tight (Warwick, 2003). Due to the fact that only radon is measured no special cleaning or preparation of the bottles was necessary. Preliminary tests showed, that the empty bottle contains no noteworthy amount of radon and the bottles are indeed sufficiently radon tight. In order to retain as much radon in the water as possible and prevent radon emanation, the bottles were carefully and slowly filled using a hose to prevent bubbling water. The hose was inserted into the bottle, letting the water flow in at the bottom and slowly raising the water level. When full, the water was left running over the rim for a few seconds and then the hose was slowly retrieved. After decanting a small amount of water to create room for the developing gases, the bottle was sealed using plastic screw tops.

Measurement setup

The samples were measured using two different techniques: an ionisation chamber with a charge measurement and a circulation measurement using a commercially available AlphaGUARD, traceably calibrated at ENEA. The ionisation chamber used in this study was a cylindrical chamber with a volume of 9.3 L and an applied voltage of 260 V. The ionisation chamber is connected to a high voltage supply and an electrometer. For small activities, like in our study, higher precision can be achieved by measuring charge instead of current, as in this way the current is integrated over a period of time and fluctuations have less influence on the result. The pressure in the ionisation chamber is lowered significantly by pumping out the air using a water jet pump connected to a tap. Then the water bottle is attached to the ionisation chamber by using a plug that has two hoses. Once the valve at the chamber is opened, air is slowly sucked through the water into the chamber, causing the water to bubble and emanating the radon from the water very efficiently. Previous studies (Friedmann, 1977) showed that an amount of air three times the volume of the liquid is sufficient to release virtually all the radon from the water into the chamber. After evacuating the chamber for approximately five minutes, this condition is easily satisfied. When the pressure in the chamber is balanced with the ambient air the bubbling stops (usually after about ten minutes). The chamber's valve is closed, bottle and hose are removed and HV is switched on. Due to build-up of Rn decay products and the production of negative ions during the emanation process leading to a very unstable and severely fluctuating current in the beginning, values are recorded after a waiting period of at least 10 min.

Fig. 2. A few select sampling locations and measurement set-up. Top left: Fischau Quelle 1, bottom left: St. Egyden 1, top right: Josephsquelle, Baden bei Wien, bottom right: measurement setup.

Before each new measurement ambient air is pumped through the whole setup and a blank value is measured to ensure an unbiased measurement. After the current measurements on a sample using the ionisation chamber setup and the electrometer are finished the chamber is disconnected from the EM and the HV and both outlets of the chamber are fitted with hoses and connected to the AlphaGUARD (see Figs. 2 and 3). To ensure that only the radon is measured a filter for the Rn decay products is included behind the circulation pump. Then the two valves of the ionisation chamber, which only has the function of a radon container in this setup, are opened and the circulation pump is switched on with a speed of 1 L/min. With a flux of 1 L/min and an overall volume of about ten litres of the whole setup this guarantees that all the air containing radon is circulated at least twice through the AlphaGUARD. After this, the pump is shut off and the ionisation chamber disconnected. The AlphaGUARD is also disconnected from the hoses and the outlets are shut to keep as much of the air sample as possible in the measurement volume. This way it is possible to continue with the measurement while the ionisation chamber is already prepared for the next sample. However, the outlets did not provide a perfect seal, resulting in a continuous leakage of gas from the Alpha-GUARD that results in a clearly visible drop in activity within the next couple of acquisition cycles. To take this fact into account the amount of leakage was estimated and compensated. After measurement with the AlphaGUARD the examination of one sample is complete and the ionisation chamber is cleaned by repeatedly lowering the pressure inside and letting ambient air flow in. This ensures the removal of all radon and thus the chamber can be reused after the Rn decay products are decayed to insignificant levels.

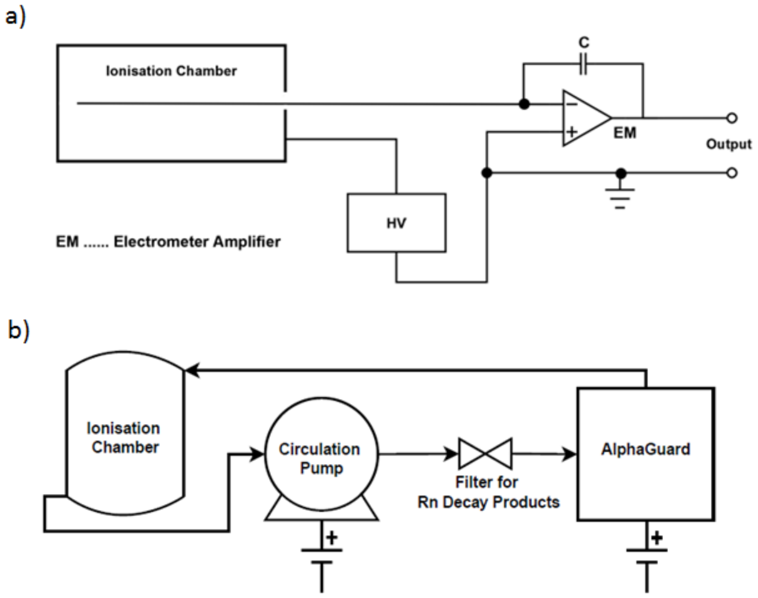

Fig. 3. Setup of the measurement system: (a) Ionisation chamber, (b) AlphaGUARD.

Uncertainty

Since this study is concentrating on the optimisation and evaluation of the measurement setups and not on the total value of activity in a sample, no measures were taken to ensure high precision on this aspect of the measurement setup. This means that the bottles were filled to approximately the same height, but no volume measurements were conducted. Consequently the additional uncertainty due to variation of volume is estimated to be 4 % of the measured value. This estimate is achieved using the formula for cylindrical volumes $V = r^2 \pi h$ and assuming a variation of 1 cm of the height h of the water level and a typical radius r for the bottle. Correcting this factor could easily be done be weighing the bottle before and after filling. This way the source of uncertainty could be reduced to the uncertainty of the weighing which should be at least an order of magnitude lower than the present uncertainty.

The second source of systematic uncertainty that is covered is much harder to estimate or minimize. Since radon is a noble gas it is extremely volatile and it is easily possible to extract it from the water it is contained in. While emanating the radon by bubbling air through the water is the basis of our measurement setup the same effect can lead to significant loss of radon during sampling or the preparation of a sample for measurement. Even though great care was taken to avoid any unnecessary disturbance it can never be ruled out that some emanation and loss of radon takes place. The best estimate for the radon loss comes from measurements, where both samples of one spring have been measured. However, the measurement of the backup samples (B samples) has been conducted only after all A samples had been measured. Therefore, nearly three half-life periods of radon elapsed before the backup samples could be investigated. This left the samples 9 A and 9B as main support of this estimate and as the mean values of them show a difference of less than 3 %, the possible uncertainty due to radon loss is conservatively estimated at 5 % of the measured value.

Results and discussion

Assuming secular equilibrium between ^{226}Ra and its progeny, the calculations of Friedmann and Hernegger (1980), that are based on the Bateman equations (Bateman, 1910) and dismissing the contribution of beta particles, give the total chamber current I_{tot} as

$$I_{\mathrm{tot}} = \left(\frac{Q_{\mathrm{Rn\text{-}222}}}{w} \cdot A_{\mathrm{Rn\text{-}222}} + \frac{1}{2} \cdot \frac{Q_{\mathrm{Po\text{-}218}}}{w} \cdot A_{\mathrm{Po\text{-}218}} + \frac{1}{2} \cdot \frac{Q_{\mathrm{Po\text{-}214}}}{w} \cdot A_{\mathrm{Po\text{-}214}}\right) \cdot \mathrm{e} \cdot K \tag{1}$$

with

$$K = \left(1 - 0.572 \cdot \frac{O}{V}\right) = 0.937 \tag{2}$$

the Duane-Laborde correction (Duane and Laborde, 1910) taking into account the loss of ionisation energy suffered by the charged particles at the walls of the ionisation chamber (Fresenius et al., 1988), where Q_{i} are the alpha energies of the respective nuclides, w the mean ionisation potential of air, e the elementary charge, O the surface of the ionisation chamber in cm^2 and V the volume of the ionisation chamber in cm^3. This means, that for every decaying ^{222}Rn atom $3.5 \cdot 10^5$ ions are produced in the chamber, resulting in a current of $5.6 \cdot 10^{-14}$ A per 1 Bq ^{222}Rn (Friedmann and Hernegger, 1980). Considering the geometric factor K of the chamber, the current to activity ratio is given by

$$I_{\text{tot}}\ (\text{pA}) \cdot 19.24 \cong A_{\text{Rn-222}}\ (\text{Bq}) \tag{3}$$

Since secular equilibrium is reached only after about ten half-life periods of the longest-lived daughter, ^{222}Rn and its progeny would only be in equilibrium after approx. five hours (ten half-lives (26.8 (9) min) of ^{214}Pb (BIPM, 2008)). Due to time constraints, especially in the field, it was investigated, if the calculated relationship can be used if the measurements starts after 20–30 min after insertion of radon gas into the chamber. The function f is a summation of the currents generated from ^{222}Rn, ^{218}Po and ^{214}Po that amount to almost the complete chamber current:

$$f(t, A_0) = \Big(I_{\text{Rn-222}}(t, A_0) + \frac{1}{2} I_{\text{Po-218}}(t, A_0) + \frac{1}{2} I_{\text{Po-214}}(t, A_0)\Big) \cdot 0.937 \tag{4}$$

with

$$I_{\text{Rn-222}}(t, A_0) = \frac{Q_{\text{t}}}{w} \cdot A_{\text{i}}(t, A_0) \tag{5}$$

and

$$A_{\text{i}}(t, A_0) \tag{6}$$

the expression of the Bateman equation for the particular nuclide. The measured current values weighted with their uncertainties are fitted using a least squares Marquardt-Levenberg algorithm where A_0 is considered the only independent variable. In this way an estimation of A_0 is computed along with an uncertainty of the fit (see Fig. 4).

To get an estimation of the detection limit of the ionisation chamber, the formula given by the Austrian Standards Institute in ÖNORM S 5250-1 (ÖNORM S 5250-1, 2002) for measurements of count rates is used. As the current of the ionisation chamber is the basis for calculating the activity is not acquired directly, but calculated from the measured charge divided by the acquisition time, it is possible to derive the following expression: As the current of the ionisation chamber is the basis for calculating the activity is not acquired directly, but calculated from the measured charge divided by the acquisition time, it is possible to derive the following expression:

$$E(R_{n,DL}) = 4.65 \cdot \sqrt{\frac{R_0}{t_0}} \text{ with } R = I \cdot K = \frac{Q}{t_0} \cdot K \Rightarrow E(I_{n,DL}) = 4.65 \cdot \sqrt{\frac{Q_0}{{t_0}^2} \cdot K} \tag{7}$$

With as the expectation value of the detection limit, R_0 the blank value count rate, t_0 the acquisition time for the blank value measurement and Q_0 the blank value charge. The blank value charge was measured using ambient air. Five measurements have been conducted with t0 varying between 62 s and 225 s and Q_0 between 10 pC and 30 pC. The calculation yields an estimation of the detection limit ranging from 0.11 pA to 0.24 pA. Using this setup, no leakage currents have been found (Friedmann, 1992). As this formula is designed for

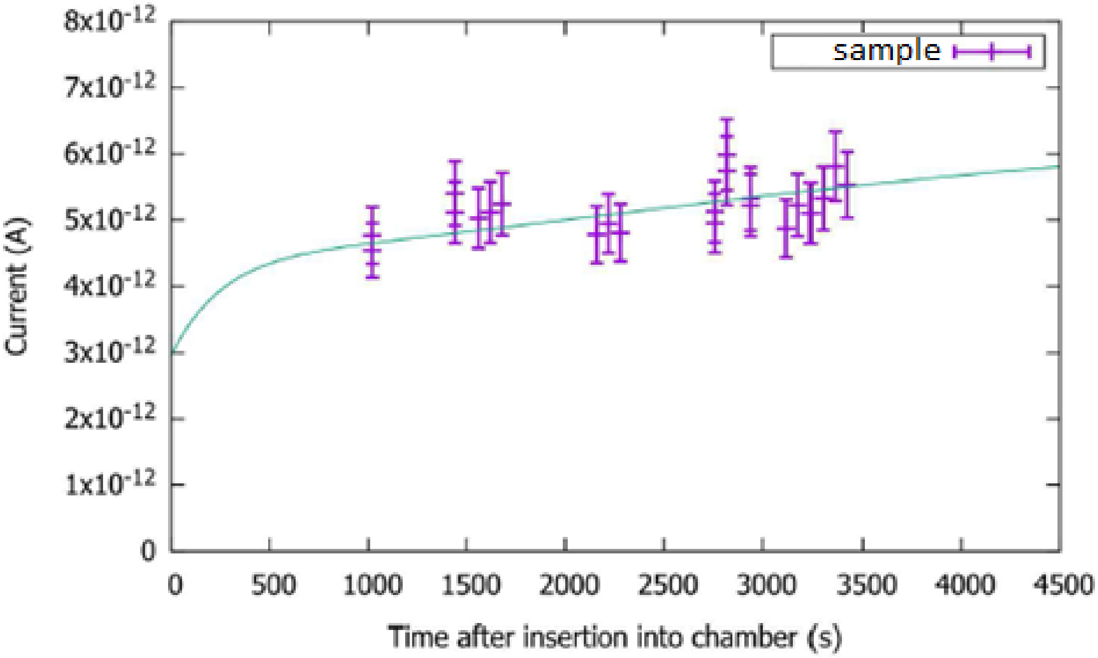

Fig. 4. Fit of the development of the current (green) for measured values (purple) of a representative sample (approx. 120 Bq/L). (For interpretation of the references to color in this figure legend, the reader is referred to the web version of this article).

measurements of count rates like in gamma detectors and Geiger-Müller counters, the result provides only an estimate of the lower limit of this measurement setup. Using the arithmetic mean and the standard deviation of the mean, the detection limits are calculated as $E(I_{n,DL}) = (0.18 \pm 0.03)$ pA and $E(R_{n,DL}) = 3.47 \pm 0.55$ Bq/L, respectively.

According to the manufacturer's data sheets, the volume of the AlphaGUARD was estimated to be 9.94 L. Due to the fact that almost 100 % of the radon is transferred from the water sample into the ionisation chamber of the AlphaGUARD, 1 Bq per L water results in 0.00994 Bq per m^3 ^{222}Rn in air. Since the volume of the AlphaGUARD was determined by the manufacturer the uncertainty of the volume has been dismissed, as it is small in comparison to the other sources of uncertainty that have been considered. During measurements it became obvious, that the setup of the AlphaGUARD is not quite gas tight and a considerable amount of radon is lost. This is especially noticeable once the circulation pump is switched off. It is assumed, that the reason for the loss is leakage in the plugs of the outlets. In order to compensate for this, the rate of radon loss was estimated and corrected with a linear correction factor p: $A_{\text{corr}}(t) = A_{\text{measured}}(t) \cdot (1 + \Delta t \cdot p)$.

For the calculation of p, five samples with at least three measurements after shutting off the pump have been selected, normalised by their mean and fitted. Due to the small number of measurements per sample the correction factor is afflicted with high uncertainties. It is remarkable that the rate of gas loss seems to be less severe for samples with less activity concentration than for those with higher activity concentration. Nevertheless, the most logical assumption is a constant rate of radon loss and it is a solid assumption, that the effect simply cannot be observed as well in less active samples due to their high relative uncertainties. Therefore, p can be given as 0.0141 ± 0.0029. Fig. 5 gives an overview over the measured samples and the different techniques. The results of the comparison between the two methods show a difference factor of 1.00 and 2.99, with all measurement except two between 1.00 and 1.55. In the two cases it was assumed that a loss of radon while switching measurement methods is the cause of the anomaly.

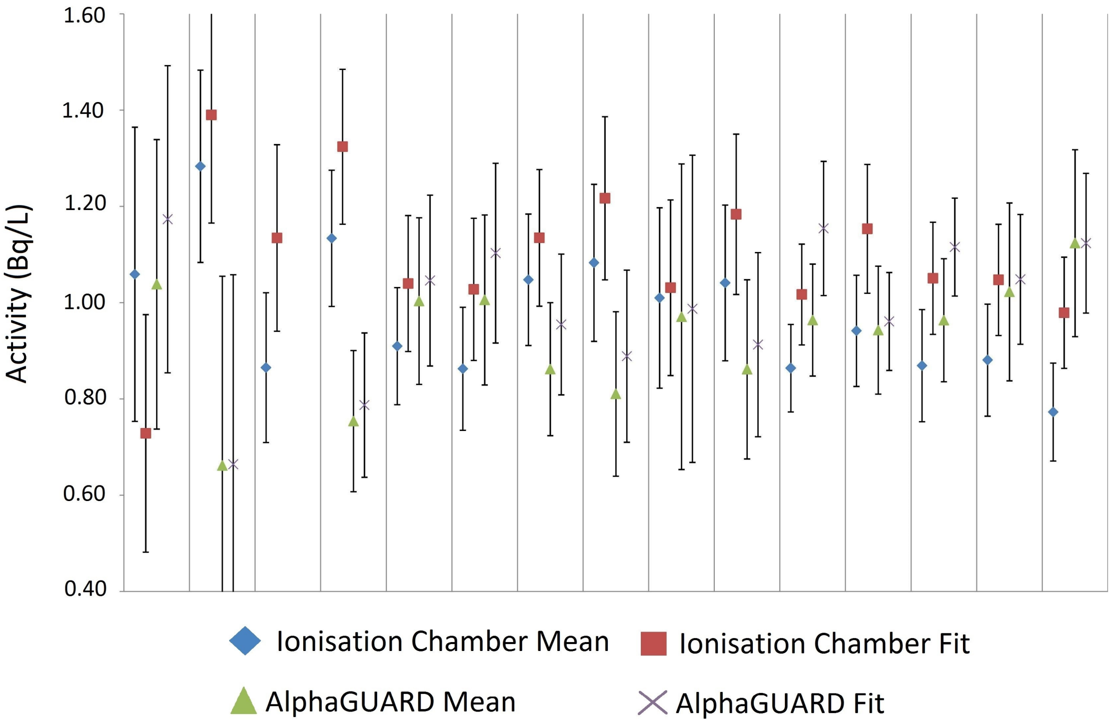

Fig. 5. Overview of select samples with their normalised activity and the respective measurement technique.

Conclusion

In this study the results and uncertainties given by the measurement using the ionisation chamber and the AlphaGUARD setup generally agree (difference factor of 1.00–1.55). The results were corrected to take into account that at the measurement time the sample was not in equilibrium using a fit of the chamber current. The relative uncertainties range from 10 % to 35 % ($k = 1$). For the future, a better estimation of the gas loss of the AlphaGUARD would be desirable and further

References

Bateman, H., 1910. Solution of a system of differential equations occurring in the theory of radioactive transformations. Proc. Camb. Philos. Soc. 15, 423–427.

BIPM, 2008. Monographie BIPM-5. Table of Radionuclides. (Volume 4–A = 133 – 252) Sèvres Cedex, France, pp. 75.

Ditto, M., et al. 2007. Strahlenexposition durch Trinkwasser in Oberösterreich – 2004 bis 2006 – Teilprojekt Strahlenexposition von Beschäftigten in oberösterreichischen Wasserwerken – Zusammenfassender Endbericht. Linz: Land Oberösterreich, Abteilung Umwelt- und Anlagentechnik, 2007.

Duane, W., Laborde, A., 1910. The quantitative measurement of radium emanation. Compt. Rend. 150, 1421–1423.

European Commission, 2001. Commission Recommendation of 20 December 2001 on the protection of the public against exposure to radon in drinking water supplies. Official Journal of the European Communities. 28. 12. 2001.

Fresenius, W., et al., 1988. Water Analysis: A Practical Guide to Physico-Chemical, Chemical and Microbiological Water Examination and quality Assurance. Springer Verlag, Berlin Heidelberg New York London Paris Tokyo, pp. 451.

Friedmann, H., 1977. Modell für die Entemanierung radioaktiver Lösungen. Anz. der Math. Nat. Kl. der österreichischen Akad. der Wiss. 114, 7. Friedmann, H., 1992. An inexpensive and highly sensitive method for continuous radon monitoring. Mém Expl. Cartes. Céologiques Et. Minières De. la Belg (Nr. 32).

Friedmann, H., et al., 2007. Das österreichische Nationale Radonprojekt – ÖNRAP Projekt Endbericht. Bundesministerium für Land- und Forstwirtschaft, Umwelt und Wasserwirtschaft und Bundesministerium für Gesundheit, Familie und Jugend, Wien (2007).

Friedmann, H., Hernegger, F., 1980. Radium- und Radonbestimmung in Luft- und Wasserproben. Anzeiger der Mathematisch Naturwissenschaftlichen Klasse der österreichischen Akademie der Wissenschaften 117. pp. 7. ÖNORM S 5250-1, 2002. Zählstatistische Aspekte bei Radioaktivitätsmessungen – Teil 1: Messunsicherheiten, Erkennungs- und Nachweisgrenzen. Österreichisches Normungsinstitut – Fachnormenausschuss 088 Strahlenschutz, Wien (2002).

Peck, D., Linsberger, A., 2010. Baden im Übergang – naturräumliche Analyse. TU WIEN Projekt 2 - Kommunale Entwicklungs- und Flächenwidmungsplanung WS2009/ SS2010. [Online] 2010. [Cited: 22 1. 2017.]. `http://p2.iemar.tuwien.ac.at/p2_09_baden/downloads/landscape/ifoer2&6_landscape.pdf`.

Rühle, H., 1997. Radon in unserer Umwelt und die damit verbundene Strahlenexposition. In: der Bevölkerung (Ed.), Karl Aurand and Horst Rühle. Radon und Trinkwasser. Berlin 101. Schriftenreihe des Vereins für Wasser-, Boden- und Lufthygiene, Berlin, pp. 39–55.

UNSCEAR (United Nations Scientific Committee on the Effects of Atomic Radiation), 2010. Sources and Effects of ionizing radiation, UNSCEAR 2008, Report to the General Assembly with Scientific Annexes VOLUME I. United Nations, 2010, New York.

Warwick, P., 2003. Environmental Radiochemical Analysis II. (Special Publication No. 291) Royal Society of Chemistry, Maidstone, United Kingdom, pp. 134.

6.4 Paper four

Study of particular problems appearing in NORM samples and recommendations for best practice gamma-ray spectrometry

Andreas Baumgartner, Michael Stietka, Franz Kabrt,
Hannah Wiedner, Franz Josef Maringer

Applied Radiation and Isotopes
Volume 126, April 2017, Pages 285-288
http://dx.doi.org/10.1016/j.apradiso.2016.12.035

Study of particular problems appearing in NORM samples and recommendations for best practice gamma-ray spectrometry

Andreas Baumgartner[a], Michael Stietka[a], Franz Kabrt[a,b], Hannah Wiedner[a,b], Franz Josef Maringer[a,b]

[a] *University of Natural Resources and Life Sciences, Vienna, Prüflabor für Umweltradioaktivität und Strahlenschutz, Low-Level Counting Laboratory Arsenal, Arsenal 214, A-1030 Vienna, Austria*
[b] *BEV – Federal Office of Metrology and Surveying, Arltgasse 35, A-1160 Vienna, Austria*
[*] *Corresponding author. E-mail address: a.baumgartner@boku.ac.at (A. Baumgartner).*

Highlights

- Comprehensive study of spectral interferences of selected natural radionuclides.
- Calculation of interference contributions for various NORM samples.
- Comparison of BIPM and IAEA gamma emission intensities for selected natural radionuclides.
- Demonstration of a simple and sensitive method for the estimation of the ^{222}Rn leakage of sample containers.

Abstract

In this paper spectral interference effects for selected gamma-emitting radionuclides of the natural decay series and ^{40}K in selected NORM samples are studied. Recommendations for the choice of γ-lines and the consideration of possible spectral interferences are provided. Special attention is given to the radon tightness of the sample containers. A simple and sensitive method for the estimation of the ^{222}Rn leakage of sample containers is introduced. The applied polystyrene sample containers show ^{222}Rn leakages lower than 1 %.

Introduction

Naturally Occurring Radioactive Materials (NORM) containing e.g. radionuclides of the ^{238}U, ^{235}U and ^{232}Th decay series as well as ^{40}K can pose health risks to workers and the public, especially when industrially exploited or used as building materials. As shown by a large number of publications on the subject (as a recent example see Mantero, 2015), the evaluation of the radioactivity content of the material is usually done using gamma-ray spectrometry, as it is a versatile and nondestructive method. The difficulties, which arise in the measurement of NORM samples, are analyzed within the Joint Research Project

IND57 MetroNORM "Metrology for processing materials with high natural radioactivity" in the framework of the European Metrology Research Programme (EMRP). MetroNORM is aimed to develop improved laboratory and in-situ measurement methods and to design standardized procedures, as well as perform testing in industrial environment. This paper describes the study of spectral interferences in selected NORM samples with special attention to the radon tightness of the applied sample containers. Based upon the work, a proposal for best practice gamma-ray spectrometry of the investigated NORM samples is given. This includes recommendations for γ-lines including the handling of interferences.

Materials and methods

The gamma spectrometric measurements were performed with a HPGe p-type coaxial broad-energy detector of Baltic Scientific Instruments (BSI). The detector (GCD-50195X; rel. eff.: 52.2 %; peak to Compton ratio: 66:1; FWHM: 1715 eV at 1332 keV, 678 eV at 122 keV, 481 eV at 14.4 keV) has a carbon epoxy window and is equipped with an ultra low-background U-type cryostat and a low-level lead (120 mm) shielding. For gamma-ray spectrometry, the sample is centered 8 mm above the endcap of the detector. The detector is operated in the Low-Level Counting Laboratory Arsenal, Vienna. The measuring room of this laboratory is designed for low-level radioactivity measurements. This is enabled by the application of a 1.6 m 4 π shield-concrete, 3 cm lead, 0.5 cm steel for the shielding against cosmic and terrestrial radiation and a special air condition to provide a radon progeny free air. All decay data in this paper were taken from BIPM (Nucleide, 2016), except the column “Gamma emission intensities (IAEA)” in Table 2 and the data for ^{230}Th are from IAEA (2016). For ^{230}T there are no data available from BIPM. Other literature sources also give comprehensive recommendations on γ-lines and their interferences (e.g Wahl, 2016). Specifically, interferences in NORM samples were studied in e.g. Živanović et al. (2012), Lavia et al. (2004).

Investigated NORM samples

The applied raw materials and processed substances within the NORM industries have a huge diversity regarding their chemical composition and physical nature. Due to this diversity, various problems may occur for gamma-ray spectrometry of NORM. Additionally, due to overlapping γ-lines as well as coincidence effects, the aimed determination of specific radionuclides is challenging and requires suitable corrections for the different NORM samples. Exemplary for spectra in which interferences occur, the following materials were selected for a detailed investigation: tuff (volcanic ash; which is a common building material), titanium dioxide waste, ion exchange resin (from a waterworks purification filter) and a filter residue (origin unknown). For these materials, the main sources of spectral interferences were evaluated for selected gamma-emitting radionuclides of the natural decay series and ^{40}K.

Sample container

For the gamma spectrometric measurements, cylindrical polystyrene containers (diameter: 64 mm; height: 11 mm; wall thickness: 1.5 mm) were used. The samples were sealed with glue and stored before the measurements to ensure secular equilibrium between ^{226}Ra and the ^{222}Rn progenies ^{214}Bi and^{214}Pb. The gamma spectrometric measurement of ^{226}Ra can be done either by a direct measurement of the 186 keV γ-line or by measuring the γ-lines of the ^{222}Rn progenies ^{214}Bi and ^{214}Pb. Due to an interfering γ-line, a direct measurement requires the deconvolution of the full energy peak (Zhang et al., 2009) and the exact knowledge of the ^{235}U activity concentration, see e.g. Justo et al., 2006. The more common method of determining ^{214}Bi and ^{214}Pb strongly relies on the radon tightness of the sample containers (Scholten et al., 2013; Mauring and Gäfvert, 2013). Scholten et al. (2013) showed that $BaSO_4$ sample matrix and plastic containers sealed with epoxy resin reduce the ^{222}Rn leakage to less than 1 %. Besides the ^{222}Rn leakage, the distribution in solid/liquid and air phases in gamma-ray spectrometry has to be considered for partially filled sample containers (Carconi et al., 2012). This paper shows a simple method for the assessment of the ^{222}Rn leakage of sample containers. The method is based upon the measurement of the ^{222}Rn activity concentration inside a 3 l desiccator. The sample and a Canary Pro ^{222}Rn in air measuring device are placed inside the desiccator and the ^{222}Rn build-up curve is measured. The Canary Pro measuring device is a small, handheld passive diffusion chamber. It uses silicon photo-diodes both to count and to measure the energy of alpha particles resulting from the decay chain of radon gas (Corentium, 2016). The equilibrium activity concentration in the desiccator is a measure for the radon tightness of the sample. The radon tightness of the applied desiccator itself was verified by measurements inside a radon calibration barrel of Genitron Ltd.

Results and discussion

Spectral interferences

The activity concentrations of the selected NORM samples together with the standard measurement uncertainties (k=1) are given in Table 1. For the determination of the activity concentrations, the actual BIPM γ-intensities (Nucleide, 2016) were applied and all interferences given in Table 2 were considered. Due to absence of ^{232}Th, its progenies ^{228}Ra and ^{228}Th are in disequilibrium in the TiO_2 sample. For the selected materials, a critical peak-by-peak evaluation on spectral interferences of selected gamma-emitting radionuclides of the natural decay series and ^{40}K was performed. Considering the γ-intensities and calculated interference contributions in Živanović et al. (2012) as well as the recommendations from Wahl (2016), some γ-lines were excluded, e.g. the 92.4 keV γ-line of ^{234}Th. The nuclides of interest, the recommended γ-lines and the potential spectral interferences are shown in Table 2. Apart from the true coincidence summing (TCS), the calculated interference contributions to the activity concentrations for the various NORM materials are independent of the applied HPGe-detector. The information about possible TCS corrections is related to the applied coaxial HPGe detector with the cylindrical sample geometry and corrections higher than 0.5 %. The TCS corrections were calculated by Monte Carlo methods with the EffCalc software of LSRM (Laboratory of Spectrometry and Radiometry). For detectors with high absolute efficiencies (e.g. welltype detectors), there could also be TCS effects for other radionuclides e.g. the 205.3 keV γ-line of ^{235}U and the 256.2 keV γ-line of ^{227}Th. The deviation due to spectral interferences (Table 2) is calculated as the ratio of the count rates of the interfering photons and the photons of the nuclide of interest. This means that neglecting the interference would cause the deviations given in Table 2 (e.g. if the peak in the spectrum at 1460.8 keV is generated equally by ^{40}K and ^{228}Ac the value for the deviation would be 100 %). The deviation due to a radon leakage is applied for ^{214}Bi and ^{214}Pb. It is calculated according to chapter 3.2. For a determination of ^{226}Ra on basis of an equilibrium with ^{214}Bi and/or ^{214}Pb, neglecting the ^{222}Rn leakage would cause the given deviations for the ^{226}Ra value (for the applied sample containers). In accordance with Živanović et al. (2012), the spectral interferences can be classified in photons with significant and variable contributions and in photons with significant and constant contributions. The 62.9 keV photons of ^{234}Th as well as the 163.1 keV photons of ^{231}Th can be considered as significant and constant contributions. Therefore, they are simple to handle. The tuff sample required the calculation of the ^{232}Th interference at the 63.3 keV γ-line of ^{234}Th (^{232}Th is only present in the tuff sample). The ^{232}Th content was estimated on basis of its γ-emitting progenies. For a direct determination of ^{226}Ra, the interference from ^{230}Th at 186.1 keV is of less importance, as can be seen in Table 2 for the filter residue. Alternatively, (e.g. in case of high ^{235}U content) ^{226}Ra can be calculated on basis of the progenies ^{214}Pb and ^{214}Bi. Regarding the determination of ^{214}Pb the 295.2 keV γ-line was preferred to the 351.9 keV γ-line because of a high interference with ^{211}Bi (13.00 (19) % at 351.0 keV). ^{214}Bi generates ^{210}Tl by a low intense alpha emission (0.0210 (13) %). The 295.2 keV γ-line of ^{214}Pb is interfered by ^{210}Tl and can be considered in equilibrium with ^{214}Pb. As a result of the low alpha emission probability and the uncertainty of the decay data (296 (3) keV), it was not considered in the calculation of the deviation. For the determination of ^{235}U with use of the 205.3 keV γ-line, the energy resolution of the most HPGe-detectors is high enough to separate it from the interference at 204.0 keV from ^{228}Ac. For the consideration of the interference at 163.1 keV, the short-lived ^{231}Th was assumed to be in equilibrium with ^{235}U. For the determination of ^{227}Th, the 256.2 keV γ-line was preferred to the 236.0 keV γ-line, since for the 256.2 keV γ-line the TCS is below 0.5 %. ^{228}Ac also causes interferences for ^{212}Bi, ^{208}Tl and ^{40}K. Those interferences are well documented in literature (e.g. Lavia et al., 2004).

Radon tightness

For the evaluation of the radon tightness of sample containers, the applied measurement setup is intended to measure the leaked radon gas directly. After installing the Canary Pro measuring device together with the sample container inside the desiccator, the ^{222}Rn activity concentration C is monitored. Two different samples have been used to check the tightness

Table 1
Radiometric characterization of the selected NORM samples.

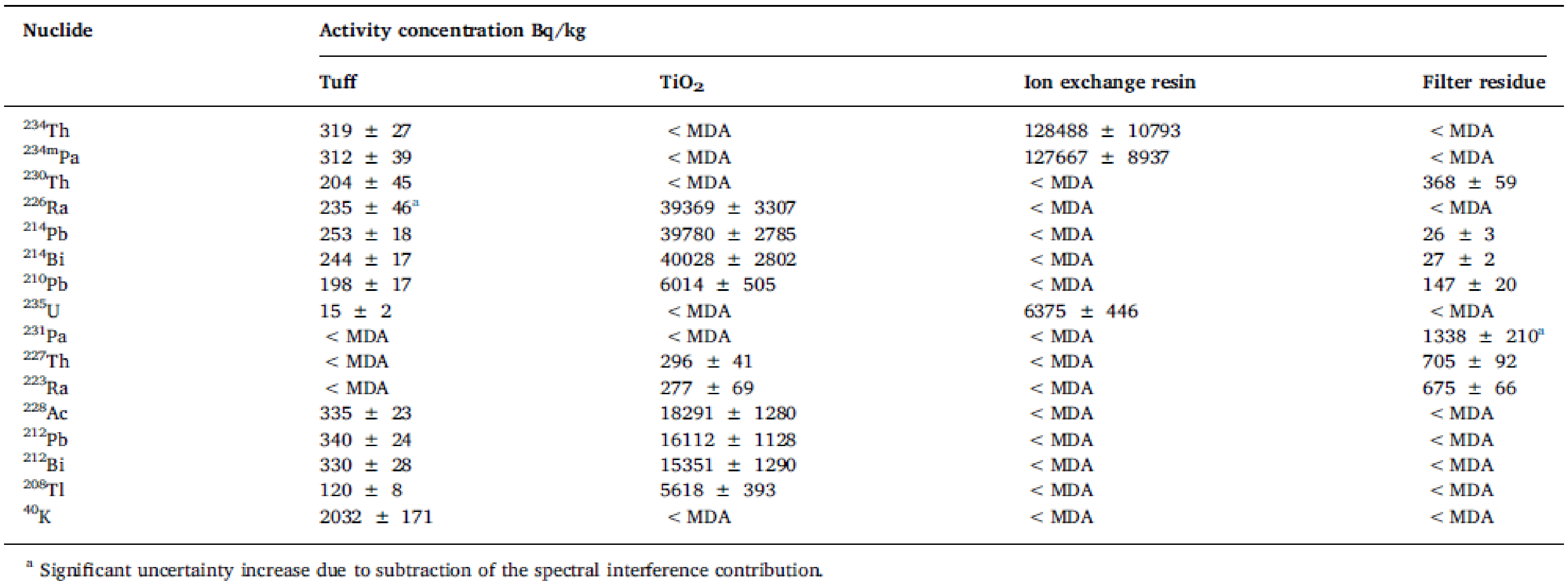

Nuclide	**Activity concentration Bq/kg**			
	Tuff	**TiO_2**	**Ion exchange resin**	**Filter residue**
^{234}Th	319 ± 27	< MDA	128488 ± 10793	< MDA
^{234m}Pa	312 ± 39	< MDA	127667 ± 8937	< MDA
^{230}Th	204 ± 45	< MDA	< MDA	368 ± 59
^{226}Ra	235 ± 46[a]	39369 ± 3307	< MDA	< MDA
^{214}Pb	253 ± 18	39780 ± 2785	< MDA	26 ± 3
^{214}Bi	244 ± 17	40028 ± 2802	< MDA	27 ± 2
^{210}Pb	198 ± 17	6014 ± 505	< MDA	147 ± 20
^{235}U	15 ± 2	< MDA	6375 ± 446	< MDA
^{231}Pa	< MDA	< MDA	< MDA	1338 ± 210[a]
^{227}Th	< MDA	296 ± 41	< MDA	705 ± 92
^{223}Ra	< MDA	277 ± 69	< MDA	675 ± 66
^{228}Ac	335 ± 23	18291 ± 1280	< MDA	< MDA
^{212}Pb	340 ± 24	16112 ± 1128	< MDA	< MDA
^{212}Bi	330 ± 28	15351 ± 1290	< MDA	< MDA
^{208}Tl	120 ± 8	5618 ± 393	< MDA	< MDA
^{40}K	2032 ± 171	< MDA	< MDA	< MDA

[a] Significant uncertainty increase due to subtraction of the spectral interference contribution.

Table 2
Evaluation of particular gamma-ray spectrometry problems on basis of selected NORM samples including the calculation of interference contributions, a comparison of BIPM and IAEA gamma emission intensities for selected natural radionuclides as well as radon leakage effects.

Nuclide	Gamma line keV	Spectral interferences and radon leakage	Gamma emission intensities (BIPM) %	Gamma emission intensities (IAEA) %	Deviation due to choice of gamma intensities %	Deviation due to spectral interferences and radon leakage (except true coincidence summing) %			
						Tuff	TiO_2	Ion exchange resin	Filter residue
^{234}Th	63.3	TCS; interference with the 62.9 keV / 0.0164 (28) % γ-line of ^{234}Th and with the 63.8 keV / 0.259 (15) % γ-line of ^{232}Th	3.75 (8)	3.7 (4)	1.4	7.7	–	0.4	–
$^{234\,m}$Pa	1001.0	TCS	0.847 (8)	0.842 (8)	0.6	0.0	–	0.0	–
^{230}Th	67.7	–	no data available	0.38 (3)		0.0	–	–	0.0
^{226}Ra	186.2	Interference with the 185.7 keV / 57.0 (3) % γ-line of ^{235}U and with the with the 186.1 keV / 0.0088 (7) % γ-line of ^{230}Th	3.555 (19)	3.64 (4)	−2.3	104.3	0.0	107 kBq/kg[b]	1 Bq/kg[b]
^{214}Pb	295.2	TCS, insignificant interference with the 296 keV / 79 (10) % γ-line of ^{210}Tl	18.414 (36)	18.42 (4)	0.0	−0.6	−0,6	–	−0.6
^{214}Bi[a]	609.3	TCS	45.49 (19)	45.49 (16)	0.0	−0.6	−0.6	–	−0.6
^{214}Bi[a]	1120.3	TCS	14.91 (3)	14.92 (3)	−0.1	−0.6	−0.6	–	−0.6
^{210}Pb	46.5	Interference with the 46,4 keV / 0.19 (1) % γ-line of ^{231}Pa	4.252 (40)	4.25 (4)	0.0	0.0	0.0	–	40.7
^{235}U	163.4	TCS; interference with the 163.1 keV / 0.156 (5) % γ-line of ^{231}Th	5.08 (3)	5.08 (6)	0.0	3.1	–	3.1	–
^{235}U	205.3	TCS; interference with the 204.0 keV / 0.114 (8) % γ-line of ^{228}Ac	5.02 (3)	5.02 (6)	0.0	41.7	377 Bq/kg[b]	0.0	–
^{231}Pa	283.7	TCS	1.72 (3)	1.70 (10)	1.2	–	–	–	0.0
^{227}Th	256.2	–	6.8 (4)	7.0 (6)	−2.9	–	0.0	–	0.0
^{223}Ra	323.9	–	4.06 (8)	3.99 (9)	1.8	–	0.0	–	0.0
^{228}Ac	911.2	TCS	26.2 (8)	25.8 (4)	1.6	0.0	0.0	–	–
^{212}Pb	238.6	–	43.6 (5)	43.6 (5)	0.0	0.0	0.0	–	–
^{212}Bi	727.3	TCS; interference with 726,9 keV / 0.68 (8) % γ-line of ^{228}Ac	6.65 (4)	6.67 (9)	−0.3	8.4	9.9	–	–
^{208}Tl	583.2	TCS; interference with the 583.4 keV / 0.120 (11) % γ-line of ^{228}Ac	85.0 (3)	85.0 (3)	0.0	0.3	0.3	–	–
^{40}K	1460.8	Interference with 1459.1 keV / 0.87 (5) % γ-line of ^{228}Ac	10.55 (11)	10.66 (13)	−1.0	1.1	1405 Bq/kg[b]	–	–

[a] Corrected for the radon leakage regarding the calculation of the ^{226}Ra activity concentration.

[b] The activity concentration of the target nuclide is lower than the MDA. Therefore, the contribution of the interfering nuclide can cause a false positive detection. The reported activity concentration values represent such false positive values of the target nuclides. These values were calculated for the applied detector system with use of the intensities of the target nuclides.

of the containers: a certified soil and a certified 226Ra standard solution. Fig. 1 shows the relative ^{222}Rn build-up curves inside the desiccator. Cmax is the theoretical maximum activity concentration in the desiccator (100 % leakage). It is calculated from the ^{226}Ra reference values of the certified soil and the standard solution and the desiccator volume. The measurement results show an asymptotic ratio of C/Cmax of approximately 0.6 % for the completely filled polystyrene container and a ratio of approximately 0.7 % for the half-filled liquid sample. Due to the fact that the liquid sample has a large void volume and a low radon retention, it gives an estimate for a high exhalation of a sample. The determined ratios of C/Cmax indicate a high grade of radon tightness of the applied sample containers and underline the sensitivity of the method.

Conclusion

Due to the huge diversity of the occurring radionuclides within NORM samples, the gamma-ray spectrometry of specific radionuclides is challenging and requires a suitable handling of spectral interferences. The comprehensive study of potential spectral interferences and the indepth evaluation of four selected NORM samples provide recommendations for the choice of γ-lines and the consideration of possible spectral interferences. The determination of ^{226}Ra based upon ^{214}Bi and ^{214}Pb strongly relies on the radon tightness of the sample containers. In this paper, a simple and sensitive method for the estimation of the ^{222}Rn leakage of sample containers was introduced. The applied polystyrene sample containers showed ^{222}Rn leakages lower than 1 %. The results presented in this paper can contribute to the improvement of measurement procedures for gamma-ray spectrometry of NORM samples.

Funding

This work was done within the Joint Research Project IND57 MetroNORM "Metrology for processing materials with high natural radioactivity" in the framework of the European Metrology Research Programme (EMRP) (Grant Contract No. IND57-REG1). The EMRP is jointly funded by the EMRP participating countries within EURAMET and the European Union.

References

Carconi, P., Cardellini, F., Cozzella, M.L., De Felice, P., Fazio, A., 2012. Correction for radon distribution in solid/liquid and air phases in gamma-ray spectrometry. Appl. Radiat. Isot. 70, 2119–2123.

Corentium, 2016. `http://www.gammadata.se/assets/Uploads/CANARY-pro-DataSheet-V2R1.pdf`.

IAEA, 2016. Live Chart of Nuclides. `https://www-nds.iaea.org/relnsd/vcharthtml/VChartHTML.html`.

Justo, J., Evangelista, H., Paschoa, A.S., 2006. Direct determination of ^{226}Ra in NORM/TENORM matrices by gamma-spectrometry. J. Radioanal. Nucl. Chem. 269 (3), 733–737.

Lavia, N., Groppib, F., Alfassic, Z.B., 2004. On the measurement of 40K in natural and synthetic materials by the method of high-resolution gamma-ray spectrometry. Radiat. Meas. 38, 139–143.

Mantero, J., Gázquez, M.J., Hurtado, S., Bolívar, J.P., García-Tenorio, R., 2015. Application of gamma-ray spectrometry in a NORM industry for its radiometrical characterization. Radiat. Phys. Chem. 116, 78–81.

Mauring, A., Gäfvert, T., 2013. Radon tightness of different sample sealing methods for gamma spectrometric measurements of 226Ra. Appl. Radiat. Isot. 81, 92–95.

Nucleide, 2016. Decay Data Evaluation Project. `http://www.nucleide.org/DDEP_WG/DDEPdata.htm`.

Scholten, J.C., Osvath, I., Pham, M.K., 2013. ^{226}Ra measurements through gammaspectrometric counting of radon progenies: how significant is the loss of radon? Mar. Chem. 156, 146–152.

Wahl, W., 2016. Radionuclide Handbook for Laboratory Workers (Version 5.1.8). ISuS Institute for Spectrometry and Radiation Protection.

Zhang, W., Ungar, K., Chen, J., St-Amant, N., Tracy, B.L., 2009. An accurate method for the determination of ^{226}Ra activity concentrations in soil. J. Radioanal. Nucl. Chem. 280 (3), 561–567.

Živanović, M.Z., Nikolić, J.D., Apostol, A.I., Anagnostakis, M.J., 2012. Analysis of interferences from full energy peaks in gamma spectrometry of NORM and TENORM samples. Nucl. Technol. Radiat. Prot. 27 (4), 380–387.

PERSONAL INFORMATION

Hannah Judith Wiedner

📍 Aurikelweg 8, 1220 Wien, Austria

☎ 0043 650 55 44 747

✉ hannah.wiedner@gmx.at

Sex Female

Date of birth 1988-02-14

Nationality Austria

WORK EXPERIENCE

Since June 2017

Coordination of EMPIR project “MetroRADON – metrology for radon monitoring”

Physikalisch-technischer Prüfdienst des Bundesamts für Eich- und Vermessungswesen, Arltgasse 35, 1160 Wien, Austria

European Joint Research Project focused on developing novel techniques and methods for measurement of radon at low activity concentrations with 17 European partners and additional collaborators.

Since October 2014

Austrian Federal Office of Metrology and Surveying

Physikalisch-technischer Prüfdienst des Bundesamts für Eich- und Vermessungswesen, Arltgasse 35, 1160 Wien, Austria

Department for Ionising Radiation and Radioactivity with the main assignment of gamma-ray spectrometry using a HPGe detector and contributing to EMRP and EMPIR projects like MetroNORM and MRTDosimetry.

23 Oct 2013 – 22 Oct 2014

Internship at Austrian Federal Office of Metrology and Surveying

Federal Office of Metrology and Surveying, Arltgasse 35, 1160 Wien, Austria

Internship at the department for Ionising Radiation and Radioactivity with the main assignment of gamma ray spectrometry, calibration of HPGe detectors and contribution to EMRP project MetroMETAL.

EDUCATION AND TRAINING

Since 10/2016

PHD student

University of Natural Resources and Life Sciences, Vienna (Austria)

PHD student in the field of ionising radiation and radiation physics on the topic of “Development of innovative methods in radionuclide metrology for applications in natural resources and life sciences”.

09/2015 – 11/2015

Early stage research mobility grant by EURAMET

Granted to work in the field of Artificial Neural Networks and gamma-ray spectrometry at Centro De Investigaciones Energéticas, Medio Ambientales Y Tecnológicas (CIEMAT, public research body, Madrid (Spain)) within EMRP JRP MetroNORM (IND057).

Research question: Can Artificial Neural Networks be used to evaluate if certain NORM (naturally occurring radioactive materials) are above the exemption limit?

10/2012 – 01/2015	Master of Science in Physical Energy and Measurement Engineering Technical University of Vienna, Vienna (Austria)
10/2007 – 07/2012	Bachelor of Science in Technical Physics

PERSONAL SKILLS

Mother tongue: German

Other language(s)

English

UNDERSTANDING		SPEAKING		WRITING
Listening	Reading	Spoken interaction	Spoken production	
Very good	Very good	Very good	Very good	Very good

Communication skills	Very good communication skills gained through coordination of a European Joint Research Project, as well as participation in several international conferences, workshops and project meetings.
Organisational/managerial skills	Excellent organisational skills gained through the coordination of a European Joint Research Project with 17 European partners and the organisation of international workshops and conferences, specifically the 20th International Conference on Radionuclide Metrology (ICRM 2015, approx. 260 participants) and the European Workshop on Quantitative Imaging for Molecular Radiotherapy (approx. 65 participants) in Vienna, as well as several international project meetings (approx. 30-40 participants).
Computer skills	Good command of Microsoft Office™ tools Good command of Canberra Genie 2000™ Basic knowledge of LabView, C/C++, HTML

ADDITIONAL INFORMATION

- High-school exit exam passed with distinction
- Diploma exam and master program passed with distinction
- Project work on “Radioactive waste management in Austria”
- Master’s thesis on “Implementation, improvement and comparison of different calibration methods of high purity germanium detectors for gamma-ray spectrometry and exemplary application in radionuclide metrology”
- Driving licence category B
- 3rd place in IRPA Young Scientist and Professional Award
- Experience in Preparing proposals for European Joint Research Projects
- 2017: Konrad Mück Award of the Austrian Association for Radiation Protection (Österreichischer Verband für Strahlenschutz) for “Application of an artificial neural network for evaluation of activity concentration exemption limits in NORM industry“